

Antimicrobial biomaterials for treatment of bone and implant infections

Inaugural-Dissertation
to obtain the academic degree
Doctor rerum naturalium (Dr. rer. nat.)

submitted to the Department of Biology, Chemistry and Pharmacy
of Freie Universität Berlin

by

Magdalena Anna Czuban
from Strzelce Opolskie (Poland)

July 2019

This PhD thesis was performed in the research groups of PD. Dr. Andrej Trampuz and Prof. Dr. Rainer Haag from **May 2015** to **February 2019** in Biofilm Infections Laboratory of Berlin-Brandenburg Center for Regenerative Therapies at Charité - Universitätsmedizin Berlin, and Berlin-Brandenburg School for Regenerative Therapies and at the Institute of Chemistry and Biochemistry of the Freie Universität Berlin,

1st Reviewer: Prof. Dr. Rainer Haag, Freie Universität, Berlin

2nd Reviewer: PD Dr. Andrej Trampuz, Charité – Universitätsmedizin Berlin

Dissertation date: 05.09.2019

Dedication

Dedicated to the memory of my father who always was proud of me and believed in my ability to be successful.

Acknowledgments

I would like to express my sincere gratitude to my PhD supervisor PD Dr. Andrej Trampuz for giving me the opportunity of conducting this PhD work in his research team, for his continuous support of my research work, his patience, motivation and great freedom he provided me during my work. I would also like to thank Prof. Dr. Rainer Haag for giving me the opportunity to conduct the chemical part of my doctorate in his research group, for his time spent discussing my project and his great support. Their guidance helped me in all the time of my research and writing this thesis. I could not have imagined having a better advisors for my PhD study.

I would like to thank the mentor of my PhD project Dr. Mariagrazia Di Luca for her help and time spent on discussions on the complex challenges associated with my experiments, her useful suggestions to all my manuscripts and this dissertation and the time working together in the lab. I am grateful to Dr. Elena Maiolo for guiding my first steps in the Trampuz's research group.

My sincere thanks go to Dr. Jose M. Mejia-Oneto for his scientific enthusiasm and introducing me to the practical application of the bioorthogonal chemistry and the subsequent long-term cooperation. I would also like to thank Prof. Maksim Royzen for his great hospitality during my research stay in his research laboratory at the University at Albany, The State University of New York. He gave me the opportunity to join his research team and provided me access to his laboratory and research facilities.

Many thanks to both of them for the cooperation during my PhD study, their help and constructive discussions on the manuscripts.

I thank my fellow labmates: Anna Koliszak and Lei Wang for their support in experiments, and inspiring discussions, for the sleepless nights we were working together before deadlines. I would also like to address my thanks and Mercedes Gonzales, Tamta Tkhilaishvili for their support and all the fun we have had in the last four years. My special thanks go to Christoph Schlaich, Michaël W. Kulka, and Leixiao Yu, for their introduction to the Haag's research group and MI-dPG synthesis, intensive and fruitful discussions on titanium coatings, as well as Alexander Oehrl for tetrazine-COOH synthesis. I would like to thank Dr. Katharina Achazi for her help in cell culture experiments. I am grateful to Dr. Carlo Fasting for his help and constructive discussions that he offered for HPLC measurements.

I would like to address my acknowledgement to Tony Lane for the manufacturing the titanium material. Furthermore, I sincerely thank Dr. Sebastian Vogt and Mirosława Chmil for their help in PMMA cement manufacturing and especially Dr. Vogt for the great cooperation during my PhD work and the inspiring guidance and discussions.

I would like to acknowledge Prof. Britt Wildemann for her suggestions during the committee meetings and for providing me with the cell lines for the cell culture experiments.

Thank you Dr. Pamela Winchester for the proofreading of this dissertation. My sincere expression of gratitude also goes to my friend Dr. Anna Koziol for her encouragement and language polishing of some of my manuscripts.

I am very grateful to my family; my mother, father and sister for their encouragement during all these years, their love and guidance, for supporting me in my life in general.

In particular, I want to express my heartfelt gratitude to my husband Rafal Czuban for his love, care, patience, continuous support, for believing in me and for his understanding during all these years. Without you this journey would not have been possible.

Table of contents

1. INTRODUCTION.....	1
2. THEORETICAL SECTION.....	2
2.1 Biofilm.....	2
2.2 Biofilm development.....	2
2.3 Implant biofilm-associated infections.....	3
2.4 Diagnosis of the implant-associated infections.....	4
2.5 Treatment procedures for selected implants (where <i>S. aureus</i> is involved).....	4
2.5.1 Prosthetic joint associated infections (PJI).....	4
2.5.2 Cardiovascular devices.....	6
2.5.3 Neurosurgical devices.....	8
2.5.4 Mammary implants.....	10
2.6 Preventive strategies for implant-associated infections.....	10
2.6.1 Implant-based preventive strategy.....	10
2.7 New approach for biofilm-based infections.....	16
2.7.1 Reaction using azido group as a latent amino group.....	17
2.7.2 Reaction between tetrazine and benzonorbornadiene.....	18
2.7.3 Tetrazine/alkene reaction.....	19
2.8 Non-antibiotic-based strategy to elimination of biofilm-based infections.....	21
2.9 Polymethyl methacrylate (PMMA) bone cement commonly used in the clinic to combat biofilm-based infections.....	22
3. SCIENTIFIC GOALS.....	23
3.1 Bio-Orthogonal chemistry-based reloadable biomaterial to enhance the treatments against <i>Staphylococcus aureus</i> infections.....	23
3.2 Mussel-inspired polyglycerol combined with bio-orthogonal chemistry - as a coating strategy for implant associated infections.....	24
3.3 PMMA bone cements with antifungals.....	26
3.4 Photodynamic-based strategy for bacterial eradication.....	26
4. PUBLICATIONS AND MANUSCRIPTS.....	27
4.1 Bio-Orthogonal Chemistry and Reloadable Biomaterial Enable Local Activation of Antibiotic Prodrugs and Enhance Treatments against <i>Staphylococcus aureus</i> Infections.....	27
4.2 Titanium coating by combining concepts from bio-orthogonal chemistry and mussel inspired polymer enhances antimicrobial activity against <i>Staphylococcus aureus</i>	58
4.3 Release of different amphotericin B formulations from PMMA bone cements and their activity against <i>Candida</i> biofilm.....	79
4.4 Electro-responsive graphene oxide hydrogels for skin bandages: The outcome of gelatin and trypsin immobilization.....	101
5. SUMMARY AND CONCLUSIONS.....	113

6. KURZZUSAMMENFASSUNG	114
7. PUBLICATIONS AND CONFERENCE CONTRIBUTION	116
7.1 Publications	116
7.2 Oral Presentations	116
7.3 Poster presentations	117
8. REFERENCES	118

1. INTRODUCTION

Medical devices inserted into the human body have revolutionized medicine and improved the quality of life or even make it possible. However, implants are prone to microorganisms seeding and are related with increased risk of infection.^{1, 2} Despite the progress in the surgical technique, implant design and biocompatibility, laminar air flow in the operating rooms, the number of medical device-associated infection raises.³ These infections represent the one of the most challenging complications and account for about 60-70% of healthcare-related infections.^{1, 2}

Infections of the biological tissue are efficiently cleared by the immune system of the host, in contrast to implant biofilm infection, representing the *locus minoris resistentiae* for infections.² It is an immune depression niche causing acute or chronic inflammation and granulation of the tissue leading to biofilm infection.⁴ Therefore there are less bacteria needed to trigger an infection when there is a foreign body present in a host than when no implant is present.⁵

According to the FDA, more than 500,000 different types of implantable medical devices are currently on the market. About one million cardiovascular devices are implanted worldwide,⁶ and more than a million hip and knee arthroplasties are performed alone in the USA.⁷

Joint prosthesis remains in the body for years to decades and infections can be classified in three types early postoperative, delayed postoperative, and late hematogenous infection. In the first 3 months after surgery can occur the early postoperative infection, the second between the third and 24th month from the operation, the late infections occur after 24 months and are related with the hematogenous implant colonization of microorganisms.^{2, 3, 8} The early stage infection is mostly induced by *Staphylococcus aureus*, the low-grade infection (delayed) is mainly caused by coagulase-negative staphylococci or *Cutibacterium* species (*C. acnes*, formerly *Propionibacterium acnes*).⁸ A similar infection classification applies to the fracture fixation devices, early within first 2 weeks after internal fixation devices, delayed between 2 and 10 weeks, and late after more than 10 weeks from the internal fixation.⁸ Staphylococci are microorganism which are the most frequent cause of infection.^{8, 9}

Systemic antibiotics used to treat implant-associated infections do not always reach the site of infection at sufficient concentration or may cause adverse effects.^{10, 11, 12} Thus, there is a critical need for efficient and modular spatiotemporal delivery of local antibiotics in order to better treat biofilm infections.¹³

An approach using biorthogonal chemistry to turn antibiotics into prodrugs will be presented in this PhD thesis. The prodrug antibiotics, which can be concentrated through click chemistry at an implanted biomaterial¹⁴ and released through a cascade reaction at the infected implant site, was investigated. Two approaches, which are based on tetrazine-modified alginate hydrogel and a coating of the titanium material with tetrazine-modified, mussel-inspired dendritic polymers (MI-dPG) using prodrugs vancomycin and daptomycin, are presented this thesis. Both concepts are inspired by the biorthogonal chemistry approaches, which have been developed until now for delivery of prodrug for cancer therapies.¹⁵ Therefore a concept of biorthogonal chemistry which found an application for prodrug activation to achieve local *in vivo* delivery of active medicaments will be described in the theoretical section. In addition, the existing antimicrobial coating achievements will be described.

In the second part of the thesis two alternative strategies for biofilm-infection will be introduced. The first one will focus on the yeast prosthetic joint and bone infections. Yeast infections are still difficult to treat and not much research is conducted in this area. Secondly, an alternative to antibiotic therapy against bacterial infection based on photodynamic therapy will be introduced.

2. THEORETICAL SECTION

2.1 Biofilm

The aggregation of microorganisms enclosed within the extracellular polysaccharide matrix (EPS) is called biofilm.¹⁶ In this 3D structure microorganisms enter into a stationary-growth modus.^{17, 18} The microorganisms within the biofilm are more resistant to antimicrobials.¹⁹

The bacterial cells within the biofilm form a stable community and communicate between each other producing and detecting signal molecules using for that a regulatory system called quorum sensing. In gram-negative bacteria, a acylhomoserine lactone and autoinducer-2 (AI-2) quorum sensing system was described, whereas in gram-positive bacteria an autoinducing peptide (AIP) system was discovered.¹⁶ For example, in staphylococci an accessory gene regulator (Agr) quorum sensing system was extensively investigated.^{20, 21} Quorum sensing has been mostly found for bacteria communication way, however, it has been also found in the biofilms of *Candida* species.^{22, 23} *C. albicans* produces farnesol which has been described as quorum sensing molecules together with other molecules including tryptophol, morphogenic autoregulatory substance, and phenylethyl alcohol.²⁴

2.2 Biofilm development

The biofilm has three phases of development, attachment, maturation, and detachment.²⁵ Firstly, the planktonic bacteria anchor to a biotic or abiotic surface or to the host matrix protein called also conditioning film. The attachment to biotic and abiotic surface involves different interaction forces like Lifshitz–van der Waals, Lewis acid–base, and electrostatic forces.^{26, 27} The electrostatic and hydrophobic interactions are present in the anchoring process to the abiotic surface like indwelling medical devices or polymeric surfaces. However, adhesins play also an crucial role in the bacteria attachment to the surface and development of biofilm. The adhesins are glycosylphosphatidylinositol-cell wall proteins.²⁸ The protein adhesins are not the only one molecule mediating the attachment, the bacterial filamentous cell appendages also can behave as adhesins and expand the bacterial adhesion to the abiotic surface.²⁹ Another attachment system is through collagens and fibronectins, which are the constituents of the ECM.³⁰ In addition, staphylococci produce autolysins, which after proteolytic cleavage produce proteins amidase and glucosaminidase.³¹ Amidase mediates the attachment to the host matrix proteins, which are available on the implant surface.²

In the case of staphylococci, autolysin or teichoic acid proteins participate in this process.³² The complex structure of staphylococcal cell matrix network is formed by interacting of teichoic acids with electrostatic interactions and by the extracellular DNA, deriving from the lysed bacteria.³³ The cell lysis is a consequence of genes controlling bacterial programmed cell death.^{20, 34} The adhesins are also present in *C. albicans* biofilm. They are called agglutinin-like sequence family adhesins (Als), whereas Als3 plays a key role in biofilm generation.³⁵ Als can also be found in *C. parapsilosis*, however, their role in this species is not well studied.²⁸ The other crucial adhesins in the *C. albicans* biofilm formation are hyphal wall proteins (Hwp), which are a constituent of germ tubes and hyphal cells.^{28, 36} The epithelial adhesion adhesins are the adhesion proteins in *C. glabrata* species.²⁸

The biofilm matrix of *Candida* differs from the Staphylococci one. The *Candida albicans* biofilm structure is a mixture of densely packed yeast cells within extracellular matrix, lipids, polysaccharides, blastophores, germ tubes, and/or young hyphae.^{28, 37} In contrast, the biofilm of *Candida glabrata* is formed by a multilayer packed or cluster of yeast cells and an

extracellular matrix with carbohydrates and proteins without hyphae.^{28, 38} In other *Candida* species, *C. parapsilosis* biofilm matrix components are yeast cells surrounded with a minimal extracellular matrix with carbohydrates and low level of proteins and pseudo hyphae.^{28, 38, 39}

Once microorganisms are attached, the maturation process starts, bacteria agglomerate, and the extracellular matrix forms. The EPS, which provides the three-dimensional structure for the biofilm, consists of polysaccharides, like hetero or homo polysaccharides, extracellular DNA, and proteins. Maturation of the biofilm is connected with adhesive and disruptive factors.²⁰ The disruptive factors determine the formation of the characteristic channels within the biofilm.³² The channels provide the nutrients to the bacterial cells placed deep in the three-dimensional biofilm matrix.²⁰ The disruptive process has been linked to the quorum sensing system.^{20, 21} In staphylococci, Agr expression drives the biofilm detachment and regrowth by downregulating the surface-anchoring proteins and upregulating the expression of degradative proteases.^{20, 40} The disruptive factors are involved in the final step of biofilm development and expansion. The planktonic bacteria are disrupted from the matrix structure and float on to form further biofilm and expand within entire body *in vivo*, possibly leading to a development of systemic dissemination. The detachment may be driven by enzymatic degradation as well as by surfactants.^{20, 25} It has been shown that the *Staphylococcus aureus* produce peptides of surfactant similar properties. These phenol-soluble modulins are amphipathic and α -helical peptides.⁴¹

Whether the host cells or bacteria occupy the medical device surface is defined as a “race to the surface.” It is crucial that the first colonizers will be host cells.⁴² Once the bacteria are seeded on the implant surface, no more prevention from biofilm formation is possible by host cells.⁴³ The importance of the host cells’ first colonization also lead to better osseointegration of the orthopedic implants where bone tissue is growing in the implant and thus integrate the implant in the body.⁴⁴

2.3 Implant biofilm-associated infections

Each implant, a foreign body induces the reaction of the host immune defense system. Once the inflammation response is active, the neutrophils’ capacity to reduce the bacteria cells is dramatically altered.^{45, 46, 47} Moreover, bacteria can defend themselves from the host immune system and has an adverse influence on immune response by production of the toxins.²

The bacteria cells are protected within the biofilm matrix. It was first believed that human leukocytes could not penetrate the dense mature biofilm and thus led to biofilm eradication difficulties.⁴⁸ However, it has been shown that indeed the leucocytes can penetrate the biofilm structure⁴⁹, the phagocytic cells could not deliver protection from the bacteria.⁵⁰ The biofilms have the ability to change the inflammatory phenotype from pro into anti-inflammatory, which is related to the production of anti-inflammatory mediators.^{51, 52, 53, 54} The interleukin-12 (IL-12), which has cytokines, secreted proteins, and signal molecules, boosts the myeloid suppressor cells. These cells supply the anti-inflammatory biofilm surrounding by their immunosuppressive activity, which leads to the phagocyte influx and biofilm reduction or removal.⁵⁵

S. aureus and *Staphylococcus epidermitis* (*S. epidermitis*) are found in around 90% cases of material associated infections. Another pathogen that plays a key role is *Candida* spp. For example, *C. albicans* forms a polymicrobial biofilm together with *S. aureus*, both of which create a barrier that reduces the sensitivity of the antimicrobial agent.⁵⁶

2.4 Diagnosis of the implant-associated infections

Diagnosis of implant-associated infections is crucial for effective treatment.⁵⁷ The traditional culture methods using peri-implant tissue or synovial fluid have limited sensitivity for biofilm detection. The sonication of the removed implant is the most sensitive diagnostic method when the implant is removed.⁵⁸ Other authors focused on histology and evaluation of biomarkers, such as α -defensin and D-lactate in synovial fluid.⁵⁹ Novel approaches include next generation sequencing technologies.⁶⁰ However, new diagnostic techniques are not used in the routine microbiological laboratories.^{61, 62}

2.5 Treatment procedures for selected implants (where *S. aureus* is involved)

2.5.1 Prosthetic joint associated infections (PJI)

The infection symptoms vary depending on the time in which the infection manifests itself. In the first, early stage of infection, which can occur in the first 2 months after surgical procedure, the infection symptoms are erythema, wound secretion, or synovitis. The delayed or later stage of infection no longer presents these symptoms and is much harder to diagnose. The infection may be suspected when the patient complains of permanent pain after surgery or shows signs of loosening of the implant.⁶³ Often this symptom is accompanied by a skin infection or pneumonia, which is not immediately associated with the symptoms of later infection, as well as arthritis, is a point for careful observation.⁵⁷ The cytology and arthroscopic synovial biopsy are methods to detect infection of total knee arthroplasty. The granulocyte fraction higher than 65% and/or leucocytes greater than 1700/ul represent an excellent infection detection factor with the sensitivity of more than 90%.⁶⁴ However, in late or delayed type of infections and in previous antibiotic therapies, the sensitivity of synovial fluid culture is limited. The method that helps detect infection in such cases is sonication of the infected implant parts.^{57, 65}

Prosthetic joint infections occurring early after the surgery can be treated with tissue debridement and implant retention. This procedure has to be very carefully performed. It should only be followed for specific patients where the symptoms of infection are no longer than 3 weeks old, the implant is stable, there is no abscess, and the treated microorganism must be susceptible to the antibiotic used.⁵⁷ To the antibiotics used in the PJI treatment belong antibiotics with antibiofilms and non-growing bacteria efficacy, i.e., fluoroquinolones. In the PJI, the bacteria are in the stationary phase and their burden is moderate 10^6 CFU/ml.⁵⁶

However, delayed and late infections involve special treatment: one- or two-stage exchange arthroplasty. Two-stage or staged exchange arthroplasty consists of several surgeries, but remains a gold-standard in treatment of PJI.⁶⁶ First, there is a debridement of all the dead tissue, and all foreign body materials are removed. The procedure is supported with several weeks' intravenous antimicrobial therapy.⁵⁷ The infected prosthesis is replaced by a bone cement spacer impregnated with antimicrobial agents, which are released from the spacer. In uncomplicated cases treating pathogens, the time of spacer application lasts from 2 to 4 weeks. In this way, the joint is immobilized and the spacer is removed in a follow-up surgery after a few weeks and a new prosthetic joint is inserted in its place.⁶⁷ In more complicated treatment of infections, an interval of 8 weeks is required with a bone cement spacer. This is so-called two-exchange revision arthroplasty with a long interval. The two-stage procedure is commonly used for patients with PJI, because it has a very high success rate > 90%, but is

associated with significantly higher costs for hospital and a patient, which is connected with two admissions, patient longer hospital stay, and a period of restricted patient mobility.^{57, 66}

One-stage or so-called direct exchange procedure, used in intact or narrowly infected soft tissues. In this procedure, the replacement of the infected implant with new prosthesis is carried out in the same surgical operation.⁶⁸ There is no antimicrobial dosage used before operation, it is applied after the tissue samples and fluids are collected.⁶⁶ The success rate in this operation is high, when the procedure is properly done and the treated pathogens are not methicillin resistant *S. aureus* (MRSA), fungi, enterococci, quinolone-resistant *P. aeruginosa*, or small-colony variants staphylococci⁵⁷ One-stage procedure can be also used after previous two-stage exchange failure or by risk of relapsing.⁶⁹ This procedure has its advantages because ex- and reimplantation of the prosthesis performed in one surgical procedure allows one to reduce the costs of PJI treatment, which have already been recently proven in a retrospective study on total hip arthroplasty PJI.^{66, 70} The two-stage procedure turned out to be related with higher complication rate comparing to one-stage exchange, however, the difference was not significant.⁷¹ One-stage revision does not belong to gold-standard treatment in PJI but there are already institutions which choose this procedure over two-stage-exchanges, i.e., ENDO Klinik in Hamburg.⁷² In recent years, it has been shown that this procedure has gained in international popularity and acceptance by appropriate usage and following strict inclusion criteria.⁶⁶ The absolute requirement needed in this procedure is the preoperative diagnosis of the pathogen causing the PJI.⁶⁶

Another procedure is only for patients who are at great risk of reinfection, such as immunosuppressed patients, or patients knowing that the insertion of a new prosthesis will be associated with an implant failure. In these patients, the infected implant is removed without inserting a new one. This procedure is called permanent removal. In case a patient is not suitable for a new operation with a new prosthetic joint, further treatment may consist of the long-term antimicrobial therapy, although often the infection returns after withdrawal of the antibiotics.⁵⁷

In order to provide the patient with a long-lasting, pain-free joint, an appropriate therapy consisting of a surgical procedure and well-chosen antimicrobial therapy is required. The treatment of implant-associated infection with antimicrobial therapy alone usually fails.⁵⁷ Early diagnosis is crucial as curing early infection is much straightforward than treating late or delayed infection. In addition, it is very important not to use antibiotics empirically until the diagnosis is made.⁵⁷

2.5.2 Cardiovascular devices

A) Pacemaker and cardioverter-defibrillators (ICD)

The implantation of cardiac pacemakers and ICD is steadily increasing due to the older population age.⁷³ There are two classes of pacemaker's infections: (a) pacemaker generator pocket infection and (b) electrodes' infection including pacemaker infective endocarditis where the pathogen has also spread along the electrodes.^{56, 74}

The early infection, which occurs within first 1 to 2 months after the implantation of the device, is called exogenous and show following symptoms: erythema, swelling, pain, erosion, warmth, and sinus tract. These are characteristic symptoms of pocket inflammation. However, the exogenous infection may manifest later symptoms when the battery pockets are infected. Hematogenous infection mostly lacks typical symptoms. It impacts the electrode and may be triggered by the bacteremia.⁵⁷

Study shows that most common pacemaker infection-causing microorganisms are coagulase-negative staphylococci (CNS), *S. aureus*, and Enterobacteriaceae. *S. aureus* is predominant in the early stages of pacemaker endocarditis infections that occur in the first month after implantation. In the infections manifested at a later stage, the dominant organisms are CNS.^{56, 75}

The suggested treatment regarding pacemakers and ICD includes removal of all infected materials and surrounding parts, implantation of a new device under bacteremia control followed by antimicrobial therapy.⁵⁶ The exception can be made in case of generator pocket infection without coexisting bacteremia, when late exogenous infection occurs. Here the therapy includes the generator replacement without explanation of electrodes, which is related with an increased risk of infection recurrence. In case of electrode infections, the exchange of all hardware is used.^{56, 57}

B) Prosthetic valve endocarditis

Prosthetic valve endocarditis (PVE) is rare but belongs to serious complications for a patient.⁷⁶ It is associated with devastating complications, i.e., ischemic stroke, increased operative morbidity, and mortality risk.⁷⁶ The highest risk of valve endocarditis occurs in the first 12 months after cardiac surgery and this infection is classified as early infection.⁷⁷ However, the most PVE death cases occur in the first 3 weeks from cardiac surgery.^{76, 78} If the PVE is developed within the first 12 months from the device implantation, it is categorized as healthcare-associated infection.⁷⁹

After 12 months the risk of PVE is reduced, although it remains present lifelong. The infection manifestation after 12 months from device implantation is called late infection^{56, 76, 80} In the case of infections immediately following cardiac surgery, we are dealing with organisms that come from the human skin of the patient or surgeons, therefore dominant pathogens are *S. aureus* and CNS about 50% of the time.^{56, 81} They are also present in the late stage of infections, but streptococci, enterococci, and HACEK (group of bacteria *Haemophilus*, *Aggregatibacter*, *Cardiobacterium*, *Eikenella*, *Kingella*) microorganisms predominate.^{77, 82} These pathogens settle on the valve through the blood, most often through the urinary tract or gastrointestinal tract.⁵⁶ The risk of bacteremia is mostly related with the patients with central venous catheters^{76, 83} or urinary catheters.⁸⁴ Murray et al. suggested that PVE risk is increased by *S. aureus* bacteremia.⁸⁵ Another risk for PVE is candidemia, which is rare and covers about 5 to 10% of cases, but the risk of death from such infection is very high.⁸⁶ Therefore the patients

with prosthetic valves and candidemia must undergo an aggressively antifungal treatment together with long-term follow up.⁷⁶ Hemodialysis has also been categorized to elevated risk of PVE development, especially to the *S. aureus* endocarditis.⁸⁷ There are two categories of valves: mechanical and bioprosthetic. The first one shows an increased risk of PVE in the first three months.^{76, 88} The reason why mechanical risk of PVE is higher is unknown. Mechanical valve infection is associated with the formation of peri/paravalvular abscesses, valve delamination, and aneurysms resulting from the connection of sewing ring and annulus. In the case of bioprosthetic valves, the infection develops on the leaflets and does not cause the same effect as in the case of mechanical valve infection, but it leads to vegetation, cusp fracture, and perforation.⁸⁹

The first PVE treatment procedure consists of antimicrobial therapy. The antibiotics used for the endocarditis treatment are the ones with the bactericidal efficacy against planktonic pathogens used for at least 6 weeks or in some cases longer. Beta lactams and aminoglycosides belong to the bactericidal drugs. It has been suggested that the reason for choosing drugs with planktonic efficacy is related to the bacteria burden that reach 10^8 - 10^{10} CFU/ml in endocarditis and therefore is classified as very high. Additionally, the bacteria are in the log phase of growth. The antimicrobial therapy may be supported with the replacement surgery of infected valves.⁵⁶ The indication for surgery is only suggested in certain cases such as valve dysfunction, left-sided infectious endocarditis caused by *S. aureus* or fungi, perivalvular abscess, bacteremia, or endocarditis relapse.^{56, 76}

C) Vascular graft infections

Vascular graft (e.g., femoropopliteal, aortic) infections are rare but when they do occur they are life-threatening⁹⁰ for patients with aortic grafts (up to 75%).⁵⁷ They also carry a high risk of morbidity, in the case of vascular grafts of lower extremities valves, up to 70% of the limbs are amputated.^{56, 57}

The symptoms of the vascular infections can be non-specific. The possible signs are fever, wound-healing difficulties, erythema, or swelling. However, low-grade fever can be the only signs associated with the infection. The infection related to erosion between anastomosis prosthesis connected with intestines show symptoms of gastrointestinal bleeding.⁹¹ The predominant microorganisms in these infections are *S. aureus*, group B-streptococci, and *S. epidermidis*.⁹²

The treatment must start with the microbiological diagnosis, which consists of fluid puncture and blood cultures that were taken prior to antibiotic therapy.⁵⁷ The CT scan is a gold standard in the diagnosis of acute infections. For chronic infections, positron emission tomography shows good sensitivity and specificity.⁹³

In the treatment of vascular prosthesis infections, it is important to control sepsis, remove the infected graft, and replace with a new one, at the same time allowing the vascular supply of the affected organ. The broad-spectrum antibiotic therapy must immediately follow after surgery, and when the microbiological results are known de-escalation therapy must be administered with the addition of at least one antibiotic that has anti-adherent properties.^{57, 93} In specific cases, e.g., aortic prosthesis infection, an extra anatomical bypass may be used. This procedure involves the expertise from cardio surgeons and infection diseases specialists.^{56, 57}

2.5.3 Neurosurgical devices

Within the neurosurgical implants commonly used are neurostimulators for the management of Parkinson's disease or diseases related to movement disorders, titanium fixation devices for craniotomy or cranioplasty, external ventricular drainage (EVD) and lumbar drainages (ELD) and shunts.⁹⁴

The shunts are used in the patients with hydrocephalus conditions that increase the pressure in the brain by the accumulation of the cerebrospinal (CSF) fluid in the ventricles.⁹⁴ In the ventriculo-peritoneal (VP), the CSF fluid drains out into abdomen or peritoneum, into the spaces surrounding lung. The CSF fluid is drained into right heart atrium in the ventriculo-atrial shunts and the CSF fluid is absorbed by blood stream.⁹⁵

The diagnosis and treatment of neurosurgical devices are not trivial, as the literature about management of these types of infections is scarce and no guidelines are reported for these types of infections. The treatment procedures are often extrapolated from the management of orthopedic-device-infection treatment guidelines. The infections are related to high morbidity, mortality, and costs. The treatment costs of neurosurgical implant-associated infection are estimated to be higher than prosthetic joint implant-associated infections.⁹⁴ The costs for prosthetic joint implant infections are three times higher than primary implantation.^{96, 97, 98}

Neurosurgical implant infection can occur at different times. They are classified as early, including acute, and later developing, i.e., delayed and late. The first ones develop in the first 4 weeks after the implant placement. Acute infections are most commonly present in the hospital and are characterized by fever, swelling, erythema, and warmth and symptoms of local inflammation. In the case of these infections, the biofilm is not yet well developed and the therapy can therefore only consist of debridement and a subsequent 12-week antimicrobial therapy.⁹⁴ Delayed infections are those developing during the first 12 months after implantation and infections occurring after a year after implant placement are classified as late.⁹⁴

The risk to develop the neurosurgical implant infection is mostly related to the skin colonized with bacteria or to mucosal flora.⁹⁴ The infection can occur in three stages, through a skin or open wound preoperatively, intraoperatively through an implant that has been infected with pathogens, and postoperatively associated with wounds and their insufficient healing or wounds resulting from the placement of a drainage system.^{99, 100, 101} Rarely there is a bloodstream infection, although this may occur in shunts. VA shunts are located endovascular and therefore in the event of bacteremia it is also possible to develop biofilm-related infection on the shunt.⁶³ For post-craniotomy infection the most frequent risk of infection origin is the use of preoperative chemotherapy or if CSF leakage occurs postoperatively, infecting the open wound, using steroids all the time, longer than usual surgery.^{102, 103} In shunt infections, the risk of infection development is first of all the earlier infected shunt, CSF leakage postoperatively, the application of a neuroendoscope, similar to the post-craniotomy infection prolonged surgery but the experience of neurosurgeons also plays an important role.^{104, 105, 106} The infection risk factors for EVD are intraventricular hemorrhage, cranial fracture with CSF leakage, but the catheterization time is also very important and prolonged hospital stay.^{107, 108,}
109

There is a general recommendation for treatment of permanent implants, which includes a surgery to remove necrotic tissue and reduce the bacteria amount followed by the application of bactericidal antimicrobial agents.^{63, 110} In order to reduce the bacteria load in acute infections, it is better to clean the implant mechanically unless the infection symptoms persist for more than four weeks, then the implant replacement is recommended.⁹⁴

There are two ways of proceeding with neurosurgical implant infection treatment: the first when the pathogen is susceptible to antibiofilm agents, the second when the microorganism is not susceptible to antibiofilm therapy. In the first case, the therapy consists of implant debridement and leaving the implant in case of early infection, or one or two-stage implant exchange in case of later infections. In each case, the treatment is combined with the use of antibiofilm agents for 12 weeks. If the microorganism is not susceptible to antibiofilm therapy, a complete removal of the implant with the antibiotic therapy is applied for about 6 weeks. The new insertion of the implant only performed after the infection has been removed. In cases of shunt infection and/or *S. aureus*, the time can be shortened to 2 weeks without the implant. The final treatment, which is possible when the implant cannot be removed, can be considered suppressive antibiotic therapy. The suggested intravenous treatment antimicrobial agents for infection caused by *S. aureus* and MRSA include vancomycin or daptomycin in combination with rifampicin. Higher doses are required for infection connected with the central nervous system.⁹⁴

A) Infections related to post-craniotomy and cranioplasty

An operation with removal of a part of skull is called craniotomy. This surgery is performed to access the intracranial brain compartment. After completing the operation, the cut part of the skull is then returned to its position and secured with titanium plates or screws.⁹⁴ Symptoms of this infection appear most frequently in the first days after surgery and the prevalent pathogen causing this infection is *S. aureus* and coagulase-negative staphylococci and some gram-negative bacteria.^{111, 112} The most common signs of this infection are changes in mental status, fever, and headaches.

In the case of craniectomy, the skull bone cut out does not return to its place immediately, here the patient can live without brain protection even for several months, which can affect CSF dynamic and cause hydrocephalus.¹¹³ Either cryopreserved autologous bone flap or a synthetic implant that is made of titanium, polymethyl methacrylate, or polyether ether ketone is used to close the skull. Here, too, the most infectious microorganisms are *S. aureus* and coagulase-negative staphylococci.^{113, 114}

The standard treatment procedure in both cases is to remove the bone flap or synthetic implant using an antibiotic therapy that can last for weeks or months. Only then is cranioplasty performed. There are also new suggested therapies. In case of acute infection, debridement and retention of the bone flap should be performed. A two-stage implant exchange with a short interval of no implant is also a consideration. Both of these procedures demand an antibiofilm therapeutic agent for the following 12 weeks after the surgery.⁹⁴

B) Ventriculoatrial and ventriculo-peritoneal shunt infection

VP shunts are most commonly used as they are related to less complication rate. The Ventriculoatrial (VA) shunts are related to more complications as: cardiac arrhythmia, myocardial injury, intra-cardiac thrombi, or endocarditis.^{115, 116} VAs are only chosen for the patients who have had abdominal surgery or who have had earlier complications with VP shunt.⁹⁴ The most common infectious pathogen in early shunt infection are microorganisms found on the skin flora, i.e., *S. aureus*, coagulase-negative staphylococci, and *C. acnes*, in later infections they are often polymicrobial.¹⁰¹ There are no clear symptoms immediately indicative of shunt infections. The signal that may indicate an infection is that the shunt will stop working and it will be recognized by the repeated hydrocephalus, which can cause a headache or vomiting. Further symptoms are ventriculitis and meningitis. In VP shunt infection additional symptoms are peritonitis or intraabdominal pseudocysts. In VA shunt infections typical symptoms are right-sided endocarditis and fever.^{101, 117, 118}

There is no gold standard for treatment of shunt infections. There are, however, suggested ways to proceed. After diagnostics based on valve puncture and SCF sample collection and blood culture, the appropriate steps are taken. If there is no meningitis, abscess, shunt dysfunction, or skin erosion, the infected implant can be retained and antibiofilm antibiotics are given for 12 weeks. If any of these is present, the infected implant must be replaced immediately. The replacement consists of removal of the implant and antibiotic therapy. When the infection is cured, a new implant can be inserted. In the case of *S. aureus* and a negative blood culture, a new implant can be inserted after 14 days. If a new implant is inserted, CSF culture is negative, a 4-week antibiofilm therapy following reimplantation is suggested.⁹⁴

2.5.4 Mammary implants

The infection rate of mammary breast implants is estimated on 2% for patients with simple augmentation⁹⁶ and higher about 12% for patient with previous breast cancer and mastectomy followed by immediate implant placement.¹¹⁹ The predominant pathogens are *S. aureus*, *Enterobacteriaceae*, and *P. aeruginosa*.⁵⁷ Swelling, pain, difficult and chronic wound healing accompanied by fever are common symptoms of mammary implant early acute infection.

The standard therapy include similarly to periprosthetic joint infection removal of the infected implant, followed by delayed replacement of an implant and long-lasting antimicrobial agents therapy.¹²⁰ However, therapy with direct implant substitution, immediate new implant insertion prior for pocket curettage, debridement, and postoperative antimicrobial application is also considered to be successful.^{120, 121}

2.6 Preventive strategies for implant-associated infections

It has been shown that the care bundle approach used by a patient before the surgery gives the maximum outcome benefit. The care bundles include whole-body decolonization with proper antiseptic agents.¹²² It has been found that one risk factor for prosthetic joint infections (PJI) is the preoperative anemia. The risk to develop the infection is doubly increased in this case.^{123, 124}

2.6.1 Implant-based preventive strategy

The implant surface is so important that changing its characteristics has a huge impact on the adhesion of microorganisms and thus on the development of biofilm. Different coatings offer surface superhydrophilicity, antifouling, and bacteria repelling surfaces.^{125, 126, 127, 128} Ideally prosthetic joint implants should also boost tissue integration by a fast host cell implant colonization.^{129, 130}

Many of the coating technologies are already advanced and tested in the clinical studies, which mostly includes materials with coating that release antimicrobial agents and repel bacteria.²

Material that is supposed to be protected by bacterial colonization should have repelling or killing properties. It is suggested that this can be achieved by modifying the surface of the material without damaging the bulk properties of the implant. Chouirfa et al. suggests dividing surface modification methods into surface modifications or coatings of the material surface. Both can be sub-divided into physical and chemical or a combination of the two.¹³¹

A) Surface modifications

Modification of the implant surface aims to introduce antibacterial properties on the implant surface by immobilizing small molecules. The molecules can be inserted into the implant surface in two ways, through adsorption, which does not necessarily provide a suitable stable coating¹³¹, and through covalent bonding of the molecule to the surface.¹³² Covalent, strong bonding can be divided into those that require a suitable anchor, the so-called "grafting to" coatings, and those that require a polymerization on the implant surface, the "grafting from" coatings.¹³¹

A.1 Grafting "from"

It has been reported a process that introduces a polymer on the surface of a titanium implant in several steps. First, the oxidation of the titanium surface was applied through sulfuric acid and hydrogen peroxide, which generates titanium hydroxide or peroxide on the surface of the implant. In the next step, by heating or UV irradiation, radicals were formed on the surface, which were used to connect to a highly concentrated styrene sulfonate monomer.^{133, 134} This method showed an effective inhibition of *S. aureus* by comparing it to an implant without coating.^{133, 135, 136} However, the "grafting from" methods are composed of multiple coating steps and need no special water and oxygen conditions and therefore have turned out to be more complicated than "grafting to" methods.¹³⁷

A.2 Grafting "to"

A coating, which binds the molecule to the implant surface, uses different anchors, i.e., silane, catechol, and phosphor.

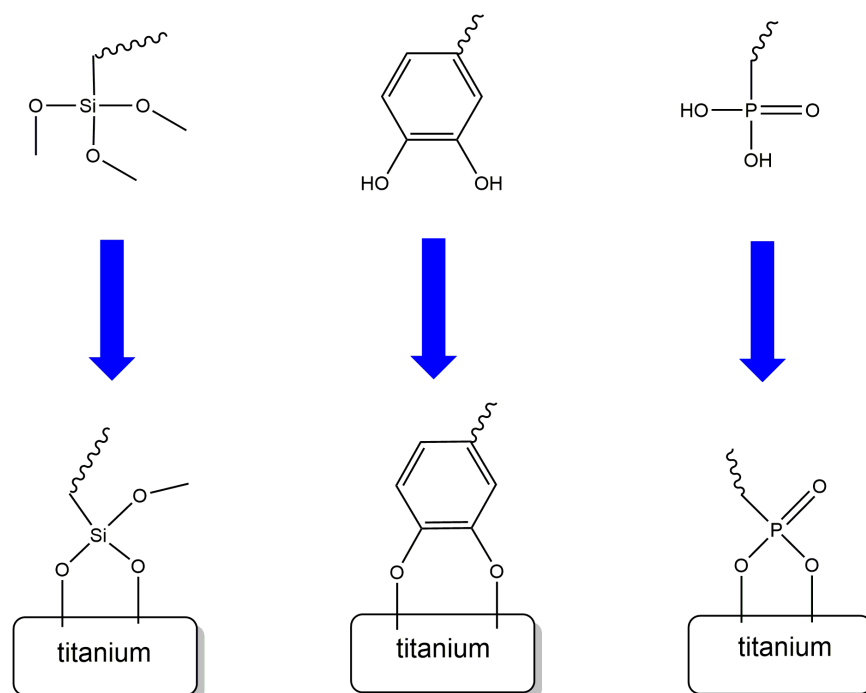


Figure 1. Titanium surface functionalization with different anchors to prepare an antimicrobial surface. Modified reprint with permission from reference¹³¹. Copyright, 2019, Acta Biomaterialia.

A.3. Silane anchor

Silanization has been used to introduce peptides, polymers, or proteins into the titanium surface. The hydroxyl groups present on the titanium surface are further modified using alkoxy silane.¹³¹ Chen et al.¹³⁸ used (3-aminopropyl)triethoxysilane to introduce amino groups on the titanium surface, then they used bifunctional linker ester to introduce the melimine on the surface. It is a synthetic peptide, which shows a wide spectrum of antibacterial and antifungal activity. This coating showed a significant *in vitro* reduction in adhesion of *S. aureus* and *P. aeruginosa* biofilm by comparison to the titanium without coating. In the *in vivo* case, where substrates were tested with a mouse and rat infection model, that coating showed a reduction in bacterial count of 2 log10.¹³⁸ A further example of the silane anchor use is the coating introduced by Gerits et al.¹³⁹, where the antimicrobial agent SPI031 was covalently bonded to titanium using (3-aminopropyl)triethoxysilane. This coating also demonstrated *in vitro* and *in vivo* reduction in *S. aureus* and *P. aeruginosa* biofilm formation.

A.4 Catechol anchor

Catechol can be used in a variety of ways as an anchor. The first option is to functionalize a polymer with catechol. Such a polymer can then be easily attached to the titanium surface.¹⁴⁰ There have been three adsorption modes according to the density function theory.¹⁴¹ Depending on the pH value used for the reaction, there are different types of bindings: in lower pH bidentate hydrogen bonding between protonated catechol hydroxyl groups and interfacial oxygen on the titanium surface, one monodentate H-bonds combined with a single coordination bond at intermediate pH, and at elevated pH values fully deprotonated catechol coordinates with interfacial oxygen on the titanium surface to form bidentate two coordination bonds.¹⁴²

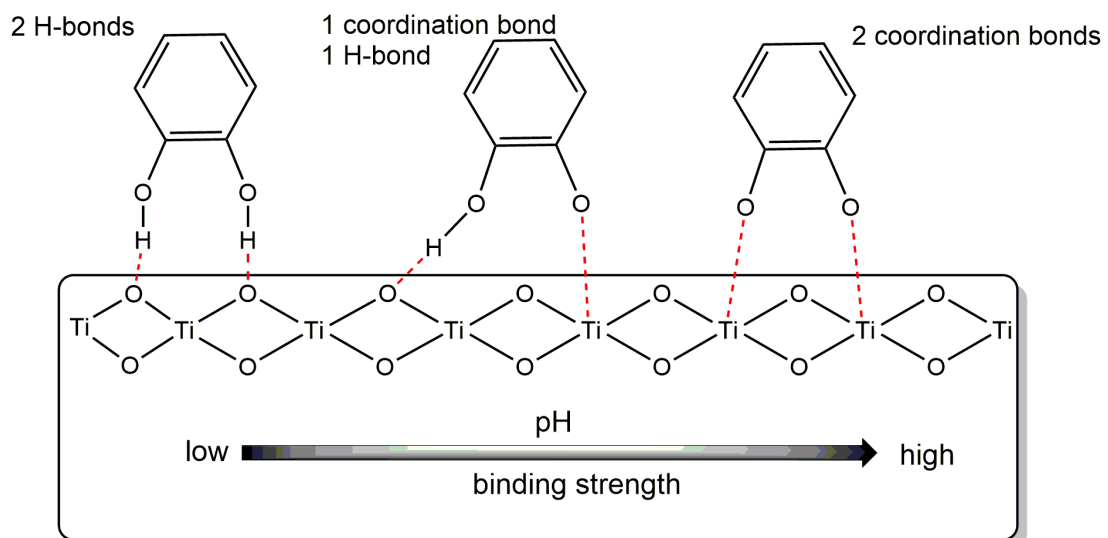


Figure 2. pH dependent binding modes of DOPA to titanium surface. Modified reprint with permission from reference¹³¹. Copyright, 2019, Acta Biomaterialia.

Another alternative is to first introduce the catechol on the titanium surface and then to connect it to a functionalized polymer by means of a reaction click.¹⁴³ The catechol can also be introduced by an initiator with catechol group in direct polymerization.¹³¹ Hu et al. showed *in vitro* a reduction of *S. aureus* adhesion to titanium where carboxymethylchitosan (CMCS) and hyaluronic acid-catechol (HAC) were grafted to the surface through a dopamine anchor. The bacteria amount was reduced to 16% for a CMCS dopamine coating and 54% with HAC coating compared to uncoated materials.¹⁴⁴

A.5 Phosphor anchor

Phosphates and phosphonates can functionalize the titanium surface by covalent binding into it and they can be connected to the desired molecule that is supposed to be attached to the surface. These types of linkers are more stable in physiological pH than silane linkers, which demonstrate instability in aqueous solutions.¹³¹

It has been shown that phosphate functionalized molecules can be directly bounded to the TiO₂ layer without a crosslinking agent.¹⁴⁵ The titanium surface with such attached molecule was incubated with *Strep. sanguinis* and showed a decrease in adhesion of this bacteria.

Pfaffenroth et al.¹⁴⁶ investigated the antimicrobial activity against *Streptococcus mutans* of the titanium surface which they previously functionalized with copolymers of 4-vinyl-N-hexylpyridinium bromide and dimethyl-[2-(methacryloyloxy)ethyl] phosphonate. The polymers formed an ultrathin layer on the titanium surface with antimicrobial properties.

B) Coating of the surface

B.1 Physical

Chouirfa suggested two sub-categories of a physical coating, bacteriostatic and bactericidal.¹³¹

a) Bacteriostatic coatings

These coatings show an electrostatic repelling bacteria activity without a bacterial killing effect. Bacteriostatic surfaces can be introduced by using hydrophobic modification of the TiO₂ layer or by polyethylene glycol (PEG) hydrogel or any other molecule forming similar gels.¹³¹

Polycations and polysaccharides coatings

It has been shown that a titanium coating based on PEG, poly(L—Lysine), and an antimicrobial peptide RGD compared to *S. aureus* and *S. epidermidis* showed a reduction of 98% and 93-95% bacteria, respectively.¹⁴⁷ Chua et al. showed that the longer the polysaccharide chain, the more Lifshitz-Van der Waals forces are reduced on the surface and the *S. aureus* adhesion decreases. A reduction of 80% has been reported.¹⁴⁸ A coating based on chitosan and alginate was introduced onto the titanium surface by the layer-by-layer self-assembly technique. The coating was first loaded with minocycline, a broad-spectrum antibiotic. After the release of the drug, the antimicrobial properties of the coating could be biostatically maintained by its surface charge and hydrophilic properties.¹⁴⁹ However, the mechanical stability of the gel coatings is still a concern. It is recommended by application of the materials with such coating to avoid screwing, this however, can be hardly avoided in implant surgery.¹³¹

Smart polymers coatings

Polymers, which respond to numerous stimuli like temperature, pH, and light, etc., are called smart polymers.¹⁵⁰ Poly(N-isopropylacrylamide) is most widely used polymer in this group, because it responds to temperature changes, is used to control the wettability properties of a surface, and displays a lower critical solubility temperature (LCST) in water at 32°C. It shows hydrophilic properties below LCST temperature, at the temperatures above LCST, it is hydrophobic, is no longer water soluble, and changes its length presenting a collapsed structure.¹³¹ Lee et al.¹⁵¹ proved that a titanium surface coated with

poly(N-isopropylacrylamide) could detach *S. aureus* and *Porphyromonas gingivalis* by decreasing the temperature below LCST.

b) Bactericidal coatings

These coatings aim to kill bacteria by interfering with the bacterial membrane.

Polycations

Polycations may be used to disrupt the bacterial outer and cytoplasmic membrane because they are attracted to the negatively charged proteins and teichoic acid in the gram-positive bacteria and to negatively charged phospholipids in the gram-negative bacteria. Schaer et al. proved the antibiofilm properties of the hydrophobic polycation N,N-dodecyl,methyl-polyethylenimine and studied this coating with *S. aureus*.¹⁵²

Coating with antimicrobial peptides

Antimicrobial peptide been developed as an alternative for the antibiotics. Rodriguez Lopez reported the release of β -amino acid-based peptidomimetic of antimicrobial peptide from the chitosan hyaluronic acid coating.¹⁵³ The materials coated with the β -peptide displayed excellent properties for mammalian cells attachment and provided long-term release of the antimicrobial peptide, which showed its antimicrobial activity against *S. aureus*. Other research groups incorporated the antimicrobial peptide Tet213 into the calcium phosphate and coated it on the titanium surface.¹⁵⁴ The authors claimed the very fast *in vitro* killing of *S. aureus* and *P. aeruginosa* within first 30 minutes.

Coating-releasing ions

Chlorine, iodine, copper, calcium, and some other chemical elements have been used to incorporate themselves into titanium or hydroxyapatite coatings. The anodic oxidation of the ion is used to introduce them into the coating. By hydroxylation, the ions can be turned into highly reactive molecules like HCl, hydrogen peroxide, or superoxide (O_2^-), which results in cell permeability and finally in cell death with oxidation.¹³¹ Iodine coating is the only ion-based coating that found an clinical application.¹⁵⁵ It also went successfully through a single Level 2 random-controlled study and gained much interest in Japan.¹⁵⁶

Coatings using photoactivity of the titanium surface

Titanium oxide is a photoactive semiconductor, which can be used for the bacteria elimination under the application of ultraviolet A light in the wavelengths between 315 and 380 nm.¹³¹ The photoactivation of titanium surface work in two steps, first the photo-activated TiO_2 surface removes the hydrocarbons by oxidation and provides super-hydrophilic surface. A second step is necessary to produce reactive oxygen species which then, by oxidation, the cell membrane leads to cell death and therefore introduces antimicrobial properties on titanium surface.¹⁵⁷ This method is limited to the light access to the implant. Therefore, not all implant-associated infections can be treated using this method.

Coatings with nanoparticles

There are several metal-based nanoparticles used for microbial eradication. These are copper, silver, gold, zinc, and magnesium nanoparticles, which range from 1 to 100 nm.¹⁵⁸ However, the antimicrobial properties of nanoparticles are under discussion as some research groups did not find any antibacterial activity of those molecules^{159, 160}, whereas the other authors reported significant (more than 90%) bacterial burden reduction.¹⁶¹ The authors who used nanoparticles together with organic or inorganic antimicrobials showed reduced bacterial attachment to the surface.^{159, 162, 163} Similarly, excellent biocidal properties against *S. aureus* and *E. Coli* have been shown with silver nanoparticles.^{164, 165}

Coating incorporating antimicrobials

Coating incorporating the antimicrobials can be prepared in different ways. The most common way is to soak the coating in the antimicrobial solution or impregnate the coating with antimicrobial drugs.¹³¹ The advantage of local antimicrobials application is that they do not cause systemic toxicity. However, the systemic application of antibiotic, as a support for the local therapy, is suggested for peri-implantitis treatment protocol.¹⁶⁶ By choosing the drug for the coating, the coating conditions have to be considered. If the coating involves high temperatures, a temperature-stable antibiotic has to be chosen.¹³¹ Metsemakers et al. reported a successful application of the gentamicin-coated tibia nails Expert Tibia Nail (ETN) PROtect in the human clinical study for 16 patients.¹⁶⁷ The coating is composed from poly(D,L-lactide) matrix containing gentamicin sulfate and is fully resorbable. The coating is introduced to the surface by the dip coating procedure and showed a burst release of 70% within the first 24 h from the implantation.¹⁶⁸ Other antibiotics, which are integrated in the release coating, are vancomycin, tetracycline, amoxicillin, and cephalothin. They all represent activity against bacterial surface colonization.^{169, 170}

Silver coatings

Silver has been broadly used in the antimicrobials coatings as it represents wide spectrum antibacterial susceptibility and, at the same time, displays antibacterial activity also against polymicrobial infections.¹⁷¹ In its ionic form, Ag⁺ eradicates bacteria in different modes of action, by inhibiting inter-membrane transport, blocking cell duplication, or disrupting the cells.⁵⁶ Silver is supposed to bind to DNA and thiol groups in the protein and thus disrupts cell membranes and proteins.¹⁷² Silver is the most commonly used metal for the antimicrobial coatings showing good antimicrobial properties with hydroxyapatite coatings^{171, 173}, silver-loaded gelatin microspheres on the porous titanium structure.¹⁷⁴ A discussion has been raised about the silver toxicity in the human body. Therefore its use has been restricted in the patients with high post-operative risk factor.¹³¹

B.2 Chemical

a) Chemical vapor deposition (CVD)

CVD, which is a reaction with gaseous reactants, found a broad application in the industry. It provides high quantity and quality coatings with a well-controlled coating process.¹³¹ Its application as a convenient coating against pathogens has not been widely used, but there are some evidences showing its usage in the antibacterial coating against *E. coli*. The graphitic C₃N₄ has been introduced onto the titanium nanotube layers through one-step CVD. Then using visible light source it demonstrated strong photocatalytic antimicrobial activity.¹⁷⁴

b) Sol-gel coating

Sol-gel is a technique, which has found many applications in coatings of various applications. This method creates a colloidal solution on the surface of the material. The colloidal solution can be an inorganic material into which organic polymers or nanomaterials can be introduced.¹⁷⁵ This method is extremely comfortable and easy to use and ultimately results in the formation of a gel on the surface of the coated material.¹³¹

Antibiotics can also be introduced this method within the gel on the surface of the material and thus create an antimicrobial coating. As it was done by Radin and Ducheye¹⁷⁶ who introduced vancomycin onto the surface of titanium material. Another antimicrobial coating was shown by Gollwitzer et al.¹⁷⁷ who introduced copper (II) acetate monohydrate to the TiO₂ surface using a sol-gel technology. Thus, coated materials were subjected to testing against *S. aureus* and exhibited reduced adhesive strength of this bacteria to the material surface.

c) Nitride coatings

Titanium nitride found its application in metals used in clinics and dentistry. It is a material that provides the surface with high corrosion resistance, it strengthens the surface structure of the material, it is chemically inert, and it has a low friction coefficient. It has also been successfully tested for its biocompatibility.¹³¹ Its antimicrobial properties remain disputable. Some of authors have indicated the lack of bacterial adhesion effect^{178, 179} while others assessed its activity on *Strep. mutants* and demonstrated bacterial adhesion reduction.¹⁸⁰

2.7 New approach for biofilm-based infections

There is not much research conducted using bioorthogonal chemistry to tackle biofilm-based infections.

Bioorthogonal reactions or click reactions, includes chemical reactions which occur in the biological milieu being at the same time inert to the biochemical processes. There are different type of biorthogonal chemistries, among others, Staudinger ligation, strain promoted azide-alkyne cycloadditions (SPAAC), copper(I)-catalyzed azide alkyne cycloaddition (CuAAC), inverse-electron demand Diels-Alder (IEDDA) reaction.¹⁸¹ Bioorthogonal chemistry has found a promising application for prodrug activation to achieve local *in vivo* delivery of active medicaments.¹⁵ For those Staudinger and inverse-electron demand Diels-Alder (IEDDA) reactions have been the most widely used.

Turning the drug into a prodrug has the benefits that undesirable drug properties such as systemic toxicity can be temporarily switched off via a temporary mask of the functional group which is the reason for undesirable properties. Additionally, the potency of the drug can be improved by tethered to a vector molecule such as antibodies, which leads to targeted delivery.

The ideal prodrug is stable while circulation in a human body and cleavable only at the desired location. There are two types of prodrug modification, one which lead to the release based on chemical reaction and second where the release of an active drug is driven by the enzymatic reaction.¹⁸² Examples of enzyme triggered reaction include, among others, hydrolysis, which causes release of an active substance from an ester prodrug.¹⁸² Prodrug, which contains disulfide linkers will be triggered by reducing agents.^{183, 184} The most common enzyme-activated prodrugs are those that contain linkers susceptible to, inter alia, esterases, proteases and phosphatases.¹⁸⁵

There are different bioorthogonal triggers for release and thus activation of products, these are among others¹⁸²:

2.7.1 Reaction using azido group as a latent amino group

The azido group is used to activate a prodrug by nucleophilic addition or self-immolative elimination. Here, the classic Staudinger reaction was modified in order to include intramolecular cyclization and it is been called Staudinger ligation. In this reaction a prodrug (Drug= R_1NH_2) is activated by azido containing compound. A Staudinger ligation followed by self-immolation has found an application in cancer therapies.¹⁸⁶ Robillard et al. reported doxorubicin (doxo) prodrug activation via the Staudinger reaction.¹⁸⁷ The doxo-prodrug **1** (Figure 3) used in his study includes azido group. This group was converted into amino group by phosphine compound **2**. The intermediate undergoes self-immolation through 1,6-elimination which leads to activation of doxorubicin and release of byproduct **11**. At 37°C in aquatic conditions the reaction between **1** and **2** was completed within 20h.

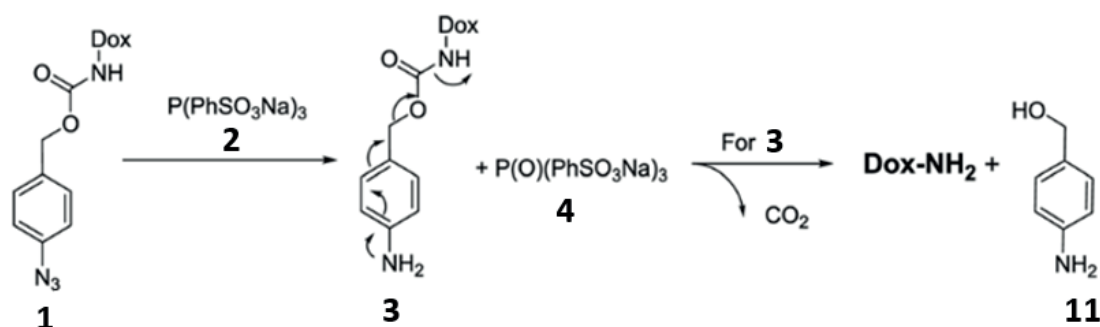


Figure 3. Staudinger reaction for the activation of the prodrug. Reprint with permission from reference¹⁸². Copyright 2019 Royal Chemical Society.

Guo et al. showed that conjugation of antibody and a fluorophore with a cleavable linker with azido group can be used to label the protein of interest.¹⁸⁸ After a treatment with a phosphine compound the intermediate released a fluorophore.

These reactions proved that reduction of azido group can be used for the activation of a prodrug. However, the reducing agent - phosphine used for this purpose can be easily oxidized in cell culture medium at 37°C. The fast oxidation was observed within the 4h. This issue limits the usage of phosphine to trigger the prodrug activation *in vivo*, as the control of its concentration is barely possible. Other drawback of this reaction is its reaction rate constant $k_2 = \sim 10^{-3} \text{ M}^{-1} \text{ s}^{-1}$ ¹⁸⁹ This means that to provide a reasonable half-life a high concentration of these two reactants has to be delivered.

Bertozzi et al. introduced a modification of Staudinger ligation, a Staudinger-Bertozzi ligation¹⁹⁰ Figure 3 where the reagent **1** and **2** reacted through click reaction forming amide **4** and releasing the **5**.

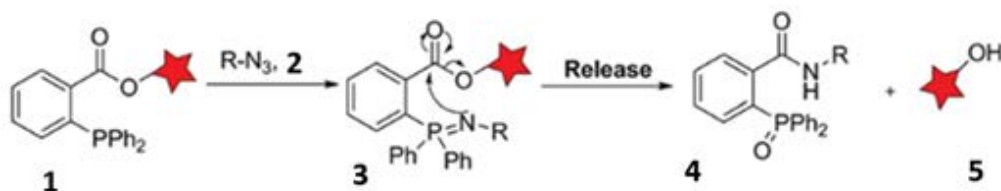


Figure 4. Staudinger ligation-based bond-cleavage reaction. Reprint with permission from reference¹⁸². Copyright 2019 Royal Chemical Society.

Gamble et al. introduced a new strategy to activate an azido group with trans-cyclooctene (TCO) without the usage of phosphine.¹⁹¹ The highly reactive TCO activated the azido prodrug (Figure 5) through the 1,3-dipolar cycloaddition and forms 1,2,3-triazoline, followed by nitrogen release and formation of aldimine, hydrolysis and 1,6-elimination.

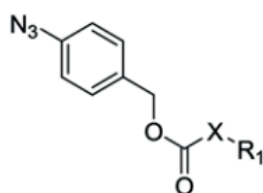


Figure 5. Azido prodrug. Reprint with permission from reference¹⁸². Copyright 2019 Royal Chemical Society.

The click reaction between TCO and azido compound is categorized by Sustmann's group¹⁹² as type-II 1,3-dipole cycloaddition in which an electron withdrawing group attached to the phenyl ring of azido prodrug (Figure 5) should decrease the LUMO energy level and thus the higher reaction rate could be achieved. It has been shown that k_2 increased from $0.017 \text{ M}^{-1} \text{ s}^{-1}$ to $0.110 \text{ M}^{-1} \text{ s}^{-1}$ when using fluoro-substitution.¹⁸² However, the introduction of fluoro group caused a slowdown in decaging of the intermediate compounds.¹⁹³ This type of reaction, compared to Staudinger reactions improved the activation of azido group by increasing the reaction rate and enhancing the stability of the activated compounds.¹⁸²

2.7.2 Reaction between tetrazine and benzonorbornadiene

The cycloaddition reaction between tetrazine and benzonorbornadiene was introduced in 2017.¹⁹⁴ This reaction (Figure 6) is combined with the elimination of nitrogen and the formation of intermediate 3, which in retro-Diels-Alder cycloreversion leads to the production of self-immolative isobenzofuran/isoindole intermediate, followed by CO₂ elimination and release of an active payload. The reaction rate constant between 1b and 2a-c was $0.190 \pm 0.029 \text{ M}^{-1} \text{ s}^{-1}$ in water. This second order rate constant was higher than present in Staudinger ligations $k_2 = \sim 0,001 \text{ M}^{-1} \text{ s}^{-1}$ and TCO and azido compounds $k_2 = 0.137 \text{ M}^{-1} \text{ s}^{-1}$.¹⁸²

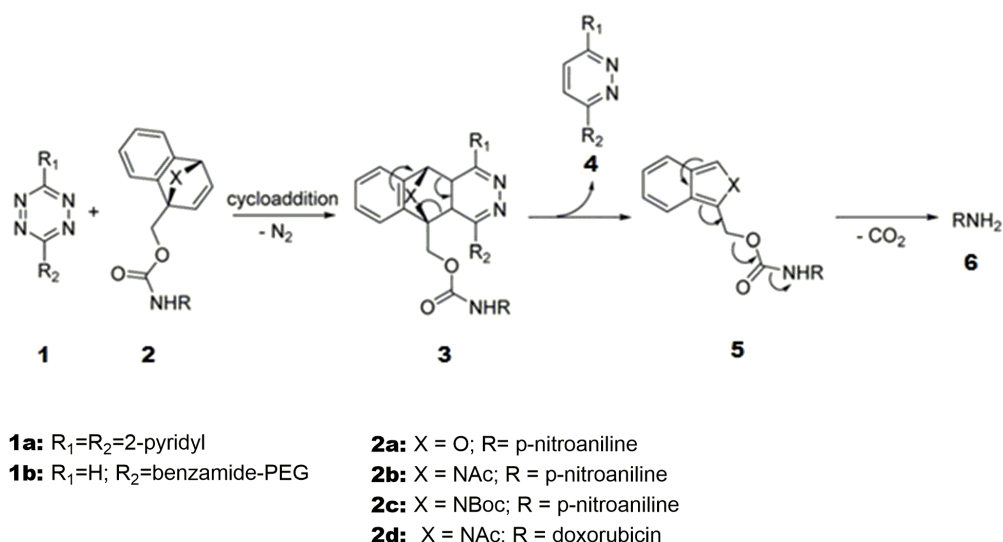


Figure 6. Cargos release from benzonorbomadiene derivatives due to tetrazine. Modified reprint with permission from reference¹⁸². Copyright 2019 Royal Chemical Society.

The reaction between 1b and 2d was studied for cancer treatment drug delivery.¹⁸² This reaction showed very fast release of a doxorubicin within 360min in a mixture of DMSO/PBS (1:1) at 37°C. No toxicity at 20µM was observed for the prodrug doxorubicin 2b and the stability in DMSO/PBS was noted for 48h.

2.7.3 Tetrazine/alkene reaction

The inverse-electron demand Diels-Alder (IEDDA) reaction between tetrazine and trans-cyclooctene (TCO) was found to be applicable for in vivo bioconjugation. This reaction yields stability in vivo but also is inert to other biological functionalities.¹⁵ Due to the very fast rate constant ($k_2 > 10^3 \text{ M}^{-1} \text{ s}^{-1}$)^{195, 196}, the reaction between trans-cyclooctene and s-tetrazines has gained much interest for use in nuclear medicine where the reaction rate and short-half lives are of priority consideration.¹⁹⁶ This reaction can undergo in aqueous conditions and thus fast due to the acceleration by the hydrophobic effect.¹⁹⁵ Several research groups have shown the application of TCO-conjugated antibodies and their reactions to tetrazine-payload to combat cancer cells.^{197, 198} The reaction between tetrazine and *trans*-alkene has been shown to be a very fast click reaction with a reaction rate which can be easily modified by using different functional groups attached to these compounds.^{199, 200, 201} There has been a lot of research done to use these two reagents to deliver drugs by using "click and release" reaction.²⁰² This reaction, reported in 2013 by Robillard et al., showed that the intermediate 1,4-dihydropyridazine 3 formed after cycloaddition between TCO and tetrazine.²⁰³ This can undergo two reactions: direct elimination or first tautomerization, which is then followed by a 1,4-elimination and ends up with the release of compound 6 and a payload compound R₁NH₂. This reaction has been employed for the doxorubicin delivery. Doxorubicin was modified with TCO. The resulting prodrug, which was incubated with 2b and 2c at 37 °C, led to very fast release within 4 and 6 minutes, respectively. It showed 55% release for 2b and 79% release for 2c. There was no release observed when prodrug was incubated alone in PBS or in serum, which proved the stability of the drug and the release driven explicitly by tetrazine.¹⁸² The fastest reaction of all tetrazines was reported between 1a and 2a, however, with a low doxorubicin release (only 7%). The low amount release was explained by the intermediate 4 and 5, which did not undergo further reactions. The doxorubicin-prodrug turned out to be about 100 times less toxic than a doxorubicin alone.

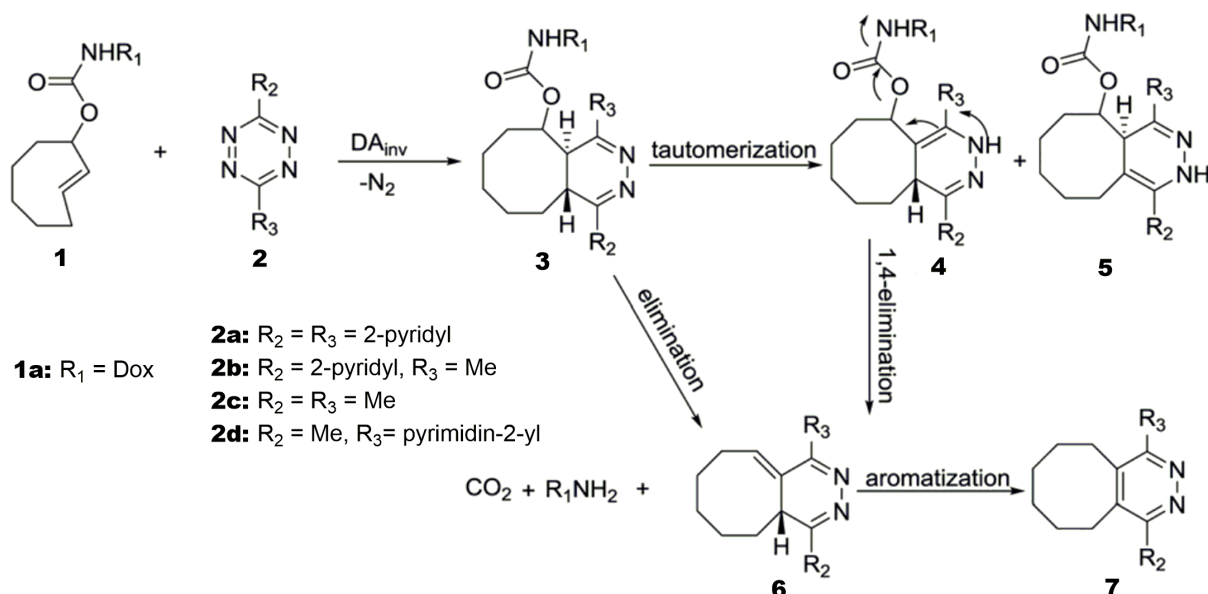


Figure 7. Inverse-electron-demand Diels-Alder reaction between trans-cyclooctene and tetrazine. Modified reprint with permission from reference¹⁸². Copyright 2019 Royal Chemical Society.

Chen et al. conducted a study with different substituents on the tetrazine ring.²⁰⁴ The electron withdrawing group (EWG) attached to the tetrazine improved the cycloaddition reaction constant rate and significantly and reduced the decaying rate. The introduction of electron donating group caused exactly the opposite effect for decaying reaction and did not improve the release yield. In order to achieve a balance between the cycloaddition reaction and the decaying rate, it was found that the use of these two groups was optimal for this purpose.

Weissleder et al. showed that the high release between 2c and 1 turned to be an artifact driven by the acidic conditions in HPLC.²⁰⁴ When this reaction performed in PBS at pH=7 the release yield after 6h of incubation was around 20%. It was thus proven that the payload release improved in an acidic environment. In response to this, they began to synthesize tetrazine with carboxylic acid groups. The addition of carboxylic group protonates the dihydropyridazine nitrogen which leads to enhanced tautomerization to dihydropyridazine followed by 1,4-elimination (Figure 8B). The introduction of two carboxylic groups on the tetrazine 2f (Figure 8A) showed almost complete release in PBS at pH=7, only trace elements of dead-end product for 2e-g was observed. The low release yield of 2c was related to the formation of a dead-end product (Figure 8C). The dead-end product coming from the intramolecular nucleophilic addition of the amidic nitrogen has no further possibility to decage the payload. To avoid the intramolecular cyclization which leads to the dead-end product formation a methyl group (3c) was introduced on the amidic nitrogen. This structure incubated in PBS with tetrazine 2c achieved a complete release.

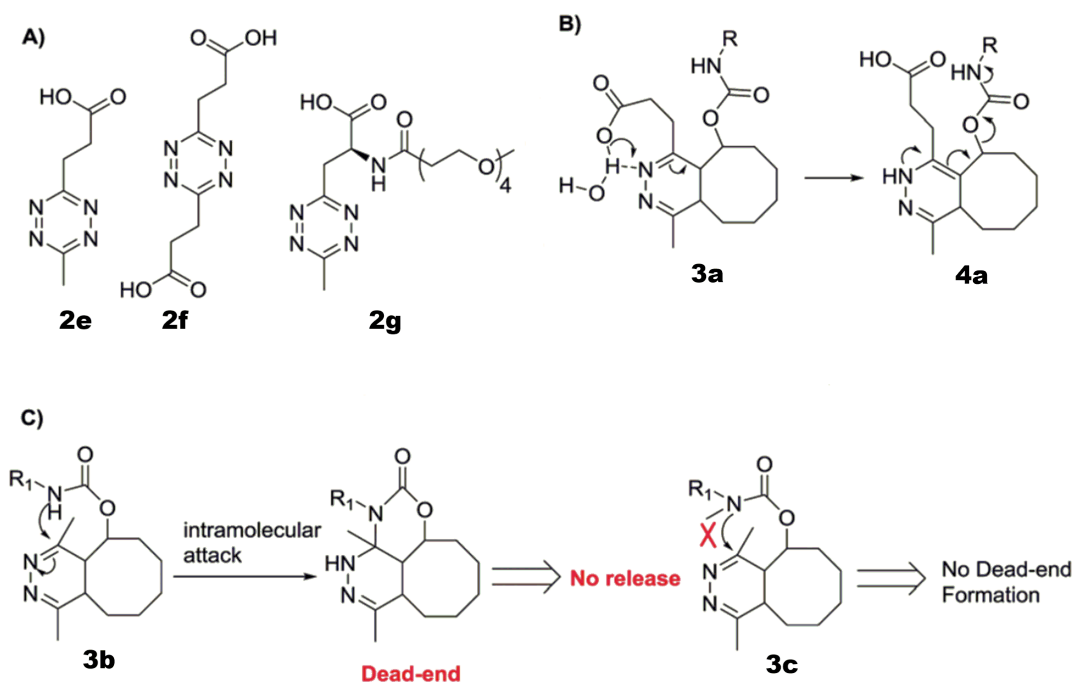


Figure 8. Dihydropyridazine intermediate (un)release mechanisms. (A) different tetrazine derivatives, (B) Intramolecular acid assisted elimination proposed mechanisms (C) The dead-end product formation. Modified reprint with permission from reference¹⁸². Copyright 2019 Royal Chemical Society.

Royzen et al. used this chemistry to image-guided prodrug activation.²⁰⁵ For that iron oxide nanoparticles (MNPs) modified with tetrazine fluorescent dye were used. The doxorubicin was modified with TCO into a prodrug 1a (Figure 7). The dye was used for MNPs tracking *in vitro* and *in vivo*. The specific localization of the nanoparticles in MDA-MB-231 breast cancer cells was confirmed. The presence of the MNPs in the tumor cells efficiently converted the doxorubicin prodrug into an active drug, which helps the dosing of the prodrug 1a. Next, the same group have introduced a new concept of biorthogonal chemistry to concentrate and activate drug at the desired location.¹⁵ In order to simply the tetrazine delivery to the targeted site and at the same time protect it from the washed out from the desired place, the alginate hydrogels were modified with tetrazine (HMT). Thus, the release of a TCO-prodrug at the location of choice (e.g. tumor) depends on the presence of the HMT. Royzen et al. demonstrated *in vivo*, in mice bearing fibrosarcoma a significant therapeutic benefit of prodrug doxorubicin released from HMT injected in the proximity of soft tissue sarcoma. The tumor was observed and after 2 weeks from the last therapy in both group TCO-doxorubicin and doxorubicin the tumor was not detectable in both groups. However, after 30 days the tumor size in the group treated with doxorubicin regrowth and was measured to have the volume of 2000 mm³, whereas the median tumor size for TCO-doxorubicin group remained furthermore not detectable.

2.8 Non-antibiotic-based strategy to elimination of biofilm-based infections

Photodynamic therapy (PDT) has found an application in the antimicrobial treatment due to the increasing number of antibiotic resistances. The microorganism killing effect of the photosensitizers (PS) is based on the generation of reactive oxygen species that eradicate pathogens by an oxidative burst.²⁰⁶

A light source activates the PS. There are 3 light sources for the PDT: lasers, light-emitting diodes (LEDs), and gas-discharge lamps.^{207, 208} In recent years, intensive research has been carried out for new PS and energy sources.²⁰⁶ Many different PS have been used and include

phenothiazinium derivatives, such as toluidine blue, which have shown inhibitory properties for *S. aureus*.²⁰⁹ Porphyrin, chlorine, and phthalocyanine derivatives have also been applied. The chlorine e6 can eliminate bacterial infection of *S. aureus* and *E. coli* and has excellent biocompatibility.²¹⁰ Curcumin, which is a component of the curcuma longa rhizome, is used to treat inflammation and has been found as well to have antimicrobials and antioxidants.^{211, 212} Most of these compounds are first used to deactivate planktonic bacteria. The most common method used is the screening method of many compounds to later select PS, which are suitable for further chemical modification in order to improve their antimicrobial efficacy.²¹³

2.9 Polymethyl methacrylate (PMMA) bone cement commonly used in the clinic to combat biofilm-based infections

The acrylic bone cement which are impregnated with antibiotics have been widely applied in the clinic for the treatment of musculoskeletal infections.²¹⁴ The cements are used in two forms: beads impregnated with antibiotics or spacers.²¹⁵ Spacers loaded with antibiotics have found the application in the knee and hip arthroplasty.^{216, 217} The choice of antibiotics used in the PMMA cement bones have to be carefully made. There are many criteria antibiotic has to fulfil in order to qualify as a good candidate for the incorporation into PMMA. Among others: the thermal stability of the antibiotic is a key property as the polymerization of the PMMA is related to production of high temperatures. Moreover, antibiotic has to be available in a powder form and ideally has a broad antibacterial spectrum. Additionally, the amount of the antibiotic and its release properties from the cements are crucial for the success of the therapy. For the eradication of methicillin sensitive or resistant infections PMMA spacers with gentamicin and vancomycin are recommended.²¹⁴

If the pathogen of the periprosthetic joint is known, the PMMA cements can be used as a specific treatment of that pathogen. They can also be applied for the prophylaxis, where the pathogen is not known and the antimicrobial treatment is then considered as non-specific. There are already industrial preparations of PMMA bone cements premixed with antibiotics. The antibiotic however can also be mixed preoperatively with the bone cement.²¹⁸

The PMMA bone cement can be used for a treatment of hip and knee arthroplasty infections. In this case they are used to improve the antibiotic delivery, stabilize the skeleton. They are used in the period between removal of an infected implant and insertion a new implant. The antibiotic spacers stays at the place of previously removed infected implant and by delivering the antibiotic in the surrounding tissue heal the infection.²¹⁸

The antibiotic-based PMMA bone cements are commonly use in the clinic, however little is known about fungal-impregnated PMMA bone cements and there is no such cement available on the market with the industrial premixed antifungals. There is also little known about fungal PJI treatment.²¹⁹ *Candida* PJI are rare but they but they are a very big threat to the patient's life.²²⁰ Therefore more investigation and research is needed in this direction.

3. SCIENTIFIC GOALS

3.1 Bio-Orthogonal chemistry-based reloadable biomaterial to enhance the treatments against *Staphylococcus aureus* infections

The theoretical part indicates that in the implant-associated infections there is no optimal strategy yet to protect the implant from bacterial colonization for the entire time the implant is located in the human body. The most common strategy in the implant infections treatment, and so far, the only one recognized worldwide, is to remove the infected implant, followed by antimicrobials administered intravenously which can be facilitated with combination of local antibiotics release from bone cements.

The first big aspect is the lack of a method that would facilitate the antibiotic local delivery which can lead to the eradication of matured biofilm without removing the infected implant.

Therefore, the main objective of this PhD work is to address the first aspect, which will be based on the development of a method that can facilitate the eradication of biofilms without removing infected implants and the development of a coating that can be loaded with antimicrobials after placing the implant in the human body.

Following the successful drug delivery approaches in the biorthogonal chemistry and keeping in mind how different substituents influence the click and release reaction, in this PhD thesis the inverse-electron demand Diels-Alder (IEDDA) reaction was used to develop a new strategy for combating biofilm associated infections and the results are reported at ACS Central Science.²⁰² The technology presented in this PhD thesis utilizes an implantable biomaterial (tetrazine-modified alginate hydrogel) and prodrugs formed by conjugating *trans*-cyclooctene (TCO) groups to antibiotics. Using the inverse electron demand Diels-Alder reaction between tetrazine and TCO the antibiotic's therapeutic index can be increased and allows a higher quantity of the antimicrobial to reach the bacterial infection site (Figure 9).

Two FDA-approved antibiotics were used: vancomycin and daptomycin. Both antibiotics are used in the treatment of *S. aureus* infections, including MRSA. Vancomycin as a "last resort" antibiotic is used in exceptional situations, including the elimination of planktonic bacteria that surround the infected implant.²²¹ It is used to combat gram-positive bacteria and the mode of action is very well known. This tricyclic glycopeptide inhibits the synthesis of bacterial cell wall^{221, 222} However, the use of vancomycin is limited because of the side effects associated with its use, such as tachycardia, nephrotoxicity and hypotension.²²³ The second antibiotic, cyclic lipopeptide daptomycin has a narrow therapeutic window: 6 mg/kg to control *S. aureus* bloodstream infections.²²⁴ The mode of action of this antibiotic is not as well-known as vancomycin, although it is known that calcium ions are needed for the antibiotic to have an impact on bacteria in order to oligomerize for permeabilization and cell membrane depolarization of the bacteria.²²⁵ Daptomycin is also used to control *S. aureus* biofilm infections, thus it is good to use it against implanted associated infections.²²⁶ However, daptomycin have shown side effects related to the use of high concentrations²²⁷ and limited biodistribution.²²⁸ Therefore, in this PhD thesis these two antibiotics were selected to increase their activities against *S. aureus* infections. Both antibiotics were modified to prodrugs with TCO and their release from hydrogel modified with tetrazine (HMT) and activity against MRSA and methicillin-sensitive *S. aureus* (MSSA) were investigated *in vitro* and *in vivo*.

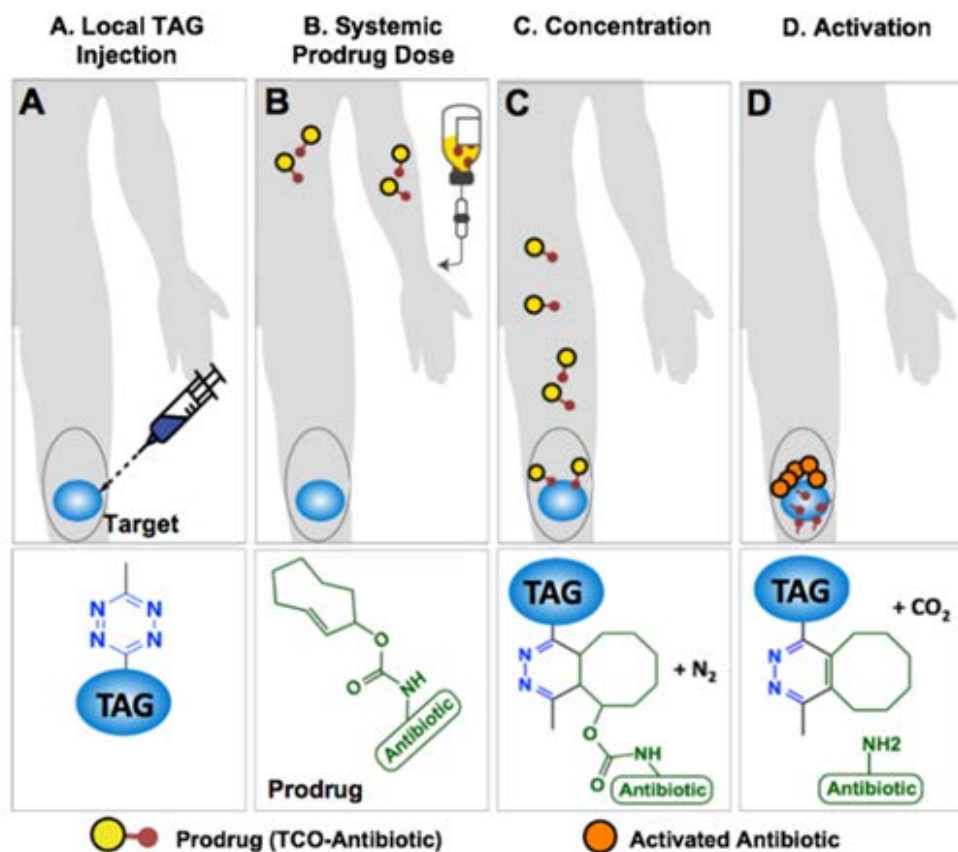


Figure 9. The click-chemistry strategy for concentration and activation of pro-drug antibiotic which are injected systemically. (A) implantation of the Tz modified alginate gel (TAG) at the infection site. (B) Intravenous injection of a pro-drug antibiotic (C) when the prodrug and the TAG come in contact, the IEDDA reaction enhances the amount of antibiotic present near the infected site. (D) Spontaneous isomerization of the cycloaddition product, following by the CO_2 release and an active antibiotic. Reprint with permission from reference²⁰². Copyright 2018 American Chemical Society.

3.2 Mussel-inspired polyglycerol combined with bio-orthogonal chemistry - as a coating strategy for implant associated infections

The antimicrobial coating strategy has been a subject of extensive research. However, these type of coatings have some limitations. The pathogen that is being fought against must be well diagnosed before implant with antibiotic coating can be inserted into the patient's body. Once the antibiotic is released, implant remains without protection from bacteria. Coating based on release of ions, nanoparticles often have tissue toxicity problems and cannot be applied to all patients.

Therefore, the second aspect that has been addressed in this PhD thesis utilizes the same bio-orthogonal chemistry as for biomaterials described above. This chemistry was used for the titanium coating where the loading of antibiotics can be done after the implant insertion into the human body (Figure 10).

A. Implantation of the tetrazine-coated prosthesis	B. TCO modified antimicrobial injected intravenously	C. Concentration of the prodrug on the implant	D. Activation and release of the antimicrobial and on the implant
----------------------------------------------------	------------------------------------------------------	------------------------------------------------	-------------------------------------------------------------------

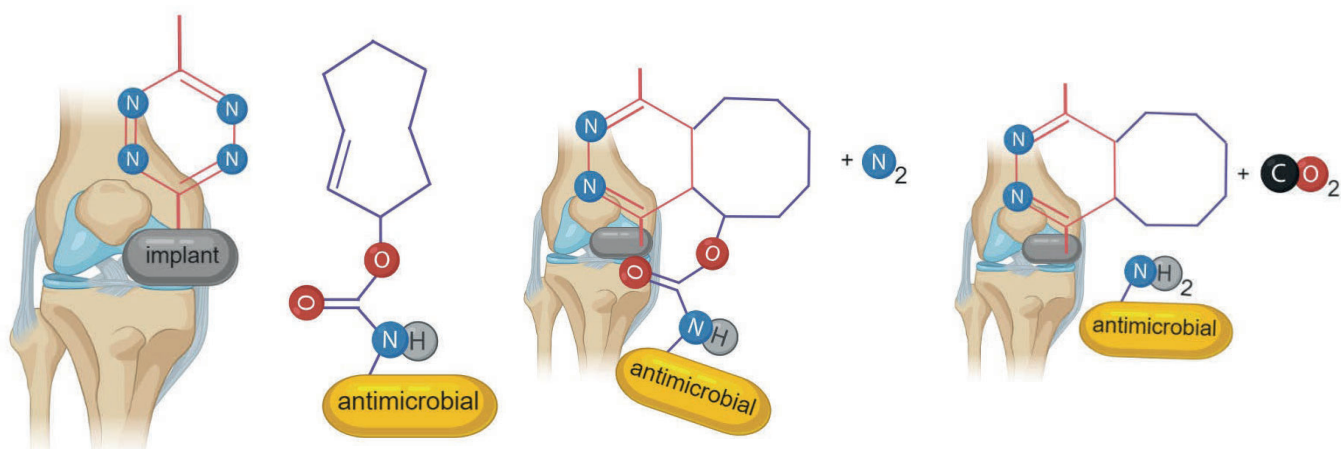


Figure 10. IEDDA-based titanium antimicrobial coating that concentrates, activates and releases intravenously infected prodrug antimicrobial. (A) The tetrazine-coated prosthesis is implanted in the infected area, (B) prodrug injected systemically, (C) prodrug covalently reacts with the coated implant, (D) The spontaneous isomerization and the release of active drug. TCO: *trans*-cyclooctene.

A tetrazine-based coating was developed. The coating for the titanium surface composes of mussel inspired polyglycerol dendritic polymer (MI-dPG) modified with tetrazine. MI-dPG mimics the properties and composition of the mussel foot proteins.¹⁴⁰ The mussels attach very quickly to any type of surface under water using mussel foot proteins (mfp-1 and mfp-5)-rich byssus.²²⁹ Both proteins contribute to surface adhesion due to lysines and 3,4-dihydroxyphenyl-L-alanine (DOPA) which interact with the surface through covalent or noncovalent bonds.^{230, 231} The amino groups in lysines crosslink each other or coordinatively crosslink with Fe³⁺ ions, which leads to byssus solidification.²³² MI-dPG is a heteromultivalent catechol- and amine-functionalized dendritic polymer which mimic the mfp-1 and mfp-5 in their functional groups, structure and molecular weight.¹⁴⁰ The MI-dPG has a similar molecular weight to the mfp-5, about 10 kDa.²³³ Due to high molecular weight as well as multivalent functional groups this polymer can form within minutes strong and stable coating.¹⁴⁰ The dopamine and its derivatives adhere to different type of surfaces, without a necessity of surface modification.^{234, 235} The coating is driven by covalent and coordinative crosslinking.²³⁶ It is a universal coating for virtually any type of surface. The catechols within the polymer were used in this work for covalent attachment to the titanium surface, amino groups used for covalent attachment of tetrazine to the coating with the goal of spatiotemporal delivery of the antibiotics to the coated surface. In this project the release of the prodrug daptomycin from the tetrazine-MI-dPG coating was tested, the activity of the released drug against MRSA was investigated, stability of the coating and biocompatibility and cytotoxicity against mouse myoblasts and human osteoblasts was examined.

3.3 PMMA bone cements with antifungals

Another aspect are the currently used PMMA bone cement spacers for treatment of bone and implant-associated infections. The PMMA commonly include only antibiotics, there are no commercially available bone cements with antifungals.

In this project different antifungal amphotericin B (AmB) formulations were evaluated in regard to PMMA bone cement incorporation. There are two available AmB formulations: non-liposomal sodium-deoxycholate and liposomal AmB. They were compared with a new formulation: non-liposomal N-methyl-D-glucamine/palmitate AmB. The reason for testing the new antifungal formulation was that the AmB deoxycholate is hardly water soluble and has a limited usage due to toxicity. Liposomal formulation due to its large amount of liposomal powder might negatively influence the mechanical properties of PMMA bone cements. The antifungals were incorporated in the PMMA bone cements by mixing the methyl methacrylate powder and monomer liquid (N,N-Dimethyl-p-toluidin) and letting the materials polymerize at room temperature. Thus, the PMMA formed cylinders have been studied for several aspects: whether there is a release of the antifungal from the material, whether the released drug is active against *Candida* biofilm, how the introduction of the antifungal into PMMA affects the compressive strength, density and porosity of the PMMA material, whether the new AmB formula might be an alternative candidate for PMMA incorporation, additionally an addition of poragen was studied.

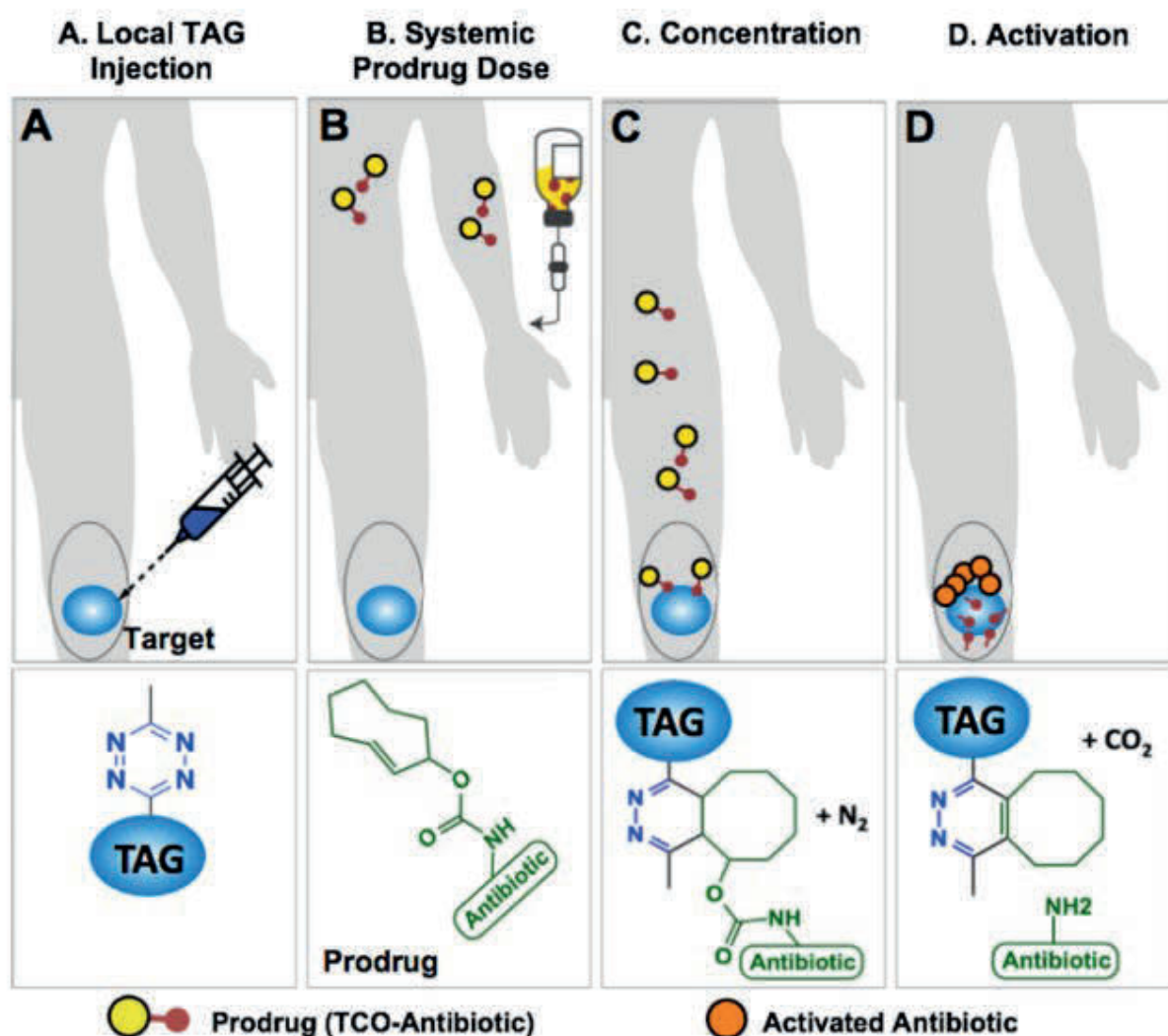
3.4 Photodynamic-based strategy for bacterial eradication

Finally, from the theoretical part, it is clear that the treatment currently used is mainly based on antibiotics. Inadequate application of antibiotics might increase the risk of resistance development. Therefore, in this project, a photosensitizer curcumin was chosen as an antimicrobial agent. As a material for curcumin incorporation a hydrogel was chosen. The hydrogel is a recognized material for wound dressing and can maintain a moist environment at the healing site. Such a highly hydrated environment can accelerate the development of pathogens and also facilitate their attachment on biomaterials. Therefore, in this project, hybrid hydrogel-containing graphene oxide was used which was loaded with an antimicrobial compound. This hydrogel has electro-responsive properties that offer highly tunable drug releasing conditions. A curcumin, which is a natural ingredient of *Curcuma longa* and a photosensitizer used in antimicrobial photodynamic therapy, was chosen as an antimicrobial agent. We applied electrical stimulations with a range of 0 to 48 V voltage and examined the response of the hydrogel. We also investigated the kinetic characterization and evaluated the curcumin release and its activity against methicillin-resistant *S. aureus*. Additionally, we tested the response and viability of human fibroblast cells.

4. PUBLICATIONS AND MANUSCRIPTS

In the following section, the scientific outcomes of this PhD thesis are listed, and the contributions of the authors are specified.

4.1 Bio-Orthogonal Chemistry and Reloadable Biomaterial Enable Local Activation of Antibiotic Prodrugs and Enhance Treatments against *Staphylococcus aureus* Infections.



Czuban M, Srinivasan S, Yee NA, Agustin E, Koliszak A, Miller E, Khan I, Quinones I, Noory H, Motola C, Volkmer R, Di Luca M, Trampuz A, Royzen M, Mejia Oneto JM. ACS Cent Sci. 2018 Dec 26;4(12):1624-1632. doi: 10.1021/acscentsci.8b00344. Epub 2018 Dec 12.

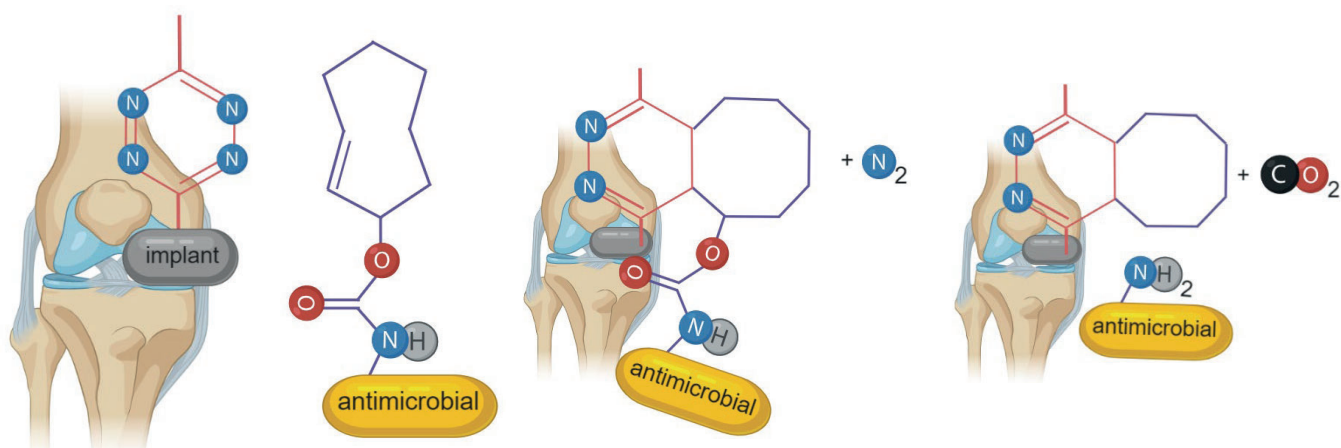
<https://doi.org/10.1021/acscentsci.8b00344>

Author contributions:

Czuban M. developed and designed the microbiological assay which enable to test the bioorthogonal-based biomaterial strategy in the isothermal microcalorimeter, co-synthesized TCO-daptomycin and TCO-vancomycin, performed the main microbiological experiments, co-wrote the paper.

4.2 Titanium coating by combining concepts from bio-orthogonal chemistry and mussel inspired polymer enhances antimicrobial activity against *Staphylococcus aureus*.

A. Implantation of the tetrazine-coated prosthesis	B. TCO modified antimicrobial injected intravenously	C. Concentration of the prodrug on the implant	D. Activation and release of the antimicrobial and on the implant
----------------------------------------------------	------------------------------------------------------	------------------------------------------------	-------------------------------------------------------------------



Czuban M., Kulka M.W, Wang L., Koliszak A., Achazi K., Schlaich C., Donskyi I., Di Luca M, Jose M. Mejia Oneto, Maksim Royzen, Rainer Haag, Andrej Trampuz, *in submission

Author contribution: Czuban M. designed the project, performed the main experiments, wrote the publication.

Titanium coating by combining concepts from bio-orthogonal chemistry and mussel-inspired polymer enhances antimicrobial activity against *Staphylococcus aureus*

Magdalena Czuban*, Michaël W. Kulka, Lei Wang, Anna Koliszak, Katharina Achazi, Christoph Schlaich, Ievgen S. Donskyi, Mariagrazia Di Luca, Jose M. Mejia Oneto, Maksim Royzen*, Rainer Haag*, Andrej Trampuz*

M. Czuban, M. W. Kulka, Dr. K. Achazi, Dr. C. Schlaich, I. Donskyi, Prof. R. Haag
Institute of Chemistry and Biochemistry, Freie Universität Berlin, Berlin, Germany
E-mail: magdalena.czuban@charite.de; haag@zedat.fu-berlin.de

M. Czuban

Berlin-Brandenburg School for Regenerative Therapies, Berlin, Germany

L. Wang, Assist. Prof. A. Trampuz

Charite Universitätsmedizin, Centrum für Muskuloskeletale Chirurgie, Berlin, Germany

E-Mail: andrej.trampuz@charite.de

Dr. M. Di Luca, A. Koliszak

Berlin-Brandenburg Center for Regenerative Therapies, Berlin, Germany

Dr. J. M. Mejia Oneto

Shasqi Inc., San Francisco, United States

Prof. Maksim Royzen

University at Albany, Department of Chemistry, Albany, New York, United States

E-mail: mroyzen@albany.edu

I. Donskyi

BAM—Federal Institute for Material Science and Testing Division of Surface Analysis and Interfacial Chemistry, Berlin, Germany

Abstract

Implant-associated infections present serious complications for patients. The implant surfaces colonized by bacteria lead to prolonged hospitalization due to patient immobilization and extended antibiotic treatments that sometimes lead to liver or kidney toxicity. In this work, we describe the inverse-electron-demand Diels-Alder reaction and hydrolytic release between mussel-inspired, dendritic tetrazine-coated titanium prosthetic materials and *trans*-cyclooctene modified daptomycin used against methicillin resistant *Staphylococcus aureus*. Characterization of the materials' properties revealed that it is hydrophobic, non-toxic, and stable for prolonged periods of time. The coating is functionalized with tetrazine and is capable of transforming a prodrug of daptomycin to the active drug. We envision that this material will be able to improve the treatment of implant-associated infections by concentrating systemically administered antibiotic prodrugs, and increasing the local concentration of active drug, thus converting the prodrugs into localized medicines.

1. Introduction

The orthopedic implant-associated infections (OIAI) cause devastating post-surgical complications.^[1] Despite of enormous progress of modern medicine and the use of laminar-flow systems in operating rooms, surgical site infections cannot be prevented completely in today's hospitals.^[2] About 5% to 10% of all inserted internal fixation devices cause implant-associated infections. The incidence may even exceed 30% after fixation of grade 3 open fractures.^[3] Despite considerable progress in prevention and treatment of OIAI, the absolute number of patients with such infections continues to rise due to the lifelong risk of bacterial seeding on the implant and aged patients requiring joint replacement.^[4]

OIAI originates from the free-floating bacteria that colonize the titanium surface of surgical implants and over time evolve as a biofilm infection. As the result, treatment of OIAI is extremely difficult as biofilm embedded bacteria are more resistant to conventional antibiotics than their planktonic counterparts.^[2,5,6] *Staphylococcus aureus* is one of the most common OIAI pathogens^[3,7] and methicillin-resistant *Staphylococcus aureus* (MRSA) is of particular concern.^[8] OIAI treatment with

conventional systemically injected antibiotics is not sufficient as they not reach their intended targets in large enough concentrations, but instead spread throughout the body. Due to the lack of specificity for the pathological site, large doses are required to achieve effective therapeutic concentrations. This leads to frequent dosing, systemic side effects, and toxicity and could potentially lead to the development of multi-drug resistance of the respective pathogen.^[9,10]

Antimicrobial coatings have been developed to overcome bacterial colonization of titanium surfaces. They include silver-based coatings that, due to toxicity concerns, have been limited to patients with high postoperative risks.^[11] Also, several vancomycin-releasing materials have been described in recent literature.^[12] Thompson et al. described a gentamicin releasing calcium-phosphate coating on titanium aluminum-niobium. However, all of these examples predetermine the antimicrobial treatment at the time of implantation. This is potentially problematic, as the treatment cannot be modulated or altered at the outset of OIAI. Ideally, the treatment should be determined at the time of an infection and the dosage adjusted based on therapeutic need.

In this work, we describe the development and characterization of a mussel-inspired tetrazine-functionalized surface coating, which is non-toxic, hydrophobic, and stable. The material is capable of activating a prodrug of daptomycin via bio-orthogonal inverse-electron demand Diels-Alder chemistry.^[13] We describe the synthesis of the coating and detailed characterization of its properties. Our long-term vision is that this material will be capable of converting systemically administered antibiotic prodrugs into active local medicines. In the event of OIAI, the modified prodrug of daptomycin will be systemically injected. It would circulate through the body in its inactive prodrug form. Upon binding the tetrazine-functionalized prosthetic surface, the prodrug will be transformed to the active daptomycin, thus locally targeting the infection. In this way, an efficient and modular spatiotemporal delivery of therapeutics will be achieved.^[14]

2. Results and Discussion

Our group previously developed a mussel-inspired dendritic polyglycerol (MI-dPG) as versatile material for surface functionalization. We have previously shown that MI-dPG can attach to virtually any surface within a short period of time. It is a stable coating that can be further functionalized with small molecules or nanoparticles.^[15-18] MI-dPG mimics the properties and composition of the mussel-foot proteins.^[19] The mussels attach very quickly to any type of surface under water using mussel foot proteins (mfp-1 and mfp-5)-rich byssus.^[20] Both proteins contribute to surface adhesion due to lysines and 3,4-dihydroxyphenyl-L-alanine (DOPA), which interacts with the surface through covalent or noncovalent bonds.^[21,22] The amino groups in lysines by crosslinkage with each other or coordinative crosslinkage with Fe³⁺ ions lead to byssus solidification.^[23] MI-dPG is a heteromultivalent catechol- and amine-functionalized dendritic polymer which mimics the mfp-1 and mfp-5 in their functional groups, structure and molecular weight.^[19] The MI-dPG has a similar molecular weight to the mfp-5, about 10 kDa.^[24] Due to high multiplicity of functional groups, this polymer can form strong and stable multivalent coatings within minutes.^[19] The dopamine and its derivatives adhere to different type of surfaces, without a necessity of surface modification.^[25,26] The coating is driven by covalent and coordinative crosslinking.^[27]

The role of the MI-dPG is dual, while the catechol groups are important for the anchoring on the titanium surface; the amino groups of MI-dPG are used for attaching a bio-orthogonal group, tetrazine (Tz). Through this modification, the titanium surface will be converted into a functional material capable of activating systemically administered antibiotic prodrugs, as illustrated in Figure 1. The strategy is related to our recent report, describing local activation of systemically administered prodrugs using bio-orthogonal chemistry.^[13,28] The strategy will involve the Tz-modified titanium surface (MI-dPG-PEG-Tz) and a daptomycin prodrug created with a modification with *trans*-cyclooctene group (pro-dapto). The systemically administered pro-dapto will react with MI-dPG-PEG-Tz and will locally activate daptomycin on the titanium surface.

A. Implantation of the tetrazine-coated prosthesis	B. TCO modified antimicrobial injected intravenously	C. Concentration of the prodrug on the implant	D. Activation and release of the antimicrobial and on the implant
----------------------------------------------------	------------------------------------------------------	------------------------------------------------	-------------------------------------------------------------------

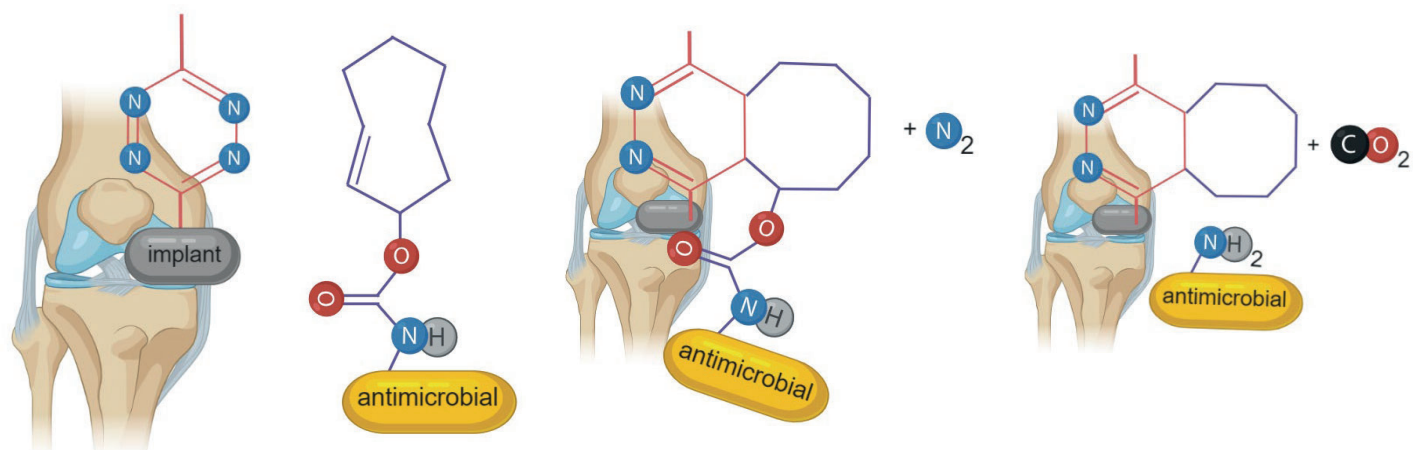


Figure 1. IEDDA-based titanium antimicrobial coating, which concentrates, activates, and releases intravenously injected prodrug antimicrobial. (A) The tetrazine-coated prosthesis is implanted in the infected area, (B) the prodrug is injected systemically, (C) prodrug covalently reacts with the coated implant, and (D) the spontaneous isomerization and the release of active drug. TCO: *trans*-cyclooctene.

2.1 Synthesis of MI-dPG-PEG-Tz

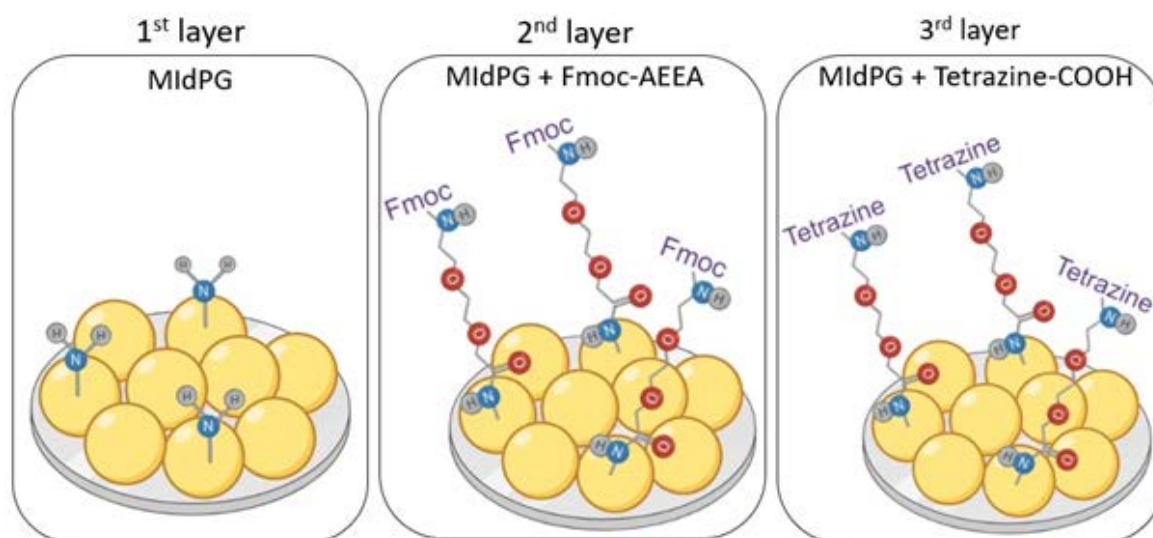


Figure 2. Coating steps for titanium coating with MI-dPG-PEG-tetrazine coating.

MI-dPG-PEG-Tz was synthesized in three steps illustrated in Figure 2. MI-dPG was synthesized following the procedure previously reported by our group.^[19] Coating of the first layer was carried out over 16 h, by treating each side of the titanium surface with a methanolic solution of MI-dPG and MOPS (pH 8.5). After subsequent washes, Fmoc-protected PEG was coupled as the second layer. The Fmoc groups were cleaved with 20% piperidine in DMF. Lastly, tetrazine was installed using HATU as a coupling reagent. The detailed synthetic procedures are described in the experimental section.

2.2. Cytocompatibility

2.2.1 Cell toxicity

The MI-dPG-PEG-Tz titanium coating, in conjunction with pro-dapto treatment, is non-toxic to myoblast cells and human osteoblasts cells. This was assessed using a cell counting kit-8 (CCK-8) cell viability assay. As illustrated in Figure 3, there was no significant difference in the viability of C2C12 cells treated with titanium, MI-dPG-PEG-Tz, or MI-dPG-PEG-Tz + pro-dapto. The cell viability was 83% in the presence of MI-dPG-PEG-Tz and 81% in the presence of MI-dPG-Peg-Tz coating previously incubated with pro-dapto. As shown in Figure 4, the MI-dPG-PEG-Tz-coated material reduced the osteoblast cells viability by 4% relative to titanium material. Meanwhile, MI-dPG-PEG-Tz + pro-dapto showed a cell viability reduction of 6%. The small reduction of cell viability has been attributed to the excessive growth of osteoblasts on titanium surface. Cell proliferation in medium has comparable viability (non-treated control), 96% and 94% for the MI-dPG-PEG-Tz and MI-dPG-PEG-Tz + pro-dapto respectively (Figure 3).

By contrast, some of the already developed silver coatings have been known to have toxicity. In fact, the broad spreading of the AgNPs coating started a debate on the toxicity of these types of coatings.^[29] A relevant toxic effect on gall bladder and midzonal hepatocellular necrosis in mice have been shown using 10 nm AgNPs size coatings, independently from the type of coating. The small AgNPs have enhanced tissue distribution and therefore found in most of the mice organs.^[29] Wentong Lu et al. reported a toxic effect on human HaCaT keratinocytes when the AgNPs citrate-coated powder was used.^[30] It has also been presented that toxicity of silver acetate and polyvinylpyrrolidone-stabilized AgNPs showed the same toxic effect against bacteria, as well human mesenchymal stem cells (hMSCs), and peripheral blood mononuclear cells. There were also controversial results doubting in the antimicrobial properties of the silver coatings that showed no significant difference between titanium coating with silver and uncoated materials.^[11]

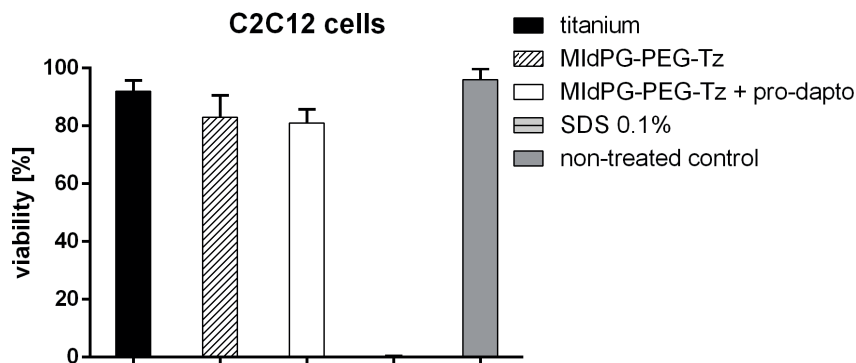


Figure 3. Viability of the C2C12 mouse myoblasts cells after cultivation with CCK-8 kit. Statistical analysis was performed using one-way ANOVA analysis. The samples were performed in triplicates; the error bars represent standard error measurement.

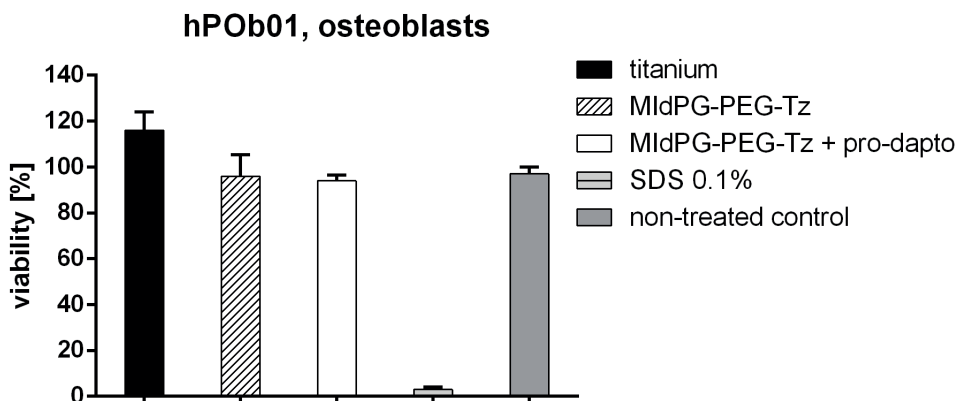


Figure 4. Viability of the osteoblast cells after cultivation with CCK-8 kit. The samples were performed in triplicates; the error bars represent standard error measurement.

2.2.2 Osteoblast adhesion

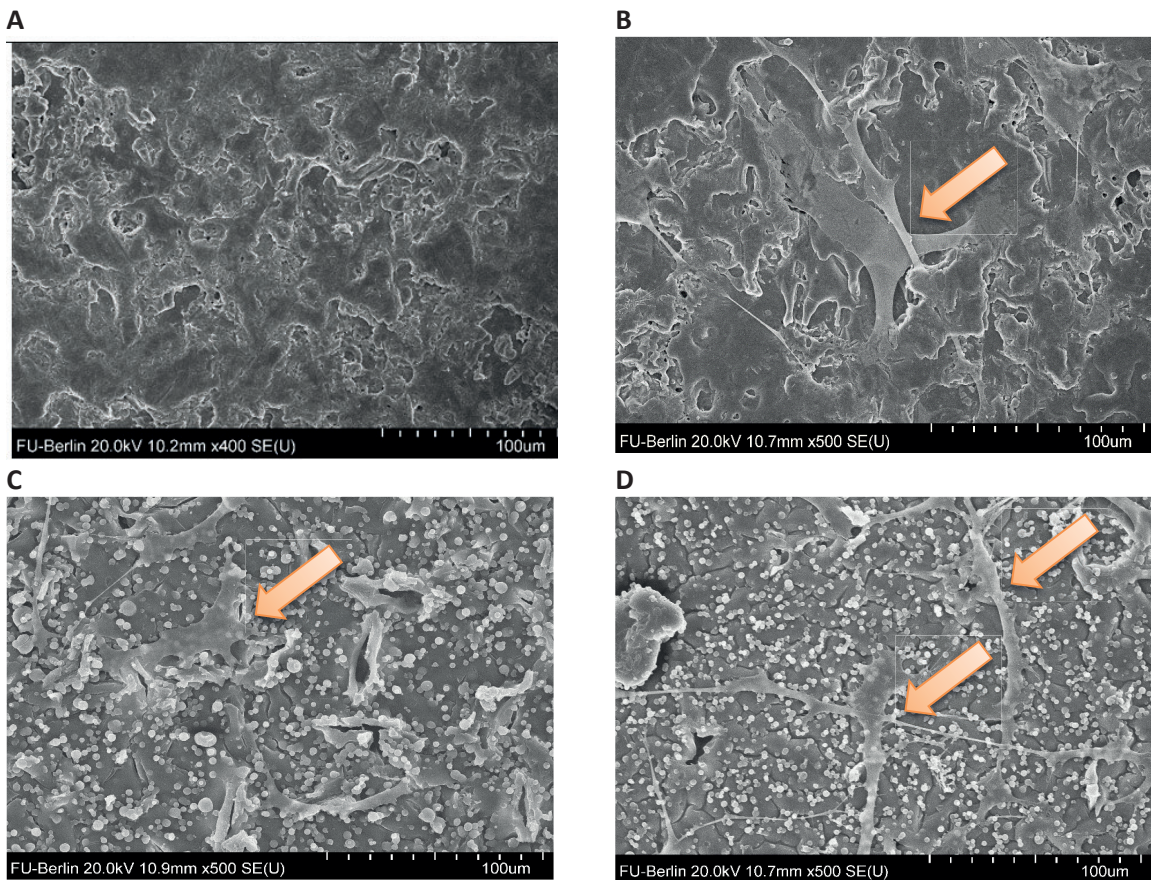


Figure 5. SEM pictures of the materials showing the attachment of the cells to the material's surface. The arrows indicate proliferated osteoblast cells. (A) Titanium without osteoblasts, (B) titanium with osteoblasts, (C) titanium coated with MI-dPG-PEG-Tz, and (D) titanium coated with MI-dPG-PEG-Tz and treated with pro-dapto for 1 h, prior to osteoblast experiment.

The morphology of osteoblasts and the attachment of the cells to the materials were analyzed using scattering electron microscopy (SEM). The osteoblasts were fixed after 24 h incubation, prior to SEM analysis. The results confirmed that the experimental materials did not create toxic microenvironment that prevented healthy cell growth. Figure 5A shows SEM images of the titanium surface without proliferated cells. Figure 5B shows growth of osteoblast cells on the untreated titanium surface. As indicated by the arrow, the attached cells had a healthy cellular morphology, the cells grew equally, and showed elongated cell bodies. The cells attached to the MI-dPG-PEG-Tz surface, shown in the Figure 5C, also represented a healthy morphology. Treatment with pro-dapto also had minimal effect on the healthy cell growth, as shown in Figure 5D. These results were complementary to the cell viability assays, confirming that MI-dPG-PEG-Tz surface and pro-dapto treatment were non-toxic to the cells.

2.3. Release kinetic results

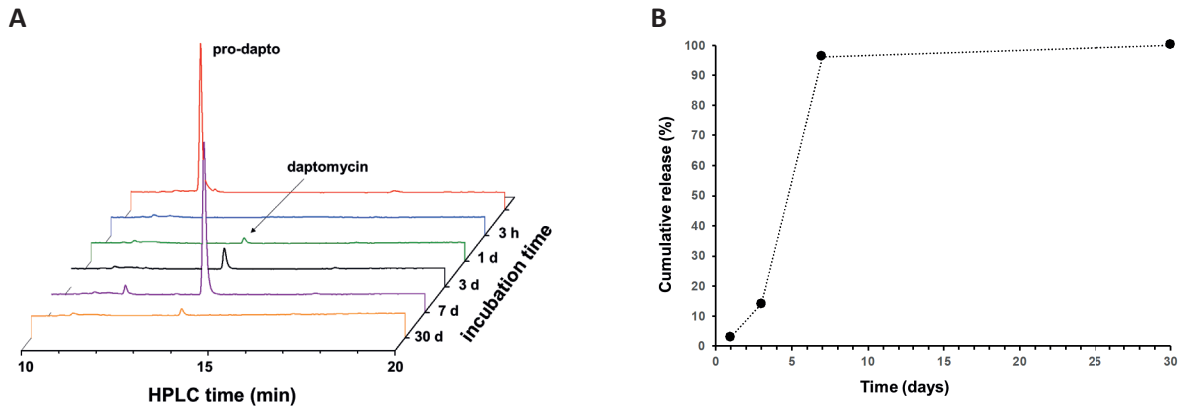


Figure 6. Release kinetic of a prodrug (A) HPLC analysis of supernatant and (B) cumulative release.

Activation of pro-dapto was tested *in vitro* by treating MI-dPG-PEG-Tz coated material with PBS solution of the prodrug pro-dapto. Upon incubation in PBS, the supernatant was collected and analyzed by HPLC. Figure 6 A illustrates the analysis of the collected supernatant solutions. Figure 6 B shows the cumulative release of daptomycin. Daptomycin was released shortly after treatment of MI-dPG-PEG-Tz with pro-dapto and continue to form for up to 1 month thereafter. Based on the observed data, over 90% of drug release occurred within 7 days after the treatment.

2.4 Surface characteristics

2.4.1 Synthesis of MI-dPG-PEG-Tz-titanium coating

In order to control the attachment of the coating to the surface, the visual observation was done as well as the static water contact angle was measured. Each coating step showed a change in the surface colors, indicating the presence of the coating on the surface. The MI-dPG-coated materials turned yellow, whereas tetrazine addition turned the materials to a pink color. Recent studies have shown that implant's hydrophilicity could enhance proliferation of osteoblasts on the implant's surface.^[31] SWCA measurements were performed to evaluate the surface properties of MI-dPG-PEG-Tz. The coating procedure consists of several steps and we used SWCA to monitor every coating step and the changes introduced to the material's surface. The SWCA for the titanium surfaces exceeded the 90° threshold, indicating considerable hydrophobicity (Table 1). The SWCA for the titanium surface was determined to be $96^{\circ} \pm 16^{\circ}$. The further coating with MI-dPG reduced the SWCA to $54^{\circ} \pm 2^{\circ}$, transforming the material's properties from hydrophobic to hydrophilic. Coating with Tz retained the hydrophilic properties with SWCA well below 90°. The SWCA increased to $63^{\circ} \pm 5^{\circ}$, which is still in the hydrophilic regime. The hydrophilic properties of MI-dPG-PEG-Tz make it a potential candidate for further *in vivo* testing.

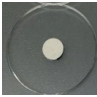
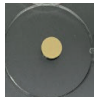

Picture of the surface	Material	Contact angle
	Titanium	$96^{\circ} \pm 16^{\circ}$
	Titanium coated with MI-dPG	$54^{\circ} \pm 2^{\circ}$
	Titanium coated with MI-dPG-PEG-Tz	$63^{\circ} \pm 5^{\circ}$

Table 1. Contact angle values for different surface coating steps. The samples were measured at least in triplicates and the mean value plus/minus standard deviation is presented in the table. Tz: tetrazine.

2.5. Coating stability

The MI-dPG-PEG-Tz coating completely covered the titanium surface. This was confirmed by the X-ray photoelectron spectroscopy (XPS) analysis of the titanium surface. As shown in Table 2, the coated samples completely lacked any Ti2p signals. Meanwhile, the C, N, and O compositions changed significantly after introduction of the coatings. Furthermore, we treated the surface with 1% SDS for 1 month and reanalyzed the samples. The percentage compositions of C1s, N1s, and O1s for the coated sample after the one month's incubation showed similar values for both coated samples. Highly resolved C1s spectra (Figure 7) showed minimal changes in C-O/C-C components' ratio from 0.82 for the freshly coated material to 0.71 for the incubated material. These results suggested that the coating was stable for the studied period of time.

	C 1s at%	N 1s at%	O 1s at %	Ti 2p at%
Titanium	29,2	0,8	50,7	17,1
Titanium 1 month in 1% SDS	34,3	1,3	47,6	14,7
Titanium coated	70,4	7,8	20,2	0,0
Titanium coated and incubated 1 month in 1% SDS	69,2	7,7	22,0	0,0

Table 2. XPS surface analysis from the coated and uncoated materials.

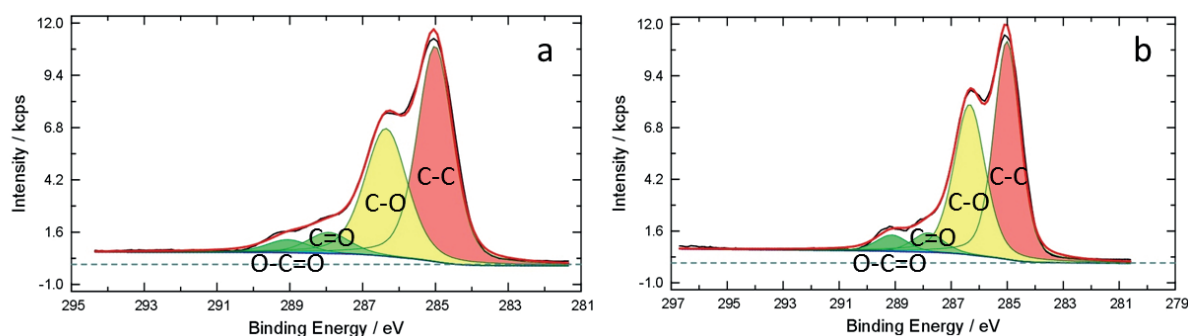


Figure 7. Highly resolved C1s spectra of (a) titanium coating with MI-dPG-PEG-Tz and (b) titanium coating with MI-dPG-PEG-Tz after 1 month of incubation in 1% SDS solution.

2.6. Coating thickness

There are several different techniques for coating thickness measurements.^[32-34] In this work SEM was employed, as it turned out to be a straightforward and optimal method, which did not involve a material breakthrough to determine the coating thickness for our samples. Before MI-dPG-PEG-Tz coating was performed, the part of materials was covered according the procedure published by Griesser et al.^[35] using poly (D,L,-lactide) (Figure 8). This enabled us to measure the coating thickness without breaking the material. The thickness was measured at three different points and the average of the three measurement points was used to determine the results. The results have shown the thickness of $49.62 \pm 5.57 \mu\text{m}$ (Figure 9).

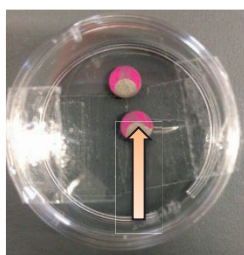


Figure 8. The titanium material coated with MI-dPG-PEG-tetrazine with uncoated parts left after poly (D,L,-lactide) layer. The arrow indicates the place where the coating thickness was measured.

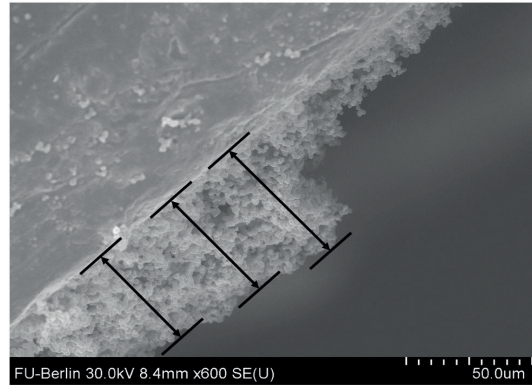


Figure 9. MI-dPG-PEG-tetrazine-coating thickness.

2.7 Ability of MI-dPG-PEG-Tz titanium coating to activate a prodrug of daptomycin

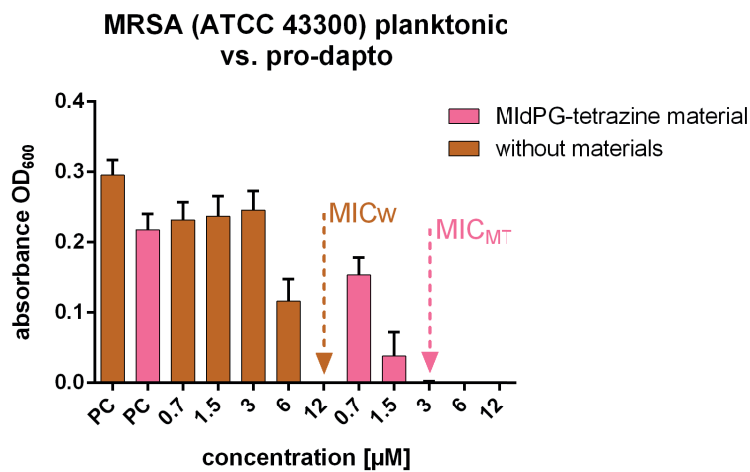


Figure 10. Minimum inhibitory concentration for planktonic MRSA versus pro-dapto for samples where no coated material was present (w) and samples, which were previously incubated with the MI-dPG-PEG-tetrazine-coated material (MT).

A series of microbiological tests was performed to evaluate the ability of MI-dPG-PEG-Tz to activate a prodrug of daptomycin (pro-dapto). We used the standardized optical density and turbidity absorbance method^[36] to measure the minimum inhibitory concentration of the supernatant (bacteria growing medium) from the pro-dapto or daptomycin incubation with MRSA. The antibiotic concentration that resulted in zero absorbance at OD₆₀₀ was identified as the minimum inhibitory concentration (MIC). Bacteria incubated with the pro-dapto prodrug showed an MIC value of 12 µM (Figure 10). In the presence of MI-dPG-PEG-Tz, pro-dapto was converted into daptomycin, thus resulting in a 4-fold reduction of MIC (3 µM). In a control experiment shown in Figure S3, we tested the antibiotic activity of daptomycin without or without the material. The observed values were virtually identical, indicating that the material did not have any anti-bacterial activity of its own.

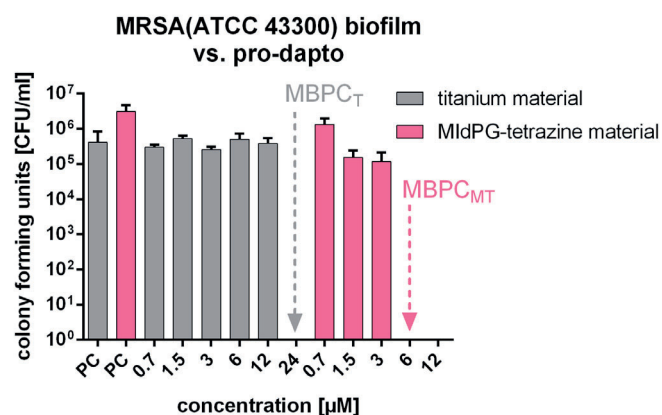


Figure 11. Minimum biofilm prevention concentration (MBPC) of the pro-dapto incubated either non-coated titanium (T) or MI-dPG-PEG-tetrazine-coated materials (MT).

The ability of MI-dPG-PEG-Tz to activate the prodrug of daptomycin was also evaluated for a biofilm-forming bacteria. The MI-dPG-PEG-Tz was pre-incubated with pro-dapto, followed by the addition of MRSA inoculum. After an overnight incubation at 37 °C, the titanium materials were washed with saline, vortexed, and sonicated. The sonication fluid was plated on the Müller-Hinton agar plates and the colony forming units (CFU) were counted. The lowest antibiotic concentration, which resulted in zero CFU on the agar plates, was considered as minimum biofilm prevention concentration (MBPC). As illustrated in Figure 11, the MBPC for pro-dapto on titanium was at 24 μM. On the other hand, pro-dapto previously incubated with MI-dPG-PEG-Tz had a 4-times lower MBPC value of 6 μM. Analogous experiments with daptomycin showed no difference in the MBPC values, indicating that the material does not have antibacterial properties of its own. In agreement with our previous published work,^[28] the material is capable of activating antibiotic prodrugs via the bio-orthogonal IEDDA chemistry.

Numerous antibacterial titanium approaches have been developed: in contrast to our study Davidson H. et al. presented covalently attached antibiotics to the titanium surface, which prevented the implant surface from the gram-negative bacteria colonization.^[37] Shu He et al. reported cefotaxime sodium immobilization on the polydopamine-coated titanium surface that prevented the materials from the *Escherichia Coli* and *Streptococcus mutants* proliferation.^[38] Min-Kyung Kang et al. showed similarly to our work a release of antibiotic from titanium coating.^[39] They present a single dose release where the majority of the drug was released within the first 24 h. Once the drug was released, no more modification of the coating or loading with the antibiotic was possible. The antibiotic pre-loaded coatings required prior planning of the targeting the bacteria. If it turns out during the treatment another bacterium is a constituent of infection, such a coating will no longer perform its function. Our approach represents a coating, which might be manipulated after the implantation of the prosthesis. The coating is a platform that can activate and release virtually any TCO-modified antimicrobial.^[28]

3. Conclusions

We have described the synthesis and characterization of a mussel-inspired dendritic polyglycerol coating for titanium surfaces that can activate antibiotic prodrugs via a bio-orthogonal IEDDA reaction. Coating with MI-dPG-PEG-Tz is non-toxic to myoblast and osteoblast cells and allows healthy adhesion of human osteoblasts to the treated surface. XPS experiments showed that the coating covered the entire titanium surface and that the coating is stable for an extended period of time. The coating was found to be hydrophobic and uniform. Our bacterial experiments showed that MI-dPG-PEG-Tz-coated titanium surface can activate the pro-dapto and release the free daptomycin. Free daptomycin released at the close proximity to the implant facilitates the eradication of the infection. Treatment of MRSA illustrated potential of this technology to battle orthopedic implant-associated infections.

4. Experimental Section

Materials: Daptomycin (Cubicin) was purchased from Novartis Pharma (Bern, Switzerland). All other chemicals were purchased from Krackeler Scientific and used without further purification. Chromatographic purifications were conducted using SiliaSphere™ spherical silica gel 5 µm, 60 Å silica gel (Silicycle). Thin layer chromatography (TLC) was performed on SiliaPlate™ silica gel TLC plates (250 µm thickness) purchased from Silicycle. Preparative TLC was performed on SiliaPlate™ silica gel TLC plates (1000 µm thickness). HPLC purification was performed on Shimadzu LC-20 Instrument using Phenomenex Luna 5u C18(2) semi-preparative column (250 x 10 mm) using a gradient of 10-70% CH₃CN (0.01% formic acid) in H₂O (0.01% formic acid). HATU and 2-[2-(Fmoc-amino)ethoxy]ethoxy acetic acid was purchased from Sigma Aldrich/Merck KGaA, Darmstadt, Germany. Analytical HPLC was performed on Shimadzu LC-20 Instrument using Phenomenex Luna 5u C18(2) column (250 x 5 mm). COSTARR Spin-X spin columns (0.22 µm cellulose acetate), purchased from Fisher Scientific (cat# 07-200-385), were used for the kinetic experiments. ¹H, ¹³C, and 2D NMR spectroscopy was performed on a Bruker 500 and 600 MHz NMR instruments. All ¹³C NMR spectra were proton decoupled. LC-MS data was acquired using Agilent Technologies 6530 Q-TOF instrument. Methyltetrazine acid was kindly provided by Alexander Oehrl, research group of Prof. Haag. Customized Ø 6 mm x 1 mm titanium plates were kindly provided by Zimmer Biomet UK Ltd (Dorcan, Swindon SN3 5HY).

Daptomycin prodrug synthesis: In our previous publication we had made an initial daptomycin prodrug modified by TCO with limited results (TCO-Dapto). This publication presents the results of pro-dapto, a daptomycin prodrug modified at its most active side ornithine (Orn6) residue with characteristics that optimized their drug properties, e.g., stability. It has been already shown by Marahiel^[40] and in our previous study^[28] that modification at this amino acid site alters the daptomycin activity.

MI-dPG- synthesis: According to the work of Sunder et al.,^[41] the synthesis of hyperbranched polyglycerol (dPG) was performed via the one-step, ring-opening, multi-branching polymerization (ROMBP) of glycidol. Next, dPG-amine was synthesized by the transformation of all terminal hydroxyl moieties to amines. This transformation was performed via (1) -OH mesylation, (2) azidation, and (3) azide reduction, as earlier described in several works by Haag and coworkers.^[42] The dPG-amine was then transformed to MI-dPG by functionalizing 40% of the terminal amine groups with 3,4-dihydroxyhydrocinnamic acid (DHHA), according to an earlier published procedure by Schlaich and coworker^[16]: dPG-NH₂ (4 g, 3.8*10⁻¹ mmol) was dissolved in 100 ml of MeOH, and the pH was adjusted to 7 using an aqueous HCl-solution (10%). Next, an aqueous buffer solution of 2-(N-morpholino) ethane sulfonic acid (MES) (100 ml, 0.1 M, pH: 4.8) was added to the solution. Subsequently, DHHA (20 g, 110 mmol, 2 eq. according to all -NH₂ moieties) and 1-ethyl-3-(3-dimethylamino)propyl)carbodiimide (EDC) (21 g, 110 mmol, 2 eq. according to all -NH₂ moieties), were added to the solution, and the reaction mixture was stirred at room temperature for 16 h.

Purification of the crude product was performed by dialysis in MeOH (dialysis molecular weight cutoff (MWCO): 2 kDa). To increase MI-dPGs' stability in solution, i.e., to prevent oxidation and subsequent crosslinking, a concentrated HCl solution (37%, 12M) was added in small amounts (i.e., 1 drop per gram of product). After purification, the solvent was removed under reduced pressure, and the product was stored in the freezer (-20 °C) under inert atmosphere (Ar).

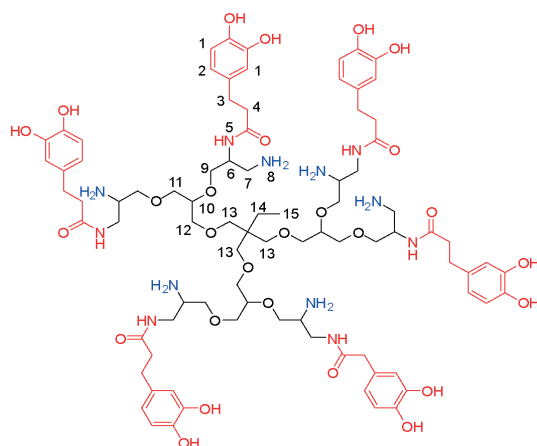


Figure 12. MI-dPG with the dPG backbone (black), and the OH moieties (red).

Coating procedure: MI-dPG was dissolved in MeOH and diluted 1:1 with 3-(N-morpholino)propanesulfonic acid MOPS pH 8.5 (final MI-dPG concentration 2 mg/ml). Coating was done overnight (at least 16 h), from each side of the material separately. Subsequently, the materials were washed three times with sterile double-distilled H₂O and one time with MeOH and dried at room temp. The 40 mg of 2-[2-(Fmoc-amino)ethoxy]ethoxy acetic acid linker (0,104 mM, final concentration 1mg/ml) in DMF was added to 71 mg of HATU (0.187 mM, 1.8 equivalent) dissolved in DMF and finally 0.343 mM (3.3 equivalent) DIPEA was added to the mixture. Each material was immersed in 300 μ l of the mixture and the liquid surrounded the material from each side. The incubation was done overnight at room temp. Next day the liquid solution was discarded and all materials were washed three times with DMF. The substrates were then transferred into new 2ml Eppendorf tubes. For the fluorenylmethyloxycarbonyl-protecting group (Fmoc) deprotection, solution of 20% piperidine in DMF was prepared. The materials were incubated in 300 μ l of the piperidine/DMF solution for 30 min. at room temp on the shaker 100 rpm. After the incubation, the fluorescence of the supernatant was measured. In order to prove the Fmoc separation, we measured dibenzofulvene–piperidine adduct, which is generated by the cleavage of base-labile Fmoc group, with 20% (v/v) piperidine in DMF at 301 nm.^[43] The results are shown in Supplementary Information (Table S1). The dibenzofulvene–piperidine adduct was then discarded and the materials were vigorously washed using vortex 3x with DMF. Finally, the supernatant was discarded and the materials were washed 3 times with DMF, using vortexing in order to wash out the Fmoc properly. Subsequently 40 mg of methyltetrazine acid was dissolved in DMF (0.19 mM, final concentration 1mg/ml, 77mg HATU in DMF (0.2 mM, 1.1 equivalent) was added and 0.37 nm of DIPEA was mixed together and 260 μ l of the mixture was added to each material, which was placed in the 2 ml Eppendorf tube. Incubation was done overnight at room temp. The next day, the liquid solution was discarded and the materials were washed 3x with DMF and 1x with MeOH.

Antibacterial analysis

Bacterial strains and growth conditions: The microbiological experiments were carried out using *Staphylococcus aureus methicillin resistant* MRSA strain (ATCC 43300). Stocks of each strain were preserved on cryovials (Roth, Karlsruhe, Germany) at -80°C. The strains were cultured on a Müller-Hinton agar (Oxoid, Hants, UK), and incubated at 37 °C for 24 h. The inoculum concentration of 2x10⁵ CFU/ml was prepared dilution of a 0.5 McFarland solution. The quantitative cultures were used in order to determine inoculum concentrations.

Minimum inhibitory concentration (MIC) determination- planktonic bacteria analysis: The pro-dapto and daptomycin dilutions were prepared in Müller-Hinton II broth (Becton, Dickinson, Le Pont-de Claix, France) (adjusted to final 50-55 mg calcium/L). The titanium materials with or without coating were incubated with 700 µl of the diluted antibiotics in order to allow the drug to attach to the coating. After 1 h incubation, 700-µl inoculum of 2×10^5 CFU/ml was added. The bacteria together with the materials and antibiotics were incubated for 24 h at 37 °C. The day after the medium of the incubated samples was tested to determine the MIC by measuring the absorbance at 600 nm, using the microplate spectrophotometer (Epoch, BioTek). MIC was defined as the minimum concentration needed to inhibit the growth of MRSA, which resulted in the same absorbance as the negative control without bacteria (medium only).

Titanium surface analysis- biofilm analysis: After 24 h incubation, the titanium materials were removed from the medium, bacteria, drug solution and washed 3 times with 0.9% NaCl to remove all planktonic bacteria. Next, the materials were placed in 500µl PBS and vortexed for 30 seconds, followed by sonication for 60 sec. at 1 MHz, lastly vortexed again for 30 sec. and the sonication fluid was plated on the Müller-Hinton agar plates. The agar plates were incubated overnight at 37 °C and the colony forming units (CFU) were enumerated the day after.

Cell viability: Cell viability was determined using a CCK-8 Kit (Sigma-Aldrich Chemie GmbH, Taufkirchen, Germany) according to the manufacturer's instructions. C2C12 (mouse myoblasts) and hPOB 01 (human primary osteoblasts) cells were kindly provided by Britt Wildemann, Julius Wolff Institut - Charité – Universitätsmedizin Berlin and cultured in DMEM (high glucose with 10% FCS, 100 U/mL penicillin and 100 µg/mL streptomycin, Thermo Fisher Scientific, Waltham, Massachusetts, USA) or DMEM/Ham's F-12 (stable glutamine with 10% FCS, 100 U/mL penicillin, 100 µg/mL streptomycin, 50 µM L-ascorbic-2-phosphate and 200 µM β-glycerolphosphate, Biochrom, Berlin, Germany), respectively. Prior to the experiment, the coated substrates were sterilized with aqueous EtOH (70%), rinsed with sterile Dulbecco's phosphate-buffered saline (DPBS without calcium and magnesium, Sigma-Aldrich, Taufkirchen, Germany), and dried in a cell culture hood. Next, the substrates were placed in a sterile 24-well plate (Sarstedt, Nümbrecht, Germany), 500 µL DMEM was added, and the plate was also placed in an incubator (Heraeus Holding GmbH, Hanau, Germany) at 37 °C and 5% CO₂.

For the cell viability test, cells were seeded in a 96-well plate at a density of 5×10^4 cells/mL in 90 µl cell culture media per well overnight at 37 °C and 5% CO₂. After overnight incubation, 40 µl per well of cell culture medium were discarded and 50 µl of medium exposed to the substrates were added to cells. SDS (1%; 0.1%) and non-treated cells served as a control. For background subtraction, also wells containing no cells but only sample were used. Cells were incubated 48 h at 37 °C and 5% CO₂. After incubation, the CCK8 solution was added (10 µl/well) and absorbance (450 nm/650 nm) was measured after approximately 3 h incubation of the dye using a Tecan plate reader (Infinite pro200, TECAN-reader Tecan Group Ltd.) Measurements were performed in triplicates and repeated three times. The cell viability was calculated by setting the non-treated control to 100% and the non-cell control to 0% after subtracting the background signal using the Excel software.

Osteoblast Adhesion and Fixation for Scanning Electron Microscopy: Frozen primary human osteoblast-like cells (hpOB 02) isolated from human donors' femoral head were kindly provided by Britt Wildemann, Charité (approval of the ethics committee from the Charité-Universitätsmedizin Berlin (EA4/035/14). For the experiment, they were thawed and cultured in Dulbecco's modified eagle medium (DMEM high glucose with 10% FCS, 100 U/mL penicillin and 100 µg/mL streptomycin, Thermo Fisher Scientific, Waltham, Massachusetts, USA) until they reached confluence. Prior to the experiment, the coated substrates were sterilized with aqueous EtOH (70%) rinsed with sterile Dulbecco's phosphate-buffered saline (DPBS without calcium and magnesium, Sigma-Aldrich, Taufkirchen, Germany), and dried in a cell culture hood. Next, the substrates were placed in a sterile 24-well plate (Sarstedt, Nümbrecht, Germany) and 500 µL DMEM containing osteoblasts (5×10^4 cells per ml) was added to the substrates. The 24-well plate containing osteoblasts and substrates was placed in an incubator (Heraeus Holding GmbH, Hanau, Germany) at 37 °C and 5% CO₂. After overnight

incubation, the cell culture medium was disposed and substrates were washed with sterile DPBS three times carefully. For the cells' fixation, the cells were incubated with glutaraldehyde solution (2.5%) at room temperature overnight. The cells were gradually dehydrated by submerging the materials with cells in EtOH/H₂O mixtures of v/v= 50/50, 70/30, and 100/0, for 10 min per mixture. Finally, the substrates were dried in hexamethyldizilane (Sigma-Aldrich, Taufkirchen, Germany) for 10 minutes at room temperature. The osteoblast cell attachment to the materials was investigated using the field emission scanning electron microscope (FE-SEM, Hitachi SU8030, Japan) at an accelerating voltage (V_{ac}) of 20 kV, a current of 20 μ A, and a working distance of 8.5 inch. Prior to the SEM experiments, all materials were sputtered with a 5-nm conductive gold layer using a compact coating unit CCU-010 by Safematic™ GmbH (Bad Ragaz, Switzerland).

Release kinetics: The coated materials were incubated with pro-dapto of 0.5 μ g/ml diluted in PBS for 24 h. Next, the supernatant was removed and the materials were incubated in PBS for 3 h, 24 h, 4 days, 7 days and 1 month. The PBS supernatant fractions were collected at each time point and a fresh buffer was added. Next the collected fractions were analyzed by HPLC. All kinetics samples were performed in triplicates.

Measurement of the water contact angle: For the contact angle measurement, the dataphysics contact angle system OCA (Data Physics Instruments, Germany) was employed with the SCA202 software version 3.12.11. The measurement of contact angle (θ) of the coated and uncoated surfaced was done at room temperature using a sessile drop method. Each surface was measured in at least 3 times with independent measurements on different locations of the material's surfaces. The Milli-Q water drop volume was 2 μ l, after the equilibration for 20 seconds the measurement of the contact angle was done.

Coating stability: To test the coating stability, the coated samples were incubated for 1 month in 1% SDS. Followed by the XPS measurement. X-ray photoelectron spectroscopy (XPS) spectra were recorded on a Kratos Axis Ultra DLD spectrometer equipped with a monochromated Al K α X-ray source using an analyzer pass energy of 80 eV for survey spectra and 20 eV for the core level spectra. The electron emission angle was 60° and the source-to-analyzer angle was 60°. The binding energy scale of the instrument was calibrated following a Kratos Analytical procedure, which used ISO 15472 binding energy data. Spectra were recorded by setting the instrument to the hybrid lens mode and the slot mode providing approximately a 300 x 700 μ m² analysis area using charge neutralization. All XPS spectra were processed with the UNIFIT program (version 2017). A Gaussian/Lorentzian sum function peak shape model GL (30) was used in combination with a Shirley background. If not otherwise denoted, the L-G mixing for component peaks in all spectra were constrained to be identical. Peak fitting of C 1s spectra was performed by fitting of all peaks to remove residual structures. After peak fitting of the C 1s spectra, all spectra were calibrated in reference to aliphatic C–C bond C 1s component at a binding energy of 285.0 eV.

Coating thickness: In order to determine the thickness of the MI-dPG-PEG-Tz coating, the titanium materials were masked according to technique described in literature.^[35] Briefly, poly(D,L,-lactide) (PDLL) was dissolved in acetone (10%, w/v), and 25 μ l of the solution was pipetted on the surface of the material, but covering only a part of the surface. The materials with the polymer were dried at 50 °C for 1 h. Next, the substrates were coated according to the MI-dPG-PEG-Tz coating procedure. Next the PDLL was removed using tweezers, which resulted in a clear step in the coating and which allowed us to identify the thickness of the coating. The vertical substrate holder (Figure 13) was used in order to enable the measurement of the thickness of the coating. The measurement was done using field emission scanning electron microscope (FE-SEM, Hitachi SU8030, Japan) at an accelerating voltage (V_{ac}) of 20 kV, a current of 20 μ A.



Figure 13. Vertical substrate holder enables the measurement of the coating thickness on the titanium material.

Click Reaction: The click reaction between tetrazine-coated titanium materials and TCO-prodrug daptomycin. Click reaction between tetrazine-coated titanium materials and TCO on daptomycin was performed similarly to described already in our previous publication.^[28] Briefly, tetrazine-coated titanium materials were placed in a freshly prepared mixture of Müller-Hinton cation adjusted medium (adjusted to final 50-55 mg Calcium/L) and pro-dapto with different concentrations (0.7 – 12 μ M) for 1 h at RT. Next MRSA was added and the reaction system was incubated overnight at 37 °C. Next day the microbiology analysis was performed.

Supporting Information

Supporting Information is available from the [_](#) or from the author.

Acknowledgements

Authors would like to express special thanks for Tony Lane from Zimmer Biomet UK Ltd (Dorcan, Swindon SN3 5HY) for the manufacturing the titanium material customized for this project, as well as Alexander Oehrl for providing CH₃-tetrazine-COOH. We are thankful to Prof. Britt Wildemann from Medical University, Charité, Berlin who provided us with mouse myoblast cells and human osteoblasts. We are also grateful to Wolfgang E.S. Unger from BAM—Federal Institute for Material Science and Testing Division of Surface Analysis and Interfacial Chemistry, Berlin, Germany for enabling us to perform XPS experiments in his institute.

Keywords: Bio-orthogonal chemistry, antimicrobial titanium coating, prodrug antibiotic, antibiotic delivery, antibiotic release.

Literature

1. Karczewski D., Winkler T., Renz N., Trampuz A., Lieb E., Perka C., Muller M., *Bone & Joint Journal*, **2019**, 101B, 132.
2. Trampuz A., Zimmerli W., *Drugs*, **2006**, 66, 1089.
3. Trampuz A., Zimmerli W., *Current Infectious Disease Reports*, **2008**, 10, 394.
4. Zimmerli W., Trampuz A., Ochsner P. E., *New England Journal of Medicine*, **2004**, 351, 1645.
5. Al Mohajer M., Darouiche R. O., *Journal of applied biomaterials & functional materials*, **2014**, 12, 1.
6. Silverstein A., Donatucci C. F., *International journal of impotence research*, **2003**, 15 Suppl 5, S150.
7. Wang J., Li J., Qian S., Guo G., Wang Q., Tang J., Shen H., Liu X., Zhang X., Chu P. K., *ACS applied materials & interfaces*, **2016**, 8, 11162.
8. Xiang Y., Xuan Y. Y., Li G., *Ther Clin Risk Manag*, **2018**, 14, 1133.
9. Weiss AJ (Truven Health Analytics) E. A. A., Bae J (Emory University), Encinosa W (AHRQ). Origin of Adverse Drug Events in U.S. Hospitals, 2011. HCUP Statistical Brief #158. July 2013. Agency for Healthcare Research and Quality, Rockville, MD.
10. Kearney C. J., Mooney D. J., *Nature materials*, **2013**, 12, 1004.
11. Chourifa H., Bouloussa H., Migonney V., Falentin-Daudre C., *Acta Biomater*, **2019**, 83, 37.
12. Han J., Yang Y., Lu J., Wang C., Xie Y., Zheng X., Yao Z., Zhang C., *Bioscience trends*, **2017**, 11, 346.
13. Mejia Oneto J. M., Khan I., Seebald L., Royzen M., *ACS Cent Sci*, **2016**, 2, 476.
14. Huebsch N., Kearney C. J., Zhao X., Kim J., Cezar C. A., Suo Z., Mooney D. J., *Proceedings of the National Academy of Sciences of the United States of America*, **2014**, 111, 9762.
15. Li M., Gao L., Schlaich C., Zhang J., Donskyi I. S., Yu G., Li W., Tu Z., Rolff J., Schwerdtle T., Haag R., Ma N., *ACS Appl Mater Interfaces*, **2017**, 9, 35411.
16. Schlaich C., Cuellar Camacho L., Yu L., Achazi K., Wei Q., Haag R., *ACS Appl Mater Interfaces*, **2016**, 8, 29117.
17. Schlaich C., Wei Q., Haag R., *Langmuir*, **2017**, 33, 9508.
18. Yu L., Cheng C., Ran Q., Schlaich C., Noeske P. M., Li W., Wei Q., Haag R., *ACS Appl Mater Interfaces*, **2017**, 9, 6624.
19. Wei Q., Achazi K., Liebe H., Schulz A., Noeske P. L., Grunwald I., Haag R., *Angew Chem Int Ed Engl*, **2014**, 53, 11650.
20. J.H. W. in *Case S.T. (eds) Structure, Cellular Synthesis and Assembly of Biopolymers. Results and Problems in Cell Differentiation (A Series of Topical Volumes in Developmental Biology)*, Vol. 19 (1992).
21. Lee B. P., Messersmith P. B., Israelachvili J. N., Waite J. H., *Annu Rev Mater Res*, **2011**, 41, 99.
22. Lee H., Scherer N. F., Messersmith P. B., *Proc Natl Acad Sci U S A*, **2006**, 103, 12999.
23. Burzio L. A., Waite J. H., *Biochemistry*, **2000**, 39, 11147.
24. LaVoie M. J., Ostaszewski B. L., Weihofen A., Schlossmacher M. G., Selkoe D. J., *Nat Med*, **2005**, 11, 1214.
25. Kang S. M., Rho J., Choi I. S., Messersmith P. B., Lee H., *J Am Chem Soc*, **2009**, 131, 13224.
26. Lee H., Dellatore S. M., Miller W. M., Messersmith P. B., *Science*, **2007**, 318, 426.
27. Faure; E., Falentin-Daudré; C., Jérôme; C., Lyskawa; J., Fournier; D., Woisel; P., Detrembleur C., *Progress in polymer science*, **2013**, 38 (1), 236.
28. Czuban M., Srinivasan S., Yee N. A., Agustin E., Koliszak A., Miller E., Khan I., Quinones I., Noory H., Motola C., Volkmer R., Di Luca M., Trampuz A., Royzen M., Mejia Oneto J. M., *ACS Cent Sci*, **2018**, 4, 1624.
29. Recordati C., De Maglie M., Bianchessi S., Argentiere S., Cella C., Mattiello S., Cubadda F., Aureli F., D'Amato M., Raggi A., Lenardi C., Milani P., Scanziani E., *Part Fibre Toxicol*, **2016**, 13, 12.
30. Lu W., Senapati D., Wang S., Tovmachenko O., Singh A. K., Yu H., Ray P. C., *Chemical physics letters*, **2010**, 487, 10.1016/j.cplett.2010.01.027.

31. Sartoretto S. C., Calasans-Maia J. d. A., Costa Y. O. d., Louro R. S., Granjeiro J. M., Calasans-Maia M. D., *Brazilian Dental Journal*, **2017**, 28, 559.
32. Pygall S. R., Whetstone J Fau - Timmins P., Timmins P Fau - Melia C. D., Melia C. D.
33. Song S. W., Kim J., Eum C., Cho Y., Park C. R., Woo Y. A., Kim H. M., Chung H., *Anal Chem*, **2019**, 91, 5810.
34. Andersson M., Folestad S., Gottfries J., Johansson M. O., Josefson M., Wahlund K.-G., *Analytical Chemistry*, **2000**, 72, 2099.
35. Hartley P. G., Thissen H., Vaithianathan T., Griesser H. J., *Plasmas and Polymers*, **2000**, 5(1), 47.
36. Baldoni D., Steinhuber A., Zimmerli W., Trampuz A., *Antimicrobial agents and chemotherapy*, **2010**, 54, 157.
37. Davidson H., Poon M., Saunders R., Shapiro I. M., Hickok N. J., Adams C. S., *Journal of Biomedical Materials Research Part B: Applied Biomaterials*, **2015**, 103, 1381.
38. He S., Zhou P., Wang L., Xiong X., Zhang Y., Deng Y., Wei S., *J R Soc Interface*, **2014**, 11, 20140169.
39. Kang M.-K., Lee S.-B., Moon S.-K., Kim K.-M., Kim K.-N., *Dental Materials Journal*, **2012**, 31, 98.
40. Grunewald J., Sieber S. A., Mahlert C., Linne U., Marahiel M. A., *Journal of the American Chemical Society*, **2004**, 126, 17025.
41. Sunder A., Hanselmann R., Frey H., Mülhaupt R., *Macromolecules*, **1999**, 32, 4240.
42. Roller S., Zhou H., Haag R., *Molecular diversity*, **2005**, 9, 305.
43. Eissler S., Kley M., Bachle D., Loidl G., Meier T., Samson D., *Journal of peptide science : an official publication of the European Peptide Society*, **2017**, 23, 757.

SUPPORTING INFORMATION

Titanium coating by combining concepts from bio-orthogonal chemistry and mussel-inspired polymer enhances antimicrobial activity against *Staphylococcus aureus*

Magdalena Czuban*, Michael Kulka, Lei Wang, Anna Koliszak, Katharina Achazi, Christoph Schlaich, Ievgen Donskyi, Mariagrazia Di Luca, Jose M. Mejia Oneto, Maksim Royzen*, Rainer Haag*, Andrej Trampuz*

M. Czuban, M. W. Kulka, Dr. K. Achazi, Dr. C. Schlaich, I. Donskyi, Prof. R. Haag
Institute of Chemistry and Biochemistry, Freie Universität Berlin, Berlin, Germany
E-mail: magdalena.czuban@charite.de; haag@zedat.fu-berlin.de

M. Czuban
Berlin-Brandenburg School for Regenerative Therapies, Berlin, Germany

L. Wang, Assist. Prof. A. Trampuz
Charité Universitätsmedizin, Centrum für Muskuloskeletale Chirurgie, Berlin, Germany
E-Mail: andrej.trampuz@charite.de

Dr. M. Di Luca, A. Koliszak
Berlin-Brandenburg Center for Regenerative Therapies, Berlin, Germany

Dr. J. M. Mejia Oneto
Shasqi Inc., San Francisco, United States

Prof. Maksim Royzen
University at Albany, Department of Chemistry, Albany, New York, United States
E-mail: mroyzen@albany.edu

I. Donskyi
BAM—Federal Institute for Material Science and Testing Division of Surface Analysis and Interfacial Chemistry, Berlin, Germany

TABLE OF CONTENTS		Page
Figure S1	¹ H NMR spectrum of MI-dPG	2
Figure S2	MI-dPG structure	2
Figure S3	Minimum inhibitory concentration measured for MRSA at the presence of daptomycin with coated materials and without the presence of materials	3
Figure S4	Minimum biofilm prevention concentration measured for MRSA at the presence of daptomycin with coated materials and with titanium materials	3
Table S1	Absorbance results from the Fmoc deprotection by 20% piperidine.	4

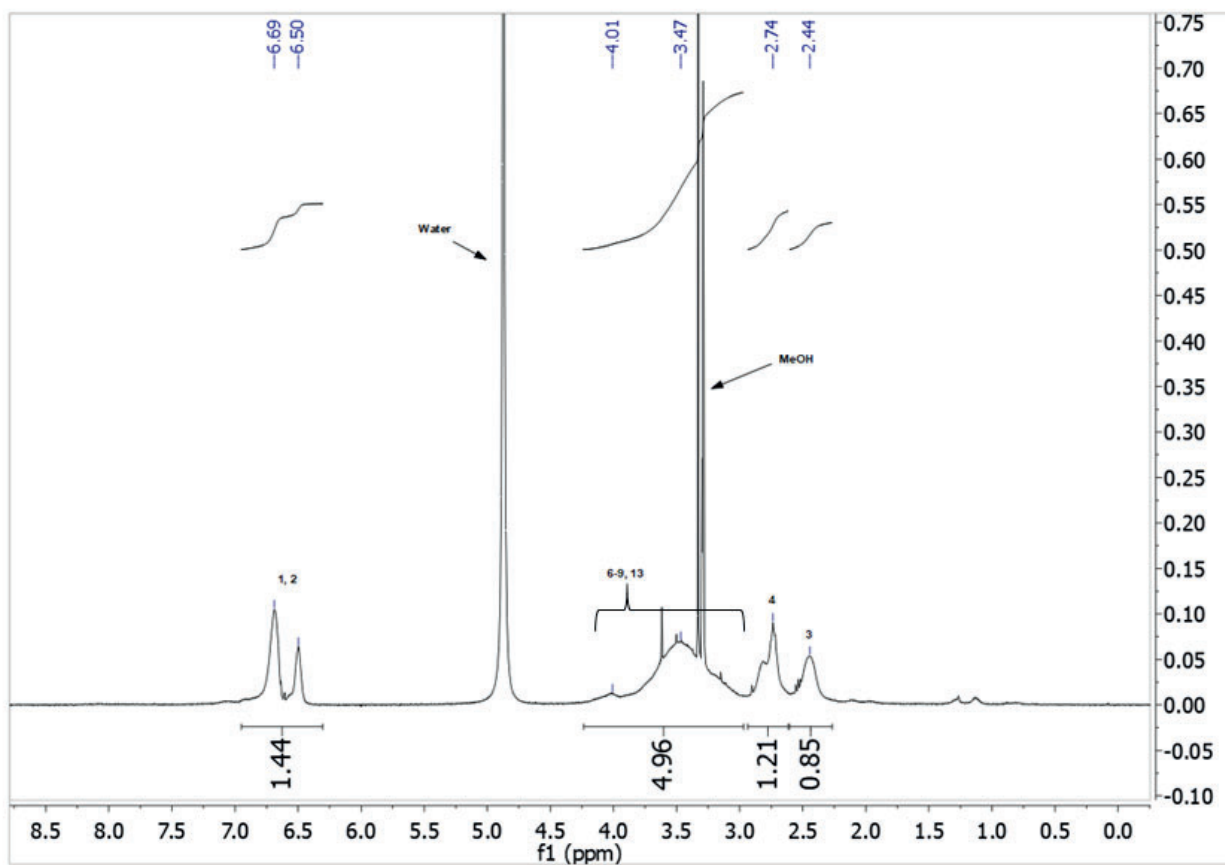


Figure S1. ^1H NMR spectrum of MI-dPG.

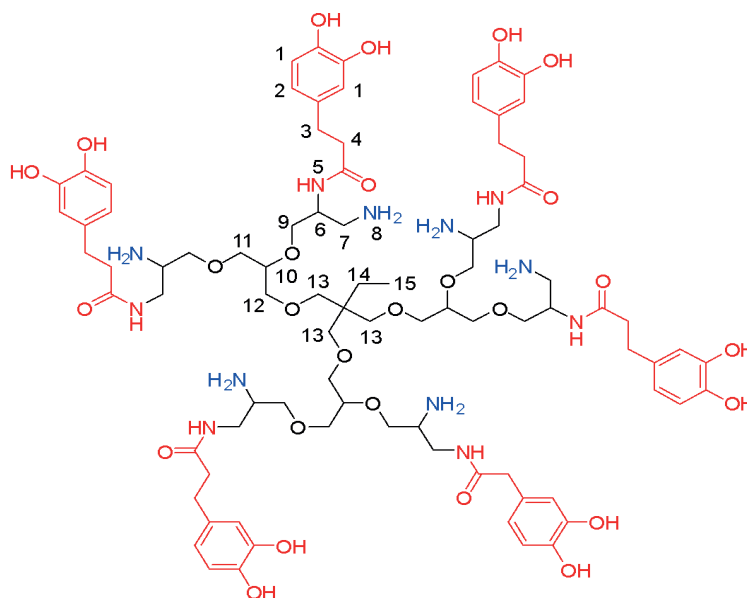


Figure S2. MI-dPG structure.

^1H NMR (500 MHz; CD_3OD): δ = 6.68-6.53 (1, 2, m, aromatic protons); 4.21-3.02 (6, 7, 8, 9, 13, m, dPG-backbone); 2.75-2.52 (3, 4, m, DHHA aliphatic protons).

MRSA (ATCC 43300) planktonic vs. daptomycin

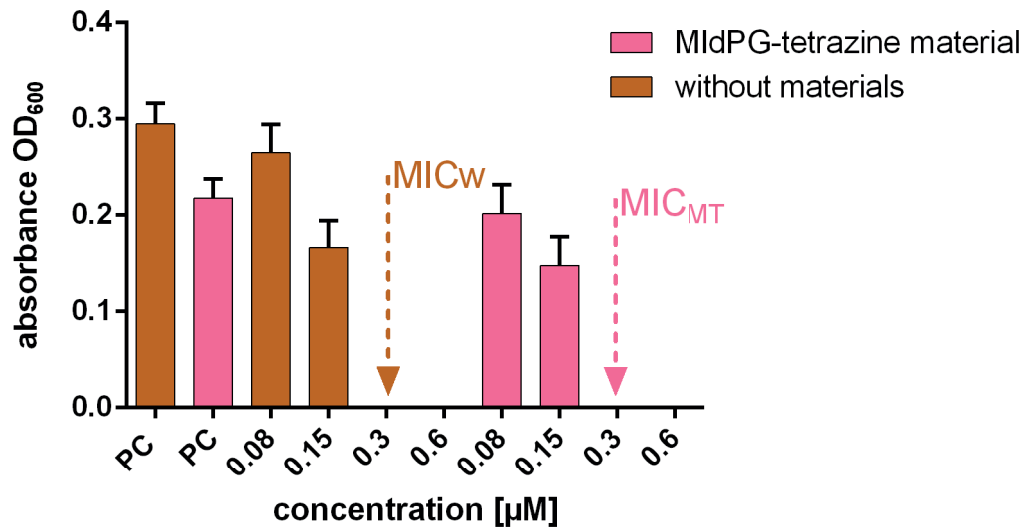


Figure S 3. Minimum inhibitory concentration for planktonic MRSA versus daptomycin for samples where no materials was present (w) and samples, which were previously incubated with MI-dPG-PEG-tetrazine-coated material (MT).

MRSA(ATCC 43300) biofilm vs. daptomycin

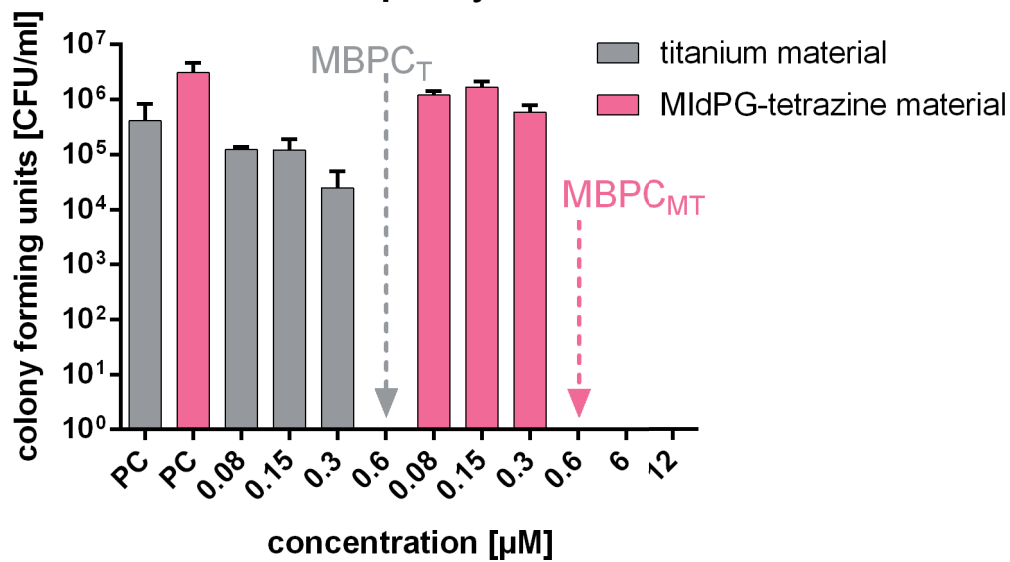


Figure S 4. Minimum biofilm prevention concentration (MBPC) of the daptomycin incubated either with not coated titanium (T) or MI-dPG-PEG-tetrazine-coated materials (MT).

2. Absorbance results: Fmoc deprotection by 20% piperidine.

The Fmoc deprotection was controlled by measuring the absorbance at 301 nm^[1] of the dibenzofulvene-piperidine adduct formation. Coated materials were incubated for 30 min with 20% piperidine/DMF solution and the absorbance of the supernatant was measured. Results shown in Table S1.

Sample	Absorbance results at 301 nm
Dibenzofulvene-piperidine adduct	1.56 ± SD 0.08
Piperidine/DMF solution	0.27 ± SD 0.03

Table S1. Absorbance results from the dibenzofulvene-piperidine adduct.

The results show the increase in absorbance for dibenzofulvene-piperidine adduct, which suggested the Fmoc's release from the surface. Incubation longer than 30 minutes did not increase the absorbance values. This indicated that the time 30 min was enough to deprotect Fmoc from the coated material's surface.

Reference

1. Eissler S., Kley M., Bachle D., Loidl G., Meier T., Samson D., *Journal of peptide science: an official publication of the European Peptide Society*, **2017**, 23, 757.

4.3 Release of different amphotericin B formulations from PMMA bone cements and their activity against *Candida* biofilm

Czuban M., Wulsten D., Wang L., Di Luca M., Trampuz A., Colloids and Surfaces B: Biointerfaces, in revision

Author contribution: Czuban M. designed the project, performed the main experiments and wrote the publication

**Release of different amphotericin B formulations from PMMA bone cements and their activity
against *Candida* biofilm**

Magdalena Czuban ^{1,2,3}, Dag Wulsten ⁴, Lei Wang ¹, Mariagrazia Di Luca ^{1,3}, Andrej Trampuz ^{1,3*}

¹ Charité – Universitätsmedizin Berlin, corporate member of Freie Universität Berlin, Humboldt
Universität zu Berlin, and Berlin Institute of Health, Center for Musculoskeletal Surgery (CMSC)

² Freie Universität, Institute of Chemistry and Biochemistry, Berlin, Germany

³ Berlin-Brandenburg School for Regenerative Therapies (BSRT)

⁴ Julius Wolff Institut, Charité - Universitätsmedizin Berlin, Berlin, Germany

Corresponding author:

Dr. Andrej Trampuz

Charité – Universitätsmedizin Berlin, Center for Musculoskeletal Surgery Charitéplatz 1,

D-10117 Berlin, Germany e-mail: andrej.trampuz@charite.de, phone: +49 30 450 615 073,

fax: +49 30 450 552 987

ABSTRACT

Amphotericin B is used for local delivery from polymethylmethacrylate to treat fungal prosthetic joint infections. The optimal amphotericin B formulation and the influence of different poragens in the bone cements are unknown. To investigate the necessary amount of amphotericin B in the bone cement to prevent *Candida* biofilm several amphotericin B formulations were studied: non-liposomal and liposomal with or without poragen gentamicin. For the non-liposomal formulation, standard bile salt, the sodium deoxycholate, was used and additionally N-methyl-D-glucamine/palmitate was applied. The activity of the released amphotericin B was tested against *C. albicans*, *C. glabrata*, *C. parapsilosis* and *C. krusei* biofilms with application of the isothermal calorimeter and standard microbiological methods. Compressive strength was measured before and after antifungal elution from the cements. There is less aggregated N-methyl-D-glucamine/palmitate amphotericin B released but its antifungal activity is equivalent with the deoxycholate amphotericin B. The minimum quantity of antifungal preventing the *Candida* biofilm formation is 12.5 mg in gram of polymer powder for both non-liposomal formulations. The addition of gentamicin reduced the release of sodium deoxycholate amphotericin B. Gentamicin can be added to N-methyl-D-glucamine/palmitate amphotericin B in order to boost the antifungal release. When using liposomal amphotericin B more drug is released. All amphotericin B formulations were active against *Candida* biofilms. Although compressive strength slightly decreased, the obtained values were above the level of strength recommended for the implant fixation. The finding of this work might be beneficial for the treatment of the prosthetic joint infections caused by *Candida spp.*

Key words: amphotericin B-loaded bone cement, fungal prosthetic joint infection, bone cement spacer, *Candida* biofilm

INTRODUCTION

Microorganisms form biofilms on the implant surfaces, which may cause persistence of infection [1, 2]. A combined surgical and antimicrobial treatment is required to efficiently eradicate implant-associated infections [3]. Periprosthetic joint infections may be caused by a wide range of microorganisms, including fungi [2, 4-6]. Among all periprosthetic joint infection, fungi are isolated in about 1 - 3%, predominantly yeasts [7-9]. Among *Candida* species, *C. albicans* has been reported to be the most prevalent pathogen, followed by *C. parapsilosis*, *C. tropicalis* and *C. glabrata* [7].

Implant-associated infections caused by *Candida* represent a serious and complex complication [10], which is further challenged due to toxicity and limited activity of antifungals against biofilms [7, 9, 11]. In addition, no uniform guidelines for the management of fungal PJI exist and most authors suggest two-stage or three-stage prosthesis exchange, combined with long-term systemic antifungal therapy with polyenes, echinocandins or azoles [3, 7, 12, 13]. Amphotericin B (AmB), one of the most active antifungals [14] is commercially available in two formulations. Amphotericin B deoxycholate (D-AmB) was initially used for the treatment of invasive fungal infections [15-17]. However, the poor water solubility and the high frequency of adverse effects after intravenous administration, such as infusion toxicity and nephrotoxicity, reduced its clinical use [18, 19]. The liposomal formulation has been developed in which amphotericin B is incorporated between lipids that compose of phospholipids and cholesterol [20]. Lipid formulations showed less nephrotoxicity [14] better tolerance and they replaced D-AmB in many institutions [19, 21].

Little data is available regarding the local use of antifungals in polymethylmethacrylate (PMMA) bone cement in the treatment of PJI, used either as temporary spacer or permanent fixation of the prosthesis [4, 6]. The thermal stability of AmB at temperature even greater than 70°C makes it an ideal candidate for inclusion into PMMA cement spacers [22]. In contrast, a commonly used echinocandin, caspofungin, shows limited thermal stability [23]. Due to low number of cases, the use of AmB-impregnated cement spacer has not been systematically investigated and its clinical efficacy remains controversial [9, 24]. Discordant results were obtained in *in vitro* and pilot clinical studies [25-27]. The analysis based on spectrophotometric measurement has shown a poor elution of non-liposomal AmB from bone cement, which is perhaps due to its covalent crosslinks in the PMMA matrix that increases the mechanical strength of the cement [22]. The liposomal formulation of AmB, although showing enhanced release of the drug, remains concerns regarding mechanical stability of the bone cements due to the high porosity resulted after polymerizing such materials [15].

The AmB structure composes of long, highly reactive unsaturated backbone, especially to the free radicals. The polymerization of the bone cements by the monomer can lead to the reaction of monomer with the double bond in the AmB. Therefore, the formed bond between the AmB and polymer chains lead to crosslinking of the antifungal within the cement matrix and the AmB cannot be released. This influences also the mechanical properties of such material by increasing the mechanical strength, a phenomenon known in polymer networks [22, 28].

Other studies showed that adding a poragen agent to PMMA improves the release of the antimicrobials, although it might decrease the strength of the cement [26, 29]. The amino-functional solubilizing agents such as polysaccharides, polyols, polyether and carboxylic acids, fatty acids encapsulate the antifungal agent and enhance the AmB release from PMMA bone cements [30]. In addition, the latter might help to disperse antifungal more homogenously and no solvent is needed for the emulsification of the drug and solubilizing agent. Thus, this might save both material and time [30].

As sodium-deoxycholate of AmB shows poor water solubility and infusion toxicity and nephrotoxicity [18, 19] and liposomal amphotericin B involves incorporation into the bone cement large amount of liposomal powder, which can negatively affect the mechanical stability of PMMA bone cements, we have investigated an alternative AmB formulation composes of amine sugar N-methyl-D-glucamine / palmitic acid (M-AmB). To our knowledge, no data was published for M-AmB release from bone cements so far. In this study we have investigated the release and activity of two standard AmB formulation from the bone cement and compared it with the M-AmB formulation. The objectives of this investigation were as follows: to determine which AmB formulation releases more active antifungal from the bone cement, to determine the AmB activity after the release from PMMA against *Candida* spp., to find AmB concentration which prevent formation of *Candida* biofilms and whether this concentration has a negative impact on the mechanical properties of bone. In addition, we have examined the same properties after addition of a poragen gentamicin to the cement.

MATERIAL AND METHODS

***Candida* strains and inoculum size.** *C. albicans* (ATCC 90028), *C. glabrata* (DSY 562), *C. krusei* (ATCC 6258) and *C. parapsilosis* (ATCC 22019) were used. The strains were plated on Sabouraud dextrose agar (SAB) and incubated for 24 h at 37°C. The $1-4 \times 10^5$ CFU/ml inoculum was prepared using McFarland standard and the exact inoculum was determined by quantitative cultures.

PMMA cement cylinders and amphotericin B formulations. Cylinders (\varnothing 6 mm x 15 mm) were manufactured by Heraeus Medical (Wehrheim, Germany). Briefly, PMMA bone cements were prepared under chemical hood at room temperature. The available on the market original packages of Palacos R® and Palacos R+G® (industrially premixed with 0.5 g gentamicin) cements were used. The non-liposomal AmB and liposomal AmB (AmBisome) were used as a powder. For the non-liposomal amphotericin B following amounts were used: 0.125, 0.25, 0.5, 0.75, 1g for 40 g of methyl methacrylate powder, with the addition of either sodium deoxycholate: 0.1, 0.21, 0.41, 0.61, 0.82g respectively or N-methyl-D-glucamine/palmitate: 0.12, 0.25, 0.5, 0.75, 1g, with 18.8 g of monomer liquid (N,N-Dimethyl-p-toluidin). For liposomal amphotericin B, 0.1, 0.2, 0.4, 0.83 and 1.66 g AmBisome was used in 10 g of polymer powder with 4.7 g of monomer liquid. PMMA cement powder, the antifungal and monomer liquid were blended properly together by hand. Next, the cement mixture was transformed to a metal mold with the wholes of \varnothing 6 mm x 15 mm. The cement cylinders dried at room temperature for 30min under a constant load of 1.3 tone. The prepared PMMA bone cement cylinders had a surface size of 0,3 cm². The conventional non-liposomal AmB formulation: sodium-deoxycholate AmB (D-AmB) was compared with an alternative non-liposomal formulation N-methyl-D-glucamine/palmitate (M). We have chosen N-methyl-D-glucamine/palmitate as it has been shown that PMMA bone cement which contain amphotericin B encapsulated fully or partly by a mixture with 1-methylamino-1-deoxy sugar alcohol and at least one fatty acid increased the water solubility of the antifungal and released effective amounts of AmB into the aqueous solutions [30].

The concentrations of different AmB-loaded PMMA cylinders evaluated in this study are summarized in Table 1.

Table 1. Amphotericin B concentrations used in this study.

Antifungal	mg drug / cylinder	Amphotericin B (mg)/ g polymer powder	Liposomal amphotericin (mg)/ g polymer powder
Amphotericin B (both D-AmB and M-AmB)	8.6	25	
	6.5	19	
	4.4	12.5	
	2.2	6	
	1.1	3	

Liposomal amphotericin B	53 mg liposomal powder (2 mg AmB)	6	166
	28 mg liposomal powder (1 mg AmB)	3	83
	14 mg liposomal powder (0.6 mg AmB)	2	41
	7 mg liposomal powder (0.3 mg AmB)	1	21
	4 mg liposomal powder (0.1 mg AmB)	0.4	10

We have used standard 0.5 g gentamicin/ 40 g polymer powder [29, 30]. As a control, cylinders without AmB were used. Following controls were used: PMMA without drug, PMMA without drug but with salts: sodium doexycolate or N-methyl-D-glucamine/palmitate, PMMA with gentamicin and salts.

Biofilm formation. The biofilm was formed on PMMA cement cylinders as previously described [31, 32]. Briefly, the PMMA cement cylinders were added to 2.7 ml advanced RPMI-1640 medium (Life Technologies corporation, NY, USA) and inoculated with 300 μ l of diluted yeast stock solution (final inoculum size 1×10^5 CFU/ml). Then, samples were incubated at 37°C for 24 h in static condition.

Quantification of adherent yeast cells by sonication. After the overnight incubation, the PMMA cylinders were transferred to new tube and washed three times with 0.9% saline. Samples were then vortexed for 30 seconds, sonicated at 40 kHz for 1 minute (BactoSonic, Bandelin electronic, Berlin, Germany) and vortexed again for 30 seconds [2]. The resulting sonication fluid was plated on the Sabouraud dextrose agar and incubated at 37°C for 24 hours for colony counting. The minimum biofilm prevention concentration (MBPC) was defined as the lower AmB concentration which determined no *Candida* colonies on agar plates. After determination of the MBPC, the additional experiment was performed. The PMMA bone cements showing MBPC were incubated with *C. albicans*, the most common PJI *Candida* spp. pathogen, for a period of 2 weeks at 37°C in static conditions.

Microcalorimetric assessment of adherent *Candida* remaining on the material after sonication.

To evaluate the viable fungi remaining on the material, cement cylinders were placed after sonication in

calorimetric disposable 4 ml-glass ampoules (Waters GmbH, Eschborn, Germany) pre-filled with 3 ml of RPMI. The metabolism-related heat production was measured at 37°C for 24 h in an isothermal microcalorimeter (TAM III; TA Instruments, New Castle, DE, USA), according the same procedures described in the previous studies [33, 34]. This method is a very sensitive technique to assess microorganism's growth. The heat production of the metabolic active pathogens is measured over a period of time [34]. The amount of fungi on the PMMA cements can be quantitatively assessed in real time. The assessment of the fungi can be done by analyzing the heat flow curve, the delay of heat production or reduction of peak heat flow. No heat production indicates no proliferating microorganisms. The results were plotted as heat flow [μW] over time. Experiments were performed in triplicates. As a control for the baseline, samples with no *Candida* spp. were used. The calorimeter manufacturer's software (TAM Assistant; TA Instruments) was used for the data analysis.

Quantification of released amphotericin B. Each PMMA cylinder loaded with AmB was incubated in 3 ml PBS, at 37°C in order to evaluate the drug release. The eluate was exchange after 24 hours and 48 hours. The elution samples were collected, after 24h, 48h and 7 days. Each of them was measured separately using spectrophotometer at the absorbance at 328 nm wavelength (Epoch Spectrophotometer, BioTek, Bad Friedrichshall, Germany). In aqueous condition, the non-liposomal AmB is aggregated and the absorption spectrum is composed of one broad peak at 328 nm [35]. For liposomal-AmB the absorbance was measured at 412 nm as indicated by Vandermeulen et al. [35]. The standard curves were prepared from AmB samples of known concentration for all tested formulations. To determine the concentration of AmB the interpolation of the standard curves was done. The release of liposomal and non-liposomal AmB was analyzed using repeated-measures ANOVA. The statistical analysis was performed using Prism 7.03 (GraphPad Software, La Jolla, CA, USA). The measurement was performed in triplicates.

Compressive strength testing. The measurement was done before and after AmB elution. This was a cumulative release over 7 days measured at 24 h, 48 h and on day 7. Experiments were performed in triplicates. For the measurement, the cylinders that showed previously MBPC values were taken as these samples show a potential perspective for the further *in vivo* studies. Each PMMA cylinder was incubated in 3 ml PBS. The elution buffer was exchanged after 24 and 48 hours, respectively. The cement cylinders were loaded to failure in axial compression according the ISO 5833 using the material

testing machine (Zwick/Roell Z010, Ulm, Germany). Compression force and displacement were recorded with a software (TestXpert II, Zwick, Ulm, Germany) at an acquisition rate of 100 Hz. The differences in the compressive strength were analyzed using a Mann-Whitney test.

Electron microscope PMMA material surface analysis

To evaluate the morphology of the surface area of PMMA samples, samples that showed MBEC were selected. The analysis of the surface was done using the scanning electron microscope and the analysis of the lateral surface was performed.

Density and porosity measurement of the PMMA bone cement samples

To assess the porosity of PMMA bone cements μ CT was performed. The height and the diameter of every single sample was measured using a caliper with LCD digital output (Digit-Cal 5S; Tesa, Switzerland) and following that samples were weighed using a microbalance (ME 36S; Sartorius, Germany) in order to calculate the samples densities.

The Specimens were then placed in a Viva40 μ CT (Scanco Medical AG, Bruettisellen, Switzerland) and a consistent ROI (212 slices) were scanned at a voltage of 45 kVp (kilovolt peak), a current of 176 μ A. The resulting images were semi-automatic segmented and analyzed in terms of radiodensity (HU).

To porosity was quantified from the micro-CT data and calculated as the ratio between the volume of residual material and the total volume of the materials, whereby a threshold of 1487 HU was used to distinguish background cavities from material. Separation is the voidspace (spacing of background).

RESULTS AND DISCUSSION

AmB is an effective antifungal molecule used as drug of choice for the management of fungal infections. AmB has a poor water solubility, therefore is commonly formulated as a sodium deoxycholate [15]. The activity and the amount of the drug released from PMMA has been a subject of much debate in the literature [15, 22, 26, 27]. Due to this fact, in the following study, an innovative approach was applied. The solubilizing agent N-methyl-D glucamine/palmitate for the AmB was used to determine its influence on the release of the drug. The local biofilm activity of liposomal and non-liposomal AmB, eluted from PMMA bone cement was studied.

Evaluation of the minimum biofilm prevention concentration of different AmB formulations released by PMMA cylinders.

PMMA cement represents an abiotic surface to which microorganisms can attach and form a biofilm on it. The ability of *C. albicans*, *C. glabrata*, *C. parapsilosis* and *C. krusei* to form biofilm on bone cement cylinders with or without AmB was evaluated by a colony counting of sonication fluids, followed by an additional analysis using isothermal microcalorimetry.

The absorbance analysis of the released AmB cannot provide information regarding the number of active molecules. However, our biofilm quantification studies showed antifungal activity of the released drugs. Similarly to the reports and studies showed by Mara et al.[27], who also used Palacos bone cements, showed clinically relevant release of AmB from acrylic bone cements in drain fluids. Wu et al. [24] reported a successful resection arthroplasty with AmB cement spacer against *Candida albicans* infection. In the case report done by Deelstra et al. [36] also was observed a significant release of AmB and voriconazole from bone cement for at least 72 hours, which finally resulted in the cure of *Candida albicans* infection in the treated patient. The MBPC of different antifungals against tested *Candida* species are reported in Table 2.

Table 2. The minimum amount of non-liposomal and liposomal amphotericin B needed to prevent the *Candida* spp. biofilm formation on the PMMA cylinders.

Antifungal formulation	Sonication fluid			
	MBPC [mg drug/ g polymer powder]			
	<i>C. albicans</i>	<i>C. glabrata</i>	<i>C. parapsilosis</i>	<i>C. krusei</i>
D	6	6	12.5	12.5
D + G	19	12.5	12.5	12.5
M	12.5	12.5	12.5	12.5
M + G	6	6	6	12.5
Liposomal amphotericin B (liposomal powder)	2 (41)	1 (21)	0.4 (10)	1 (21)

MBPC: minimum biofilm prevention concentration, D: sodium deoxycholate, M: N-methyl-D-glucamine/palmitate, G: gentamicin [0.5 g/ 40 g polymer powder].

The MBPC results show that to cover all tested *Candida spp.* D-AmB and M-AmB provide the same biofilm prevention activity 12.5 mg / g polymer powder. The addition of gentamicin to M-AmB decreased the MBPC from 12.5 mg / g PP to 6 mg / g PP for tested *Candida* species, except for *C. krusei*.

D-AmB cement with gentamicin as poragen increased MBPC from 12 mg to 19 mg AmB / g polymer powder. In contrast to the results showed by Kweon, the addition of poragen in our study did not improve significantly the release of AmB. Using the same cylinder size, Kweon showed that after 15 days of time there was 12.76 µg AmB released per cylinder when poragen was used and 1.74 µg / cylinder when no poragen was present [26]. We have observed that addition of the poragen decreased the MBPC only when M-AmB was used. Kweon [26] used 50 times more poragen than AmB. We have tested the following, much lower, ratios: 1 AmB: 1 poragen, 2 AmB: 1 poragen, 1.5 AmB: 1 poragen, 0.5 AmB: 1 poragen and 0.25 AmB: 1 poragen. Using less poragen might explain why in our study the addition of poragen did not enhance the release of the AmB. We have used 0.5 g gentamicin / 40 g polymer powder, which is a standard amount used in the commercial cements within the range of 1.25-2.5% gentamicin of the powder component in PMMA cements [37, 38]. More poragen might improve the release rate of the drug but it might also diminish the mechanical properties of the cements [37].

Compared to non-liposomal-AmB formulations, the MBPC of liposomal-AmB was lower for all the *Candida spp.* ranging from 0.4 to 2 mg of pure AmB / g polymer powder (Table 1). One has to notice that to reach 0.4÷2 mg of AmB / g PP, there is 4÷53 mg of L-AmB / g polymer powder needed. These data support the hypothesis that all released non-liposomal and liposomal AmB showed anti-*Candida* activity. Figure 2 A-D depicts *Candida spp.*, showing that all four species incubated for 24 h formed biofilm on PMMA, both with and without AmB (i.e. growth controls).

The results from the 2 weeks of incubation of PMMA cements with *C. albicans* showed that there is no growth of fungi for samples with M-AmB, M/G-AmB, D-AmB, D/G-AmB. It indicates that the non-liposomal AmB amounts which showed MBPC values, turned to be enough to protect materials from *C. albicans* colonization for a prolonged incubation period. However, *Candida* growth was observed for samples with L-AmB (2 mg drug / g PP). The amount of *C. albicans* cells found after 2 weeks of incubation was 3.8×10^3 CFU/ml. It indicates that for the liposomal samples in order to protect the materials from *Candida* growth for longer period of time, higher liposomal AmB concentration would be needed.

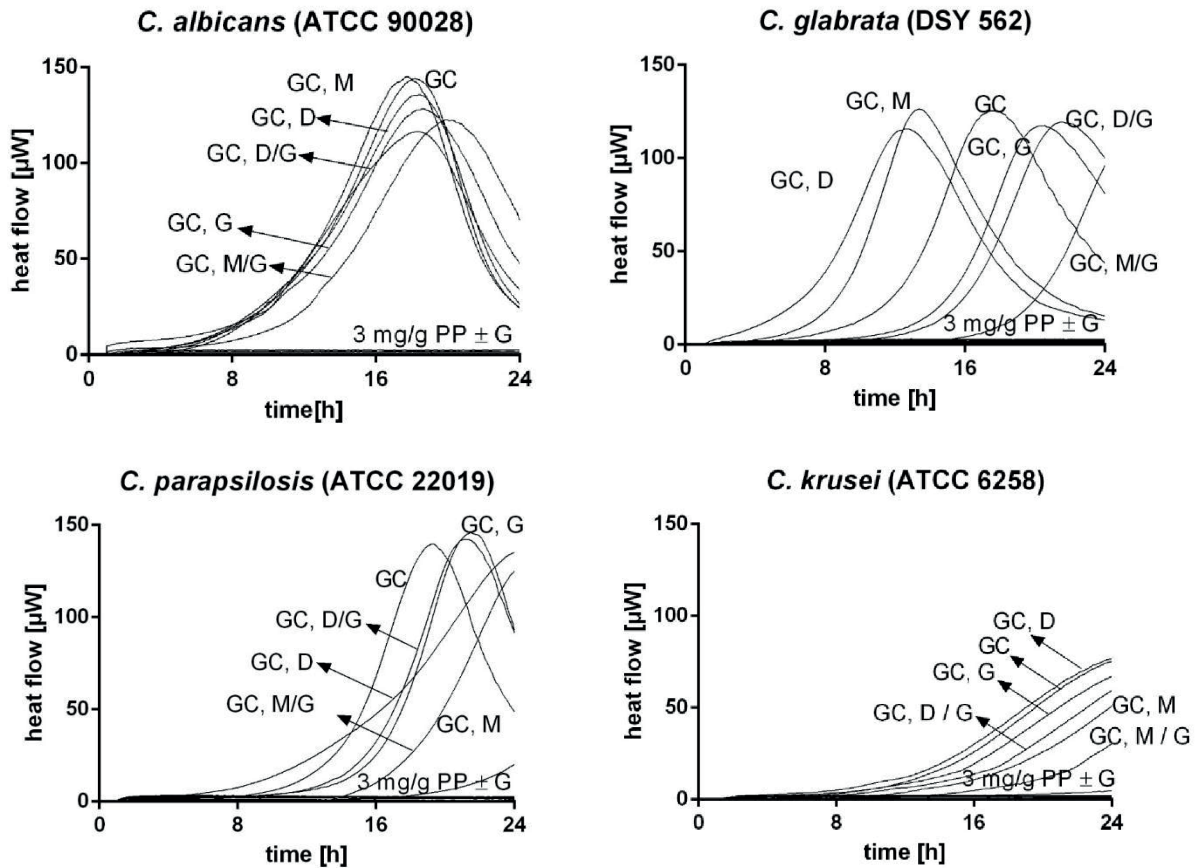


Figure 2 A-D. Heat flow produced by **A:** *C. albicans*, **B:** *C. glabrata*, **C:** *C. parapsilosis*, **D:** *C. krusei* remained on the PMMA cylinders with non-liposomal amphotericin B after sonication. The control arms are the samples named GC (growth controls) without antifungals but with solubilizing agents and with or without poragen. GC: growth control without antifungal drug, PP: polymer powder, G: gentamicin, D: sodium deoxycholate, D/G: sodium deoxycholate with gentamicin, M: N-methyl-D-glucamine/palmitate and M/G: N-methyl-D-glucamine/palmitate with gentamicin. Negative controls (PMMA materials without *Candida* spp.) did not show heat production. The concentration given in mg of the drug in gram of the polymer powder.

In order to evaluate the presence of viable *Candida* cells remaining on the cylinders after the sonication procedure, isothermal microcalorimetry analysis of all the materials was performed. The sonicated materials were placed in the fungi growing medium and transferred into the isothermal microcalorimeter for the analysis. The presence of the *Candida* cells on the materials was associated with producing the heat curves, as the proliferating cells produce heat. As shown in Figure 3 A-D, no heat production was detected during 24 hours for the tested samples, indicating that all the biofilm-embedded cells were removed from the cylinders by sonication.

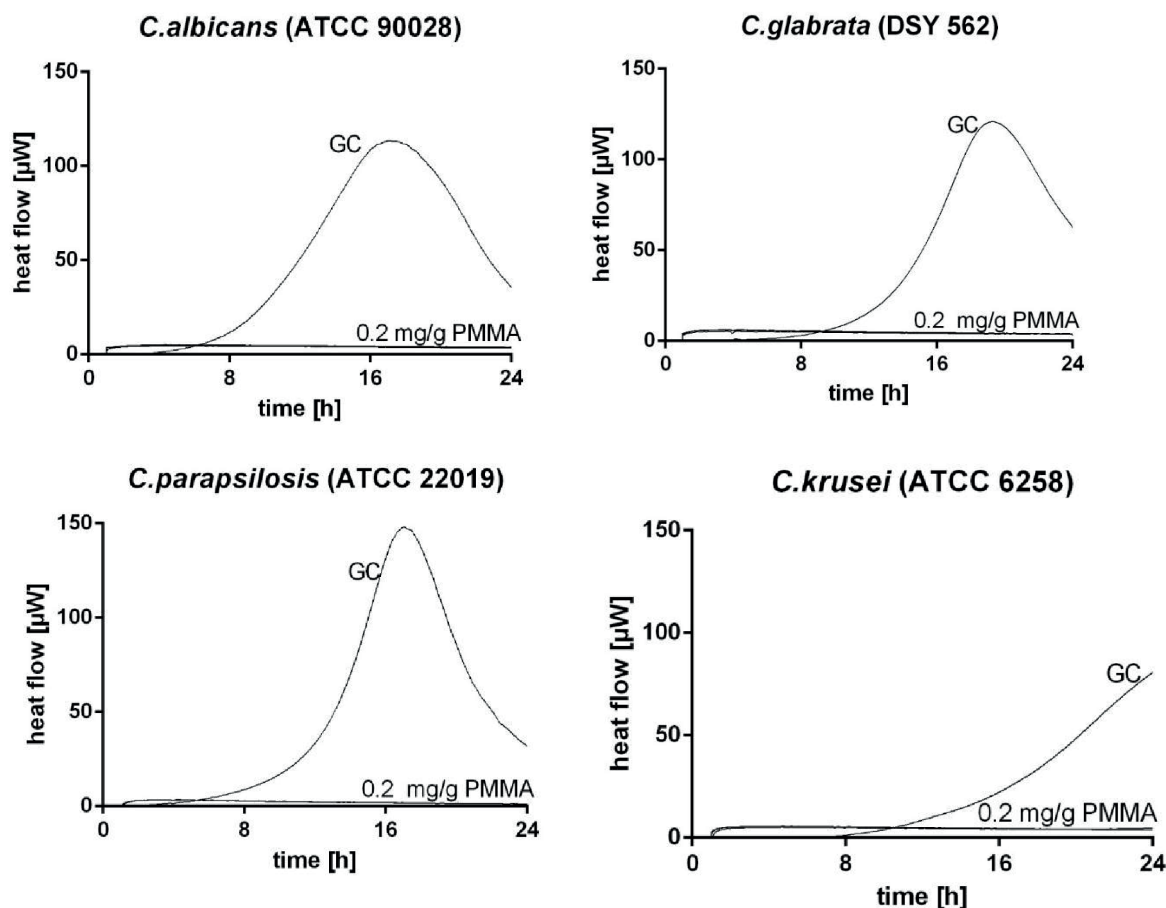


Figure 3 A-D. Heat flow produced by **A:** *C. albicans*, **B:** *C. glabrata*, **C:** *C. parapsilosis*, **D:** *C. krusei* remained on the PMMA cylinders with liposomal amphotericin B after sonication.

By contrast, the heat production was observed in the samples of cylinders without the antifungal, suggesting that a strong biofilm was formed on PMMA in absence of AmB, as the sonication procedure was not able to completely dislodge it. Moreover, comparing the elution results with sonication fluid results we showed that AmB was released in active form causing *Candida* inhibition growth. The heat flow produced by the control samples from *C. krusei* might indicate that this strain do not produce so much biofilm as the other *Candida* species tested in this work.

Quantification of different amphotericin B formulations, with and without gentamicin, released by PMMA cylinders. The cumulative drug amounts released from PMMA cylinders, after 7 days incubation in PBS, are reported in Figure 1A and 1B, respectively for non-liposomal and liposomal AmB. Besides, the effect of gentamicin addition in the cement on antifungal release was investigated as well (Figure 1A).

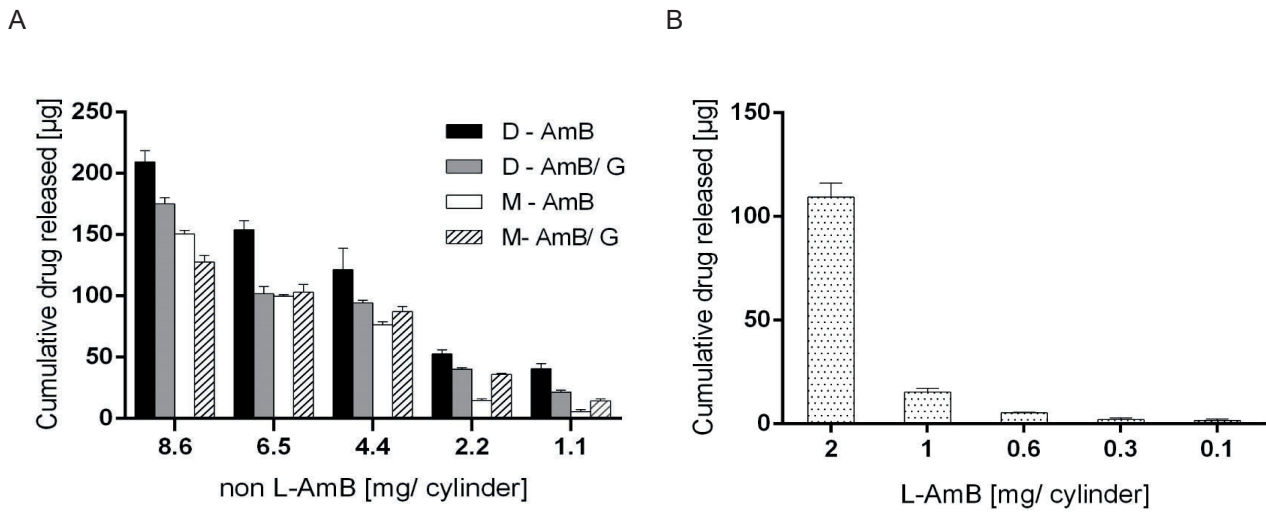


Figure 1. A) The cumulative release at day 7 for the non-liposomal amphotericin B at 328 nm in four different formulations: non L-AmB: non liposomal amphotericin B, D- AmB: sodium deoxycholate amphotericin B, D- AmB/ G: sodium deoxycholate amphotericin B with gentamicin, M-AmB: N-methyl-D-glucamine palmitate amphotericin B and M-AmB/ G: N-methyl-D-glucamine palmitate with gentamicin. The drug amounts are given per PMMA cylinder. B) The cumulative release at day 7 for the liposomal amphotericin B at 412 nm based on formulation and dose. L-AmB: liposomal amphotericin B. The drug amounts given per PMMA cylinder. The whiskers represent standard error measurement.

The presence of sodium deoxycholate released more non-liposomal-AmB in comparison to N-methyl-D-glucamine/palmitate AmB, even though this difference was not statistically significant. Although more D-AmB (range $209 \div 41 \mu\text{g}$) than M-AmB ($151 \div 6 \mu\text{g}$) was released, the D-AmB antifungal activity was inferior to the M-AmB activity. For both AmB there was 12.5 mg drug / g polymer powder needed to reach minimum biofilm prevention concentration (MBPC) for all tested *Candida* spp. These findings might suggest that not all the released D-AmB was biologically active. Although, less amount of released M-AmB was observed, its activity against *Candida* was analogous to that obtained with higher amount of D-AmB released. A possible explanation might be related to the solubility of these two bile salts. Sodium deoxycholate water solubility is lower (0.02 g / ml at 20°C) [39], in comparison to N-methyl-D-glucamine solubility in water (up to 1 g / ml at 20°C) [40]. This might result in a different aggregation state of AmB which is visible by the cumulative data. There was more D-AmB (absorbance at 328 nm [35]) than M-AmB in aggregate state. We hypothesize that M-AmB has a different particle size within the bone cements due to N-methyl-D-glucamine/palmitate, which might affect the activity of the released

AmB and its aggregation state [37]. The less aggregated state of AmB is favorable as there is weaker interaction of AmB with mammalian cell membranes [41].

In contrast to Chang et al. who reported the release of 86 $\mu\text{g} / \text{ml}$ for AmB with xylitol as an inert filler and 52 $\mu\text{g} / \text{ml}$ for powder AmB, after 10 days from initial 2 g AmB load 40 g polymer powder, our study showed 209 $\mu\text{g} / \text{ml}$ D-AmB and 154 $\mu\text{g} / \text{ml}$ M-AmB release after 7 days from the cylinders with 1 g AmB / 40 g polymer powder. Interestingly, Chang et al. used cylinders of the higher surface size $\sim 1,3 \text{ cm}^2$, than used in our study $0,3 \text{ cm}^2$.

These findings do not support the theory that the larger the surface the more drug is available on it and hence more drug is released [37]. However, they lead us to speculate that there are two factors which might explain the difference in the amount of AmB in eluates. Firstly, Chang used a bone cement by a different manufacturer. These bone cements have various copolymers and additives when compared to the cement used in our studies [37]. Secondly, we believe that the solubilizing agents used in our study for AmB formulations are of major importance for the release of the drug.

The AmB formulation seems to be crucial, as already reported by Chang the drug, although released, shows no inhibition zone for *Candida albicans* for the powder AmB and AmB/xylitol. In our study, all AmB formulations, after release, maintained antifungal activity against all tested *Candida* spp.

Our results showed lower elution of D-AmB when gentamicin was used. Its addition reduced the release of D-AmB from $209 \div 41 \mu\text{g}$ to $175 \div 21 \mu\text{g}$. These results show that the addition of gentamicin to the cement with D-AmB did not improve the release rate of this antifungal, on the contrary, there was less D-AmB released. It was also reflected in the MBPC results. Interestingly, Goss et al. [22] reported that the addition of tobramycin to D-AmB cements reduced the total elution rate of tobramycin. This could also have happened with the gentamicin used with D-AmB. These two antibiotics belong to the same group of aminoglycosides. Both are well soluble in water, hydrophilic drugs [42, 43]. According to the above mentioned, we hypothesize that the hydrophobic properties of the poragen and highly hydrophobic AmB [44] might interact with each other and, in consequence, influence the release. This might result in the diminished elution rate of both antibiotic and antifungal.

Adding a gentamicin to M-AmB loads of $0.75 \div 0,125 \text{ g} / 40\text{g}$ polymer powder showed a beneficial effect by improving the AmB elution amounts. The release amounts were higher $103 \div 14 \mu\text{g}$ as compared to $100 \div 6 \mu\text{g}$ where no poragen was used. These results imply that M-AmB interaction with gentamicin is different from D-AmB. Following this line of reasoning, it might be assumed that hydrophobic vs. hydrophilic interaction between cement ingredients contribute to the difference in the release of the

molecules, as well as the particle size of active substance and their distribution among the cement. Potentially, these findings show that M-AmB might be a better choice if use non-liposomal AmB for bone cements. M-AmB releases less aggregated AmB at the same time having equal antifungal activity to the D-AmB. We report that non-liposomal D-AmB and M-AmB have been released from the bone cement without any help of a poragen. Our data are in line with those of Houdek [45] and Cunningham [15] studies. Houdek et al. [45] reported a detectable amount of D-AmB in the eluate, which is consistent with our study. However, we cannot compare the amount of released D-AmB with our findings as the w / w of D-AmB used in Houdek study was 7.5% whereas our maximum D-AmB w / w was 2.5%. Cunningham [15] reported the release of 23 µg D-AmB after 7 days from 800 mg initial amount in the cement. Our 750 mg D-AmB load in the cement released 154 µg of the drug after 7 days. Closer inspection of this study reveals that the cylinder size used in our study is slightly bigger 0.34 cm² than the one used by Cunningham 0.28 cm². Moreover, the amounts of elution buffer differ from 3 ml in our study to 5 ml in Cunningham study. We believe that these two factors together with different cements used in our study and their powder components [37], might provide an explanation for the difference in the released amounts of D-AmB.

We report the release of D-AmB from each tested cylinder, regardless of either absence or presence of poragen. These findings do not support the data showed by Goss et al. [22]. He reported that after 168 h of elution, there was no D-AmB detected in the eluate. Within the sensitivity limit 1 µg/L, no drug could be measured. In contrast to our study, Goss et al. used cements with different composition of the powder components, which might have an impact on the release. Apparent discrepancies might be due to the amount of elution buffer used by Goss et al. that was 250 ml. In our study, there was only 3ml used. In other words, the concentration of released D-AmB in our study was higher and hence the drug detection was possible. Another possible explanation is that the amount of D-AmB used in our study was higher than those used by Goss et al. This might be a reason why here more drug was released, accordingly more powder in the cement create more porous cements and the release is therefore facilitated. As shown in Figure 1B, a dose-dependent release of L-AmB was observed. After 7 days, a total release of 109 µg, 15 µg, 5 µg, 2 µg and 1.6 µg L-AmB was observed from initial 2 mg, 1, 0.6, 0.3, 0.1 L-AmB/cylinder, respectively (corresponds to 1.7, 0.8, 0.4, 0.2, 0.1 g L-AmB / 10 g polymer powder).

Our results are comparable to those reported by Cunningham [15] where higher release was shown with L-AmB than with D-AmB and the release increased for greater load of AmB in the cement. As the

antimicrobial release rate from the bone cements depends on the roughness and porosity of the cement [37] we assume that the higher release observed for L-AmB is related to its formulation which has a larger volume of powder. The L-AmB composes of AmB powder and liposomes powder. At the same time, it provides a larger porous structure of the cement. These results support the hypothesis that more powder of the active substance within the bone cement releases more drug [37]. As the complete release of AmB from the PMMA was not observed, we assumed that crosslinking between AmB and PMMA might occur and not all AmB can be released, as already reported by Nugent et al [29].

Analysis of the cement cylinders strength.

After 7-days elution of AmB, the compressive strength resulted slightly reduced in all the eluted cement samples, as shown in Figure 4.

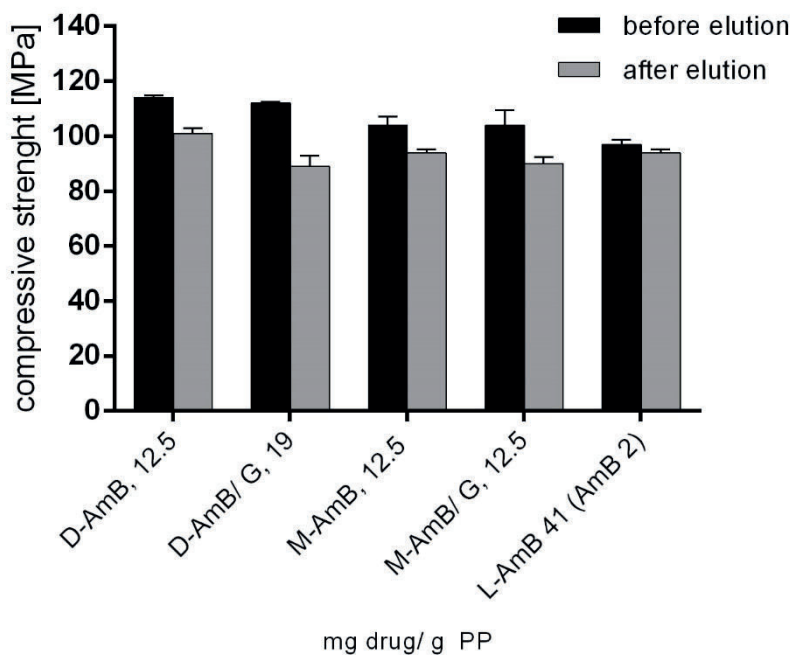


Figure 4. Compressive strength in MPa of the bone cements which showed the MBPC (amount of amphotericin B (AmB) in g/ 40 g polymer powder). Black bars are the compressive strengths for the materials before elution and grey represents the results after elution. D-AmB: sodium deoxycholate amphotericin B, D-AmB/ G: sodium deoxycholate amphotericin B with gentamicin, M-AmB: N-methyl-D-glucamine/palmitate amphotericin B, M-AmB/ G: N-methyl-D-glucamine/palmitate amphotericin B with gentamicin, L-AmB: liposomal amphotericin B

The average compressive strength of non-eluted samples ranged between 114 MPa to 97 MPa, while after elution the values varied from 101 MPa to 89 MPa. However, none of the tested AmB formulations showed a statistically significant difference in the compressive strength after elution. The MBPC for the liposomal formulation caused a non-significant change in the compressive strength after elution.

In contrast to results reported by Cunningham et al., we report compressive strength of 94 MPa for liposomal bone cements after elution, which is above the recommended level by ISO 5833 (70 MPa) [15]. The difference might be in higher volumes of the elution buffer and different amount liposomal AmB used by Cunningham et al. For the non-liposomal deoxycholate formulation, our results were consistent with those obtained by Cunningham et al. [15] Goss et al. [22] and Kweon et al. [26] (compressive strength above 100 MPa). Nevertheless, contrary to our results, Kewon et al. observed significant decrease in compressive strength after elution when high-dose of poragen was used. The low-dose of poragen used in our study might be the explanation. We report no significant decrease in compressive strength when 12.5 mg gentamicin / g PP was added, as already reported by Goss et al. when 1g of tobramycin / batch was used as poragen [22].

We have shown no significant change in compressive strength regardless the AmB formulation which are comparable findings with Chang et al. [46] Although compressive strength slightly decreased, the obtained values were above the strength recommended for the implant fixation. However, we hypothesize that in larger scale (patient treatment) the compressive strength of materials with L-AmB might decrease significantly.

Electron microscope PMMA material surface analysis

Figure S1. Shows the results from the SEM surface analysis of the samples that showed MBEC were selected. On each surface there are visible irregularities and scratches, which probably result from the polymerization process in metal molds. The sample with liposomal AmB (Figure S1, B) shows black spots which are the pores resulting of mixing large amounts of liposomal AmB powder with PMMA bone cement constituents. In this case the porosity visible on the surface is greater than in PMMA bone cement where D-AmB or M-AmB was used. The greater porosity of liposomal AMB PMMA bone cement surface, might explain why liposomal AmB in larger than D-AmB or M-AmB quantity is released to the liquid medium. Higher porosity allows better liquid penetration of the PMMA material. In the case of M-AmB mixed with gentamicin, more pores are visible than without gentamicin. The addition of gentamicin, resulted in higher number of pores which is beneficial as the PMMA material penetration by a liquid. This may also explain why the addition of gentamicin has led to a lower MBEC for M-AmB.

PMMA bone cement density and porosity measurement

The porosity results are summarized in Table S1 in the supplementary information. The smallest porosity was found in PMMA bone cement with M-AmB 0.0100, the largest porosity appeared in samples with liposomal AmB 0.0257 (Table S1). The difference between these two groups is significant. Higher porosity provides higher elution rate for the drug from PMMA bone cements [47, 48]. Therefore, an increase in porosity in the liposomal AmB PMMA may explain why from these materials more antifungal is released than if other AmB forms are used.

The density measurement showed that there were no significant differences between the samples. The results are summarized in Table S2 in supporting information. The lowest density was recorded for M-AmB PMMA 1.222 g/cm³ and the highest for PMMA bone cement with M+G-AmB 1.238 g/cm³.

CONCLUSIONS

The following study provides the data about the minimal amount of AmB that prevents *Candida spp.* biofilm growth on the PMMA, representing the standard PMMA quantity used in a clinical approach for antibiotic impregnated cement. Sonication and microcalorimetry experiments indicated that AmB released from bone cements prevented *Candida* biofilm formation in all cement forms. The addition of poragen gentamicin has an advantage when used with M-AmB, but there is no improvement when used with D-AmB.

In conclusion, our study showed that AmB has been released from bone cement regardless of the AmB formulation. Each of the tested AmB amounts remain the antifungal activity after the release. N-methyl-D-glucamine/palmitate AmB showed advantage over the conventional deoxycholate formulation which potentially might be beneficial when choosing the AmB formulation for bone cement formulation. The release profile of AmB might depend on the composition of the powder components of the cements, particle size of the active substance and its hydrophobic and hydrophilic properties.

We report that gentamicin poragen does not enhance the elution rate of D-AmB but improves the release of M-AmB. None of the tested cements showed a significant decrease in the compressive strength.

There are further *in vivo* studies required in order to deeply study the antifungal properties of released AmB and research, test, diagnose the mechanical stability of the cements with AmB on larger scale.

ACKNOWLEDGMENTS

This work was supported by PRO-IMPLANT Foundation, Berlin, Germany (<https://www.pro-implantfoundation.org>), a non-profit organization supporting research, education, global networking and care of patients with bone, joint or implant-associated Infection, providing an unrestricted educational grant.

The authors wish to thank Sebastian Vogt for his valuable comments to this work and assistance in fabrication of the PMMA bone cement materials and the materials surface analysis with SEM.

Author contribution statement:

MC: substantial contribution to research design, performed the experiments, analysis and interpretation of data, drafting the paper

DW: contribution to mechanical tests, porosity and density experiments, revising the manuscript

LW: contribution to the biofilm experiments

MDL: supervising and revising the manuscript

AT: original idea, substantial contribution to research design, revising the manuscript, approval of the submitted and final version

All authors have read and approved the final submitted manuscript.

REFERENCES

1. Delattin, N., et al., *Repurposing as a means to increase the activity of amphotericin B and caspofungin against Candida albicans biofilms*. J Antimicrob Chemother, 2014. **69**(4): p. 1035-44.
2. Trampuz, A., et al., *Sonication of removed hip and knee prostheses for diagnosis of infection*. New England Journal of Medicine, 2007. **357**(7): p. 654-663.
3. Zimmerli, W., A. Trampuz, and P.E. Ochsner, *Prosthetic-joint infections*. N Engl J Med, 2004. **351**(16): p. 1645-54.
4. Cui, Q., et al., *Antibiotic-impregnated cement spacers for the treatment of infection associated with total hip or knee arthroplasty*. J Bone Joint Surg Am, 2007. **89**(4): p. 871-82.
5. Mahmud, T., et al., *Assessing the gold standard: a review of 253 two-stage revisions for infected TKA*. Clin Orthop Relat Res, 2012. **470**(10): p. 2730-6.
6. Anagnostakos, K., *Therapeutic Use of Antibiotic-loaded Bone Cement in the Treatment of Hip and Knee Joint Infections*. J Bone Jt Infect, 2017. **2**(1): p. 29-37.
7. Dutronc, H., et al., *Candida prosthetic infections: case series and literature review*. Scand J Infect Dis, 2010. **42**(11-12): p. 890-5.
8. Kwong, C.A., S.K. Puloski, and K.A. Hildebrand, *Fungal periprosthetic joint infection following total elbow arthroplasty: a case report and review of the literature*. J Med Case Rep, 2017. **11**(1): p. 20.
9. Ueng, S.W., et al., *What is the success of treatment of hip and knee candidal periprosthetic joint infection?* Clin Orthop Relat Res, 2013. **471**(9): p. 3002-9.
10. Maiolo, E.M., et al., *Antifungal activity against planktonic and biofilm Candida albicans in an experimental model of foreign-body infection*. J Infect, 2016. **72**(3): p. 386-92.
11. Ji, B., et al., *Single-Stage Revision for Chronic Fungal Periprosthetic Joint Infection: An Average of 5 Years of Follow-Up*. J Arthroplasty, 2017. **32**(8): p. 2523-2530.
12. Yang, S.H., J.L. Pao, and Y.S. Hang, *Staged reimplantation of total knee arthroplasty after Candida infection*. J Arthroplasty, 2001. **16**(4): p. 529-32.
13. Schoof, B., et al., *Fungal periprosthetic joint infection of the hip: a systematic review*. Orthop Rev (Pavia), 2015. **7**(1): p. 5748.
14. Botero Aguirre, J.P. and A.M. Restrepo Hamid, *Amphotericin B deoxycholate versus liposomal amphotericin B: effects on kidney function*. Cochrane Database Syst Rev, 2015(11): p. Cd010481.
15. Cunningham, B., et al., *Liposomal formulation increases local delivery of amphotericin from bone cement: a pilot study*. Clin Orthop Relat Res, 2012. **470**: p. 2671-6.
16. Salzer, H.J.F., et al., *Diagnosis and Management of Systemic Endemic Mycoses Causing Pulmonary Disease*. Respiration, 2018. **96**(3): p. 283-301.
17. Thielen, B.K., et al., *Widespread Lichtheimia Infection in a Patient with Extensive Burns: Opportunities for Novel Antifungal Agents*. Mycopathologia, 2019. **184**(1): p. 121-128.
18. Mobasher, M., et al., *Solubilization Behavior of Polyene Antibiotics in Nanomicellar System: Insights from Molecular Dynamics Simulation of the Amphotericin B and Nystatin Interactions with Polysorbate 80*. Molecules, 2015. **21**(1): p. E6.
19. Jarvis, J.N., et al., *Short-course High-dose Liposomal Amphotericin B for Human Immunodeficiency Virus-associated Cryptococcal Meningitis: A Phase 2 Randomized Controlled Trial*. Clin Infect Dis, 2019. **68**(3): p. 393-401.
20. Adler-Moore, J. and R.T. Proffitt, *AmBisome: liposomal formulation, structure, mechanism of action and pre-clinical experience*. J Antimicrob Chemother, 2002. **49** Suppl 1: p. 21-30.
21. Bagshaw, E., et al., *Economic impact of treating invasive mold disease with isavuconazole compared with liposomal amphotericin B in the UK*. Future Microbiology, 2018. **13**(11): p. 1283-1293.
22. Goss, B., et al., *Elution and mechanical properties of antifungal bone cement*. J Arthroplasty, 2007. **22**(6): p. 902-8.
23. Karavas, E., et al., *Pharmaceutical composition containing an echinocandin antifungal agent and method for the preparation thereof technical field of the invention*. 2016.
24. Meng-Huang Wu and K.-Y. Hsu, *Candidal arthritis in revision knee arthroplasty successfully treated with sequential parenteral-oral fluconazole and amphotericin B-loaded cement spacer*. Knee Surgery, Sports Traumatology, Arthroscopy, 2011: p. 1433-7347.
25. Hann, I.M. and H.G. Prentice, *Lipid-based amphotericin B: a review of the last 10 years of use*. International Journal of Antimicrobial Agents, 2001. **17**(3): p. 161-169.

26. Kweon, C., et al., *Amphotericin B delivery from bone cement increases with porosity but strength decreases*. Clin Orthop Relat Res, 2011. **469**(11): p. 3002-7.
27. Fawziah Marra, G.M.R., Bassam A. Masri, Clive Duncan, Kishor M. Wasan, Evan H. Kwong, Peter J. Jewesson., *Amphotericin B-loaded bone cement to treat osteomyelitis caused by Candida albicans*. Canadian Journal of Surgery, 2001.
28. Nielsen, L.E., *Cross-Linking–Effect on Physical Properties of Polymers*. Journal of Macromolecular Science, Part C, 1969. **3**(1): p. 69-103.
29. Nugent, M., et al., *Strength of antimicrobial bone cement decreases with increased poragen fraction*. Clin Orthop Relat Res, 2010. **468**(8): p. 2101-6.
30. Vogt, S., *Antimycotic polymerisable bone cement and a method for the production thereof*. 2016.
31. Clauss, M., et al., *Biofilm formation on bone grafts and bone graft substitutes: comparison of different materials by a standard in vitro test and microcalorimetry*. Acta Biomater, 2010. **6**(9): p. 3791-7.
32. Clauss, M., et al., *Biofilm formation by staphylococci on fresh, fresh-frozen and processed human and bovine bone grafts*. European Cells and Materials, 2013. **25**: p. 159-166.
33. Boillat-Blanco, N., et al., *Susceptibility testing of Mycobacterium abscessus by isothermal microcalorimetry*. Diagn Microbiol Infect Dis, 2015. **83**(2): p. 139-43.
34. Gonzalez Moreno, M., A. Trampuz, and M. Di Luca, *Synergistic antibiotic activity against planktonic and biofilm-embedded Streptococcus agalactiae, Streptococcus pyogenes and Streptococcus oralis*. J Antimicrob Chemother, 2017. **72**(11): p. 3085-3092.
35. Vandermeulen, G., et al., *Encapsulation of amphotericin B in poly(ethylene glycol)-block-poly(epsilon-caprolactone-co-trimethylenecarbonate) polymeric micelles*. Int J Pharm, 2006. **309**(1-2): p. 234-40.
36. Deelstra, J.J., D. Neut, and P.C. Jutte, *Successful treatment of Candida albicans-infected total hip prosthesis with staged procedure using an antifungal-loaded cement spacer*. J Arthroplasty, 2013. **28**(2): p. 374.e5-8.
37. Kühn, K.-D.-. *PMMA Cements*. 2014: Springer.
38. Ayre, W.N., et al., *A novel liposomal drug delivery system for PMMA bone cements*. Journal of Biomedical Materials Research Part B: Applied Biomaterials, 2016. **104**(8): p. 1510-1524.
39. *Sodium deoxycholate, Merck safety data sheet according to Regulation (EC) No. 1907/2006*.
40. *The Merck Index, 11th ed., Entry# 5995*.
41. Alvarez, C., D.H. Shin, and G.S. Kwon, *Reformulation of Fungizone by PEG-DSPE Micelles: Deaggregation and Detoxification of Amphotericin B*. Pharm Res, 2016. **33**(9): p. 2098-106.
42. Hilmer, S.N., et al., *Gentamicin pharmacokinetics in old age and frailty*. Br J Clin Pharmacol, 2011. **71**(2): p. 224-31.
43. Pfeifer, C., et al., *Purity determination of amphotericin B, colistin sulfate and tobramycin sulfate in a hydrophilic suspension by HPLC*. J Chromatogr B Analyt Technol Biomed Life Sci, 2015. **990**: p. 7-14.
44. Tan, T.R., et al., *Characterization of a Polyethylene Glycol-Amphotericin B Conjugate Loaded with Free AMB for Improved Antifungal Efficacy*. PLoS One, 2016. **11**(3): p. e0152112.
45. Houdek, M.T., et al., *Elution of High Dose Amphotericin B Deoxycholate From Polymethylmethacrylate*. J Arthroplasty, 2015. **30**(12): p. 2308-10.
46. Chang, Y.H., et al., *Liquid antibiotics in bone cement: an effective way to improve the efficiency of antibiotic release in antibiotic loaded bone cement*. Bone Joint Res, 2014. **3**(8): p. 246-51.
47. Rasyid, H.N. and S. Soegijoko, *Influence of Soluble Fillers in Improving Porosity of Handmade Antibiotic-Impregnated Polymethyl Methacrylate (PMMA) Beads: An in-vitro Study*. Malays Orthop J, 2016. **10**(2): p. 6-10.
48. Slane, J., B. Gietman, and M. Squire, *Antibiotic elution from acrylic bone cement loaded with high doses of tobramycin and vancomycin*. J Orthop Res, 2018. **36**(4): p. 1078-1085.

Total number of words: 7499

Number of figures/tables: 8

4.4 Electro-responsive graphene oxide hydrogels for skin bandages: The outcome of gelatin and trypsin immobilization.

Di Luca M, Vittorio O, Cirillo G, Curcio M, **Czuban M**, Voli F, Farfalla A, Hampel S, Nicoletta FP, Iemma F. *Int J Pharm.* 2018 Jul 30;546(1-2):50-60.

<https://doi.org/10.1016/j.ijpharm.2018.05.027>

Author contribution:

Czuban M. performed the microbiological activity assays for the curcumin released from the hydrogels

5. SUMMARY AND CONCLUSIONS

Implant-associated infections are devastating complications. The implant surface is very easy to be colonized by bacteria, which then form a biofilm. The biofilm on the implant surface is difficult to eradicate. Therefore, the prevention procedures for an implant surface are of crucial importance.² Prevention of the implants begins with knowledge of the factors that cause the risk of infection, which can lead to the development of infection in different stages: pre-operatively, intraoperatively, or postoperatively.²³⁷ The systemically injected antibiotic spreads through the entire body. As a result, the concentration, which arrives to the infection site is mainly sublethal, causes a persister cell formation.²³⁸ The insufficient dosage of such antimicrobials leads to unresolved infection because it often does not reach the infected site. Therefore, there is a critical need for a novel solution, either one, which allows the drug to reach the infection with high concentration and improve the biofilm penetration, or the one, which helps the implant surface hinder bacteria colonization.

In this PhD work few strategies for biofilm-based infections were introduced: prodrug antibiotic local delivery based on biorthogonal chemistry, antimicrobial coating against *S.aureus* utilizing the inverse-electron demand Diels-Alder reaction and MI-dPG polymer, antifungal impregnated PMMA bone cements against *Candida* spp. biofilms and electro-responsive hydrogels with photosensitizer curcumin release against MRSA.

In the first project it has been shown that the tetrazine-modified biomaterial, boost the activation of multiple doses of TCO-prodrugs *in vitro* and *in vivo*. These results indicate that therapeutic efficacy of antibiotics can facilitate the removal of bacterial infections, at the same time antibiotic side-effects can be reduced. Bio-orthogonal chemistry for prodrug antibiotic delivery has a wide range of applications and can be a potential candidate for the clinical usage in the treatment of implant-associated infections. In conclusion, the flexibility of placing the tetrazine-alginate hydrogel as a target for the antibiotics in any desired location allows to use it for any type of implant-associated infection regardless the kind of implant material.

In the second project the introduction of tetrazine to the MI-dPG coating was capable of daptomycin prodrug concentration and activation at the implant surface. The release of an active drug it into the implant surrounding enhanced the elimination of the MRSA bacteria. The results showed that MI-dPG-tetrazine coating does not require the incorporation of an antibiotic into the coating immediately. Such an implant coating allows for a drug modification already after the implant has been inserted into the patient's body. The benefit is that the pathogen does not need to be known at the time of the implant insertion. As a future perspective it is expected that such coated implant can be loaded with several different antibiotics, which can be reloaded and released multiply times from the implant, by simply injecting the antibiotic intravenously without the need for further surgery.

In the third project, the PMMA studies with different AmB formulations showed that all tested formulations are releasable from PMMA bone cements and remained active against *Candida* spp. Although the compressive strength was reduced for liposomal AmB, it was still within the ISO 5833 standard. The density remained at the same level for all tested formulation, whereby the porosity of the materials was greatest for liposomal AmB. The new N-methyl-D-glucamine/palmitate AmB formula showed comparable efficacy to the AmB deoxycholate with an enhanced activity and release, when poragen was added. In conclusion, the results showed a potential use for N-methyl-D-glucamine/palmitate AmB for incorporation into the PMMA bone cement as an alternative to AmBs, which are currently available on the market.

In the fourth project the results from the electro-stimulated hydrogels showed that curcumin can be released from the such materials and the release kinetic can be modulated. The viability of the human fibroblast cells was higher than 94% and released curcumin showed 90% growth inhibition of MRSA. In conclusion, it was demonstrated that curcumin loaded electro-responsive hydrogels can be applied for antimicrobial approaches.

6. KURZZUSAMMENFASSUNG

Implantat-assoziierte Infektionen können zu verheerenden Komplikationen führen. Die Implantatoberfläche lässt sich sehr leicht von Bakterien besiedeln, die dann einen Biofilm bilden. Der Biofilm auf der Implantatoberfläche ist schwer zu beseitigen. Daher sind die Präventionsverfahren für eine Implantatoberfläche von entscheidender Bedeutung.² Die Prävention der Infektion beginnt mit dem Wissen über die Infektionsverursachenden Faktoren, welche präoperative, intraoperative sowie postoperative Infekte verursachen können.²³⁷

Systemisch injizierte Antibiotika haben zum Nachteil, dass sie sich im gesamten Körper verteilen und somit nur eine geringe Dosis der Anfangskonzentration am Infektionsort ankommt. Die unzureichende Dosierung solcher antimikrobieller Mittel führt zu einer ungelösten Infektion.²³⁸ Daher besteht ein dringender Bedarf an neuartigen Lösungen, entweder eine, die es dem Medikament ermöglicht, die Infektion mit hoher Konzentration zu erreichen und die Biofilmdurchdringung zu verbessern, oder eine andere, die dazu beitragen kann, die Implantatoberfläche vor einer Bakterienbesiedlung zu schützen.

In dieser Doktorarbeit werden einige Strategien gegen biofilmbasierte Infektionen vorgestellt: lokale Prodrug Antibiotika Verabreichung basierend auf bioorthogonale Chemie, antimikrobielle Beschichtung gegen *S. aureus* unter Verwendung der Diels-Alder-Reaktion mit inversem Elektronenbedarf und MI-dPG-Polymer, antimykotisch imprägnierte PMMA-Knochenzemente gegen Candida Biofilme und elektroreaktive Hydrogele mit photosensibler Curcumin Freisetzung gegen methicillinresistente *S. aureus*.

Im ersten Projekt wurde gezeigt, dass das Tetrazin-modifizierte Biomaterial die Aktivierung mehrerer Dosen von TCO-prodrug *in vitro* und *in vivo* fördert. Diese Ergebnisse deuten darauf hin, dass die therapeutische Wirksamkeit von Antibiotika die Beseitigung bakterieller Infektionen erleichtern kann, während gleichzeitig die antibiotischen Nebenwirkungen reduziert werden können. Die bioorthogonale Chemie zur Verabreichung von Prodrug-Antibiotika hat ein breites Anwendungsspektrum und kann ein potenzieller Kandidat für den klinischen Einsatz bei der Behandlung von Implantat-assoziierten Infektionen sein.

Im zweiten Projekt war die Einführung von Tetrazin in die MI-dPG-Beschichtung in der Lage, die Prodrug-Konzentration und Aktivierung von Daptomycin an der Implantatoberfläche zu erreichen. Die Freisetzung eines aktiven Medikaments in der Implantat Umgebung erhöhte die Ausrottung der MRSA Bakterien. Die Ergebnisse zeigten, dass die MI-dPG-Tetrazin Beschichtung nicht sofort die Einarbeitung eines Antibiotikums in die Beschichtung erfordert. Eine solche Implantatbeschichtung ermöglicht eine Modifikation mit Antibiotika bereits nach dem Einsetzen des Implantats in den Körper des Patienten. Der Vorteil ist, dass der Erreger zum Zeitpunkt der Implantat Insertion nicht bekannt sein muss. Als Zukunftsperspektive wird erwartet, dass ein derart beschichtetes Implantat mit mehreren verschiedenen Antibiotika beladen werden kann, die durch einfache intravenöse Injektion des Antibiotikums ohne weitere Operation mehrfach aus dem Implantat freigesetzt und wieder eingesetzt werden können.

Im dritten Projekt wurde gezeigt, dass alle getesteten Amphotericin B (AmB) Formulierungen aus PMMA-Knochenzementen freigesetzt wurden und ihre Aktivität gegenüber *Candida spp.* nicht verlieren. Die Druckfestigkeit wurde für das Liposomale AmB reduziert, lag aber immer im Rahmen der ISO 5833 Norm, die Dichte bleibt für alle getesteten Formulierungen gleich, die Porosität der Materialien war für das Liposomale AmB am größten. Die neue N-Methyl-D-glucamin/Palmitat-AmB-Formel zeigte eine vergleichbare Wirksamkeit wie das AmB-Desoxycholat, mit einer erhöhten Aktivität und Freisetzung bei Zugabe von einem Porogen. Zusammenfassend zeigten die Ergebnisse eine Wirksamkeit für N-Methyl-D-glucamin/Palmitat AmB als Alternative zu den auf dem Markt erhältlichen AmBs, die in den PMMA-Knochenzement eingebaut werden können.

Im vierten Projekt wurde festgestellt, dass Curcumin aus den elektrostimulierten Hydrogelen freigesetzt wurde und die Freisetzungskinetik moduliert werden kann. Die Lebensfähigkeit der menschlichen Fibroblastenzellen war höher als 94% und freigesetztes Curcumin zeigte 90% Wachstumshemmung von methicillin-resistentem *S. aureus*. Weiterhin wurde gezeigt, dass Curcumin beladene, elektroreaktive Hydrogele für antimikrobielle Ansätze eingesetzt werden können.

7. PUBLICATIONS AND CONFERENCE CONTRIBUTION

7.1 Publications

1. Bio-Orthogonal Chemistry and Reloadable Biomaterial Enable Local Activation of Antibiotic Prodrugs and Enhance Treatments against *Staphylococcus aureus* Infections. Czuban M, Srinivasan S, Yee NA, Agustin E, Koliszak A, Miller E, Khan I, Quinones I, Noory H, Motola C, Volkmer R, Di Luca M, Trampuz A, Royzen M, Mejia Oneto JM. ACS Cent Sci. 2018 Dec 26;4(12):1624-1632. doi: 10.1021/acscentsci.8b00344. Epub 2018 Dec 12.
2. Titanium coating by combining concepts from bio-orthogonal chemistry and mussel inspired polymer enhances antimicrobial activity against *Staphylococcus aureus*. Czuban M, Kulka M.W, Wang L., Koliszak A., Achazi K., Schlaich C., Donskyi I., Di Luca M, Jose M. Mejia Oneto, Maksim Royzen, Rainer Haag, Andrej Trampuz, *in submission
3. Release of different amphotericin B formulations from PMMA bone cements and their activity against *Candida* biofilm
Czuban M., Wulsten D., Wang L., Di Luca M., Trampuz A., Colloids and Surfaces B: Biointerfaces, *in revision
4. Real-Time Antimicrobial Susceptibility Assay of Planktonic and Biofilm Bacteria by Isothermal Microcalorimetry.
Butini ME, Gonzalez Moreno M, Czuban M, Koliszak A, Tkhalishvili T, Trampuz A, Di Luca M. Adv Exp Med Biol. 2018
5. Electro-responsive graphene oxide hydrogels for skin bandages: The outcome of gelatin and trypsin immobilization.
di Luca M, Vittorio O, Cirillo G, Curcio M, Czuban M, Voli F, Farfalla A, Hampel S, Nicoletta FP, Iemma F. Int J Pharm. 2018 Jul 30;546(1-2):50-60. doi: 10.1016/j.ijpharm.2018.05.027. Epub 2018 May 11.

7.2 Oral Presentations

1. "Activity of amphotericin B released from bone cement against *Candida* biofilm".
M.Czuban
Workshop on Prosthetic Joint Infection, Pro-Implant Foundation, April 2019, Berlin
2. "Catch and release system for local antibiotic delivery - a new strategy to treat biofilm infections",
M. Czuban, M. Royzen, S. Srinivasan, E. Miller, N. Yee, A. Trampuz, J. Mejia Oneto
ECCMID Congress, the European Congress of Clinical Microbiology and Infectious Diseases 2018, Madrid, Spain.
3. "Catch & release strategy for treatment of infection".
M.Czuban
Workshop on Prosthetic Joint Infection, Pro-Implant Foundation, September 2018, Berlin
4. "Novel approaches for local antibiotic therapy".
M.Czuban
Workshop on Prosthetic Joint Infection, Pro-Implant Foundation, October 2016, Berlin

7.3 Poster presentations

1. "Activity of rifampin on planktonic and biofilm *Candida* spp. (alone and in combination with amphotericin B) determined by microcalorimetry"
Czuban M., Maiolo E., Trampuz A.
ECCMID Congress, the European Congress of Clinical Microbiology and Infectious Diseases,
2016, Amsterdam, Netherlands
2. "Amphotericin B - loaded PMMA cement strongly inhibits *Candida* biofilm formation"
Czuban M., Di Luca M., Trampuz A.
ECCMID Congress, the European Congress of Clinical Microbiology and Infectious Diseases,
2017, Vienna, Austria
3. "Titanium coating by combining concepts from bio-orthogonal chemistry and mussel inspired polymer enhance antimicrobial activity against *Staphylococcus aureus*"
Czuban M., Kulka M.W., Wang L., Koliszak A., Achazi K, Donskyi I., Di Luca M., Mejia Oneto J.M, Royzen M., Haag R., Trampuz A.,
EBJIS Annual Meeting of the European Bone and Joint Infection Society
2019, Antwerp, Belgium
4. "Amphotericin B-loaded PMMA cement inhibits *Candida* biofilms"
Czuban M., Wang L., Di Luca M. Trampuz A.
eCM Cells and Materials Conference,
2019, Davos, Switzerland

8. REFERENCES

1. Veerachamy, S.; Yarlagadda, T.; Manivasagam, G.; Yarlagadda, P. K., Bacterial adherence and biofilm formation on medical implants: a review. *Proc Inst Mech Eng H* **2014**, *228* (10), 1083-99.
2. Arciola, C. R.; Campoccia, D.; Montanaro, L., Implant infections: adhesion, biofilm formation and immune evasion. *Nat Rev Microbiol* **2018**, *16* (7), 397-409.
3. Trampuz, A.; Zimmerli, W., Antimicrobial agents in orthopaedic surgery: Prophylaxis and treatment. *Drugs* **2006**, *66* (8), 1089-105.
4. Gristina, A. G., Implant failure and the immuno-incompetent fibro-inflammatory zone. *Clinical orthopaedics and related research* **1994**, (298), 106-18.
5. Southwood, R. T.; Rice, J. L.; McDonald, P. J.; Hakendorf, P. H.; Rozenbils, M. A., Infection in experimental hip arthroplasties. *The Journal of bone and joint surgery. British volume* **1985**, *67* (2), 229-31.
6. McIntyre, W. F.; Healey, J. S., Cardiac implantable electronic device infections: From recognizing risk to prevention. *Heart rhythm* **2017**, *14* (6), 846-847.
7. Andersen, O. Z.; Offermanns, V.; Sillassen, M.; Almtoft, K. P.; Andersen, I. H.; Sorensen, S.; Jeppesen, C. S.; Kraft, D. C.; Bottiger, J.; Rasse, M.; Kloss, F.; Foss, M., Accelerated bone ingrowth by local delivery of strontium from surface functionalized titanium implants. *Biomaterials* **2013**, *34* (24), 5883-90.
8. Trampuz, A.; Zimmerli, W., Diagnosis and treatment of implant-associated septic arthritis and osteomyelitis. *Current Infectious Disease Reports* **2008**, *10* (5), 394-403.
9. Trampuz, A.; Zimmerli, W., Diagnosis and treatment of infections associated with fracture-fixation devices. *Injury* **2006**, *37* Suppl 2, S59-66.
10. Weiss, A. J.; Elixhauser, A.; Bae, J.; Encinosa, W., Origin of Adverse Drug Events in U.S. Hospitals, 2011: Statistical Brief #158. In *Healthcare Cost and Utilization Project (HCUP) Statistical Briefs*, Agency for Healthcare Research and Quality (US): Rockville (MD), 2006.
11. Li, C.; Yu, D. F.; Inoue, T.; Yang, D. J.; Tansey, W.; Liu, C. W.; Milas, L.; Hunter, N. R.; Kim, E. E.; Wallace, S., Synthesis, biodistribution and imaging properties of indium-111-DTPA-paclitaxel in mice bearing mammary tumors. *Journal of nuclear medicine : official publication, Society of Nuclear Medicine* **1997**, *38* (7), 1042-7.
12. Kearney, C. J.; Mooney, D. J., Macroscale delivery systems for molecular and cellular payloads. *Nature materials* **2013**, *12* (11), 1004-17.
13. Huebsch, N.; Kearney, C. J.; Zhao, X.; Kim, J.; Cezar, C. A.; Suo, Z.; Mooney, D. J., Ultrasound-triggered disruption and self-healing of reversibly cross-linked hydrogels for drug delivery and enhanced chemotherapy. *Proceedings of the National Academy of Sciences of the United States of America* **2014**, *111* (27), 9762-9767.
14. Mejia Oneto, J. M.; Gupta, M.; Leach, J. K.; Lee, M.; Sutcliffe, J. L., Implantable biomaterial based on click chemistry for targeting small molecules. *Acta Biomater* **2014**, *10* (12), 5099-5105.
15. Mejia Oneto, J. M.; Khan, I.; Seebald, L.; Royzen, M., In Vivo Bioorthogonal Chemistry Enables Local Hydrogel and Systemic Pro-Drug To Treat Soft Tissue Sarcoma. *ACS Cent Sci* **2016**, *2* (7), 476-82.
16. I., L.; M., L.; S., A.; SA., M.; HM, T., Biofilm Formation, Maturation and Prevention: A Review. *Journal of Bacteriology and Mycology* **2019**, *6* (1: 1092).
17. Flemming, H. C.; Wingender, J., The biofilm matrix. *Nat Rev Microbiol* **2010**, *8* (9), 623-33.
18. Burmolle, M.; Webb, J. S.; Rao, D.; Hansen, L. H.; Sorensen, S. J.; Kjelleberg, S., Enhanced biofilm formation and increased resistance to antimicrobial agents and bacterial

- invasion are caused by synergistic interactions in multispecies biofilms. *Appl Environ Microbiol* **2006**, 72 (6), 3916-23.
19. Lee, K. W. K.; Periasamy, S.; Mukherjee, M.; Xie, C.; Kjelleberg, S.; Rice, S. A., Biofilm development and enhanced stress resistance of a model, mixed-species community biofilm. *The ISME Journal* **2013**, 8 (4), 894-907.
 20. Otto, M., Staphylococcal infections: mechanisms of biofilm maturation and detachment as critical determinants of pathogenicity. *Annu Rev Med* **2013**, 64, 175-88.
 21. Vuong, C.; Saenz, H. L.; Gotz, F.; Otto, M., Impact of the agr quorum-sensing system on adherence to polystyrene in Staphylococcus aureus. *J Infect Dis* **2000**, 182 (6), 1688-93.
 22. Dongari-Bagtzoglou, A.; Kashleva, H.; Dwivedi, P.; Diaz, P.; Vasilakos, J., Characterization of Mucosal Candida albicans Biofilms. *PLOS ONE* **2009**, 4 (11), e7967.
 23. Bamford, C. V.; Mello, A.; Nobbs, A. H.; Dutton, L. C.; Vickerman, M. M.; Jenkinson, H. F., Streptococcus gordonii Modulates Candida albicans Biofilm Formation through Intergeneric Communication. *Infection and Immunity* **2009**, 77 (9), 3696.
 24. Kruppa, M., Quorum sensing and Candida albicans. *Mycoses* **2009**, 52 (1), 1-10.
 25. Kim, S. J.; Chang, J.; Rimal, B.; Yang, H.; Schaefer, J., Surface proteins and the formation of biofilms by Staphylococcus aureus. *Biochimica et Biophysica Acta (BBA) - Biomembranes* **2018**, 1860 (3), 749-756.
 26. Bos, R.; van der Mei, H. C.; Busscher, H. J., Physico-chemistry of initial microbial adhesive interactions - its mechanisms and methods for study. *Fems Microbiology Reviews* **1999**, 23 (2), 179-230.
 27. Ribeiro, M.; Monteiro Fj Fau - Ferraz, M. P.; Ferraz, M. P., Infection of orthopedic implants with emphasis on bacterial adhesion process and techniques used in studying bacterial-material interactions. *Biomatter*. **2012** (2159-2535 (Electronic)).
 28. Cavalheiro, M.; Teixeira, M. C., Candida Biofilms: Threats, Challenges, and Promising Strategies. *Front Med (Lausanne)* **2018**, 5, 28.
 29. Mandlik, A.; Swierczynski, A.; Das, A.; Ton-That, H., Pili in Gram-positive bacteria: assembly, involvement in colonization and biofilm development. *Trends Microbiol* **2008**, 16 (1), 33-40.
 30. Hori, K.; Matsumoto, S., *Bacterial adhesion: From mechanism to control*. 2010; Vol. 48, p 424-434.
 31. Bose, J. L.; Lehman, M. K.; Fey, P. D.; Bayles, K. W., Contribution of the Staphylococcus aureus Atl AM and GL murein hydrolase activities in cell division, autolysis, and biofilm formation. *PLoS One* **2012**, 7 (7), e42244.
 32. Gross, M.; Cramton, S. E.; Gotz, F.; Peschel, A., Key Role of Teichoic Acid Net Charge in Staphylococcus aureus Colonization of Artificial Surfaces. *Infection and Immunity* **2001**, 69 (5), 3423-3426.
 33. Whitchurch, C. B.; Tolker-Nielsen, T.; Ragas, P. C.; Mattick, J. S., Extracellular DNA required for bacterial biofilm formation. *Science* **2002**, 295 (5559), 1487.
 34. Ratner, A. J.; Mann, E. E.; Rice, K. C.; Boles, B. R.; Endres, J. L.; Ranjit, D.; Chandramohan, L.; Tsang, L. H.; Smeltzer, M. S.; Horswill, A. R.; Bayles, K. W., Modulation of eDNA Release and Degradation Affects Staphylococcus aureus Biofilm Maturation. *PLoS ONE* **2009**, 4 (6), e5822.
 35. Nobile, C. J.; Andes, D. R.; Nett, J. E.; Smith, F. J., Jr.; Yue, F.; Phan, Q.-T.; Edwards, J. E., Jr.; Filler, S. G.; Mitchell, A. P., Critical Role of Bcr1-Dependent Adhesins in C. albicans Biofilm Formation In Vitro and In Vivo. *PLOS Pathogens* **2006**, 2 (7), e63.
 36. Henriques, M.; Azeredo, J.; Oliveira, R., Candida Species Adhesion to Oral Epithelium: Factors Involved and Experimental Methodology Used. *Critical Reviews in Microbiology* **2006**, 32 (4), 217-226.

37. Chandra, J.; Kuhn, D. M.; Mukherjee, P. K.; Hoyer, L. L.; McCormick, T.; Ghannoum, M. A., Biofilm formation by the fungal pathogen *Candida albicans*: development, architecture, and drug resistance. *Journal of Bacteriology* **2001**, *183* (18), 5385.
38. Silva, S.; Henriques, M.; Martins, A.; Oliveira, R.; Williams, D.; Azeredo, J., Biofilms of non-*Candida albicans* *Candida* species: quantification, structure and matrix composition. *Medical Mycology* **2009**, *47* (7), 681-689.
39. Lattif, A. A.; K. Mukherjee, P.; Chandra, J.; Swindell, K.; Lockhart, S. R.; Diekema, D. J.; Pfaller, M. A.; Ghannoum, M. A., Characterization of biofilms formed by *Candida parapsilosis*, *C. metapsilosis*, and *C. orthopsilosis*. *International Journal of Medical Microbiology* **2010**, *300* (4), 265-270.
40. Yarwood, J. M.; Schlievert, P. M., Quorum sensing in *Staphylococcus* infections. *Journal of Clinical Investigation* **2003**, *112* (11), 1620-1625.
41. Wang, R.; Braughton, K. R.; Kretschmer, D.; Bach, T. H.; Queck, S. Y.; Li, M.; Kennedy, A. D.; Dorward, D. W.; Klebanoff, S. J.; Peschel, A.; DeLeo, F. R.; Otto, M., Identification of novel cytolytic peptides as key virulence determinants for community-associated MRSA. *Nat Med* **2007**, *13* (12), 1510-4.
42. Gristina, A., Biomaterial-centered infection: microbial adhesion versus tissue integration. 1987. *Clinical orthopaedics and related research* **2004**, (427), 4-12.
43. Stones, D. H.; Krachler, A. M., Against the tide: the role of bacterial adhesion in host colonization. *Biochem Soc Trans* **2016**, *44* (6), 1571-1580.
44. Gristina, A. G., Biomaterial-centered infection: microbial adhesion versus tissue integration. *Science* **1987**, *237* (4822), 1588-95.
45. Patel, J. D.; Krupka T Fau - Anderson, J. M.; Anderson, J. M., iNOS-mediated generation of reactive oxygen and nitrogen species by biomaterial-adherent neutrophils. *J Biomed Mater Res A* **2007**, *80* (1549-3296 (Print)), 381-90.
46. Kaplan, S. S.; Basford, R. E.; Mora, E.; Jeong, M. H.; Simmons, R. L., Biomaterial-induced alterations of neutrophil superoxide production. *Journal of biomedical materials research* **1992**, *26* (8), 1039-51.
47. Zimmerli W Fau - Waldvogel, F. A.; Waldvogel Fa Fau - Vaudaux, P.; Vaudaux P Fau - Nydegger, U. E.; Nydegger, U. E., Pathogenesis of foreign body infection: description and characteristics of an animal model. *J Infect Dis.* **1982**, (0022-1899 (Print)).
48. Thurlow, L. R.; Hanke, M. L.; Fritz, T.; Angle, A.; Aldrich, A.; Williams, S. H.; Engebretsen, I. L.; Bayles, K. W.; Horswill, A. R.; Kielian, T., *Staphylococcus aureus* biofilms prevent macrophage phagocytosis and attenuate inflammation in vivo. *J Immunol* **2011**, *186* (11), 6585-96.
49. Leid, J. G.; Shirliff, M. E.; Costerton, J. W.; Stoodley, P., Human leukocytes adhere to, penetrate, and respond to *Staphylococcus aureus* biofilms. *Infect Immun* **2002**, *70* (11), 6339-45.
50. Hanke, M. L.; Angle, A.; Kielian, T., MyD88-dependent signaling influences fibrosis and alternative macrophage activation during *Staphylococcus aureus* biofilm infection. *PLoS One* **2012**, *7* (8), e42476.
51. Benoit, M.; Desnues, B.; Mege, J. L., Macrophage polarization in bacterial infections. *J Immunol* **2008**, *181* (6), 3733-9.
52. Gries, C. M.; Kielian, T., Staphylococcal Biofilms and Immune Polarization During Prosthetic Joint Infection. *The Journal of the American Academy of Orthopaedic Surgeons* **2017**, *25 Suppl 1*, S20-s24.
53. Hanke, M. L.; Kielian, T., Deciphering mechanisms of staphylococcal biofilm evasion of host immunity. *Front Cell Infect Microbiol* **2012**, *2*, 62-62.
54. Mbalaviele, G.; Novack, D. V.; Schett, G.; Teitelbaum, S. L., Inflammatory osteolysis: a conspiracy against bone. *The Journal of clinical investigation* **2017**, *127* (6), 2030-2039.

55. Heim, C. E.; Vidlak, D.; Scherr, T. D.; Hartman, C. W.; Garvin, K. L.; Kielian, T., IL-12 promotes myeloid-derived suppressor cell recruitment and bacterial persistence during *Staphylococcus aureus* orthopedic implant infection. *J Immunol* **2015**, *194* (8), 3861-3872.
56. Moriarty, T. F.; Zaat, S. A. J.; Busscher, H. J., *Biomaterials Associated Infection. Immunological Aspects and Antimicrobial Strategies*. Springer: 2012.
57. Bjarnsholt, T.; Jensen, P. Ø.; Moser, C.; Høiby, N., *Biofilm Infections*. Springer: New York, NY, 2011.
58. Fernandez-Sampedro, M.; Farinas-Alvarez, C.; Garces-Zarzalejo, C.; Alonso-Aguirre, M. A.; Salas-Venero, C.; Martinez-Martinez, L.; Farinas, M. C., Accuracy of different diagnostic tests for early, delayed and late prosthetic joint infection. *BMC infectious diseases* **2017**, *17* (1), 592.
59. Deirmengian, C.; Kardos, K.; Kilmartin, P.; Gulati, S.; Citrano, P.; Booth, R. E., Jr., The Alpha-defensin Test for Periprosthetic Joint Infection Responds to a Wide Spectrum of Organisms. *Clinical orthopaedics and related research* **2015**, *473* (7), 2229-35.
60. Deurenberg, R. H.; Bathoorn, E.; Chlebowicz, M. A.; Couto, N.; Ferdous, M.; Garcia-Cobos, S.; Kooistra-Smid, A. M.; Raangs, E. C.; Rosema, S.; Veloo, A. C.; Zhou, K.; Friedrich, A. W.; Rossen, J. W., Application of next generation sequencing in clinical microbiology and infection prevention. *Journal of biotechnology* **2017**, *243*, 16-24.
61. Tagini, F.; Greub, G., Bacterial genome sequencing in clinical microbiology: a pathogen-oriented review. *European journal of clinical microbiology & infectious diseases : official publication of the European Society of Clinical Microbiology* **2017**, *36* (11), 2007-2020.
62. van Belkum, A.; Welker, M.; Pincus, D.; Charrier, J. P.; Girard, V., Matrix-Assisted Laser Desorption Ionization Time-of-Flight Mass Spectrometry in Clinical Microbiology: What Are the Current Issues? *Annals of laboratory medicine* **2017**, *37* (6), 475-483.
63. Zimmerli, W.; Trampuz, A.; Ochsner, P. E., Prosthetic-Joint Infections. *New England Journal of Medicine* **2004**, *351* (16), 1645-1654.
64. Trampuz, A.; Hanssen, A. D.; Osmon, D. R.; Mandrekar, J.; Steckelberg, J. M.; Patel, R., Synovial fluid leukocyte count and differential for the diagnosis of prosthetic knee infection. *Am J Med* **2004**, *117* (8), 556-62.
65. Trampuz, A.; Piper, K. E.; Jacobson, M. J.; Hanssen, A. D.; Unni, K. K.; Osmon, D. R.; Mandrekar, J. N.; Cockerill, F. R.; Steckelberg, J. M.; Greenleaf, J. F.; Patel, R., Sonication of Removed Hip and Knee Prostheses for Diagnosis of Infection. *New England Journal of Medicine* **2007**, *357* (7), 654-663.
66. Rowan, F. E.; Donaldson, M. J.; Pietrzak, J. R.; Haddad, F. S., The Role of One-Stage Exchange for Prosthetic Joint Infection. *Curr Rev Musculoskelet Med* **2018**, *11* (3), 370-379.
67. Leite, P. S.; Figueiredo, S.; Sousa, R., Prosthetic Joint Infection: Report on the One versus Two-stage Exchange EBJIS Survey. (2206-3552 (Print)).
68. Leite, P. S.; Figueiredo, S.; Sousa, R., Prosthetic Joint Infection: Report on the One versus Two-stage Exchange EBJIS Survey. *J Bone Jt Infect* **2016**, *1* (2206-3552 (Print)), 1-6.
69. Osmon, D. R.; Berbari Ef Fau - Berendt, A. R.; Berendt Ar Fau - Lew, D.; Lew D Fau - Zimmerli, W.; Zimmerli W Fau - Steckelberg, J. M.; Steckelberg Jm Fau - Rao, N.; Rao N Fau - Hanssen, A.; Hanssen A Fau - Wilson, W. R.; Wilson, W. R., Diagnosis and management of prosthetic joint infection: clinical practice guidelines by the Infectious Diseases Society of America. *Clin Infect Dis.* **2013**, (1537-6591 (Electronic)).
70. Negus, J. J.; Gifford, P. B.; Haddad, F. S., Single-Stage Revision Arthroplasty for Infection-An Underutilized Treatment Strategy. (1532-8406 (Electronic)).
71. Choi, H. R.; Kwon, Y. M.; Freiberg, A. A.; Malchau, H., Comparison of one-stage revision with antibiotic cement versus two-stage revision results for infected total hip arthroplasty. *J Arthroplasty* **2013**, *28* (8 Suppl), 66-70.

72. Gehrke, T.; Zahar A Fau - Kendoff, D.; Kendoff, D., One-stage exchange: it all began here. *Bone Joint J.* **2013**, *95-B(11 Suppl A):77-83* (2049-4408 (Electronic)).
73. Klug, D.; Balde, M.; Pavin, D.; Hidden-Lucet, F.; Clementy, J.; Sadoul, N.; Rey, J. L.; Lande, G.; Lazarus, A.; Victor, J.; Barnay, C.; Grandbastien, B.; Kacet, S.; Group, P. S., Risk factors related to infections of implanted pacemakers and cardioverter-defibrillators: results of a large prospective study. *Circulation* **2007**, *116* (12), 1349-55.
74. Baddour, L. M.; Bettmann, M. A.; Bolger, A. F.; Epstein, A. E.; Ferrieri, P.; Gerber, M. A.; Gewitz, M. H.; Jacobs, A. K.; Levison, M. E.; Newburger, J. W.; Pallasch, T. J.; Wilson, W. R.; Baltimore, R. S.; Falace, D. A.; Shulman, S. T.; Tani, L. Y.; Taubert, K. A.; Aha, Nonvalvular cardiovascular device-related infections. *Circulation* **2003**, *108* (16), 2015-31.
75. Chua, J. D.; Wilkoff, B. L.; Lee, I.; Juratli, N.; Longworth, D. L.; Gordon, S. M., Diagnosis and management of infections involving implantable electrophysiologic cardiac devices. *Ann Intern Med* **2000**, *133* (8), 604-8.
76. Fayaz, A.; Nashy, M. R.; Eapen, S.; Firstenberg, M. S., Prosthetic Valve Endocarditis. **2018**.
77. Karchmer, A. W.; Longworth, D. L., Infections of intracardiac devices. *Infect Dis Clin North Am* **2002**, *16* (2), 477-505, xii.
78. David, T. E.; Feindel, C. M.; Armstrong, S.; Sun, Z., Reconstruction of the mitral anulus. A ten-year experience. *J Thorac Cardiovasc Surg* **1995**, *110* (5), 1323-32.
79. Francischetto, O.; Silva, L. A. P. d.; Senna, K. M. S. e.; Vasques, M. R.; Barbosa, G. F.; Weksler, C.; Ramos, R. G.; Golebiovski, W. F.; Lamas, C. d. C., Healthcare-associated infective endocarditis: a case series in a referral hospital from 2006 to 2011. *Arq Bras Cardiol* **2014**, *103* (4), 292-298.
80. Gnann Jw Fau - Dismukes, W. E.; Dismukes, W. E., Prosthetic valve endocarditis: an overview. *Herz* **1983**, *8*, 320-331.
81. Murdoch, D. R.; Corey, G. R.; Hoen, B.; Miro, J. M.; Fowler, V. G., Jr.; Bayer, A. S.; Karchmer, A. W.; Olaison, L.; Pappas, P. A.; Moreillon, P.; Chambers, S. T.; Chu, V. H.; Falco, V.; Holland, D. J.; Jones, P.; Klein, J. L.; Raymond, N. J.; Read, K. M.; Tripodi, M. F.; Utili, R.; Wang, A.; Woods, C. W.; Cabell, C. H.; International Collaboration on Endocarditis-Prospective Cohort Study, I., Clinical presentation, etiology, and outcome of infective endocarditis in the 21st century: the International Collaboration on Endocarditis-Prospective Cohort Study. *Arch Intern Med* **2009**, *169* (5), 463-73.
82. Gandelman, G.; Frishman, W. H.; Wiese, C.; Green-Gastwirth, V.; Hong, S.; Aronow, W. S.; Horowitz, H. W., Intravascular device infections: epidemiology, diagnosis, and management. *Cardiol Rev* **2007**, *15* (1), 13-23.
83. Mermel, L. A., Prevention of intravascular catheter-related infections. *Ann Intern Med* **2000**, *132* (5), 391-402.
84. Conway, L. J.; Liu, J.; Harris, A. D.; Larson, E. L., Risk Factors for Bacteremia in Patients With Urinary Catheter-Associated Bacteriuria. *Am J Crit Care* **2016**, *26* (1), 43-52.
85. Murray, R. J., Staphylococcus aureus infective endocarditis: diagnosis and management guidelines. *Intern Med J* **2005**, *35 Suppl 2* (1445-5994 (Electronic)), S25-44.
86. Nguyen, M. H.; Nguyen, M. L.; Yu, V. L.; McMahon, D.; Keys, T. F.; Amidi, M., Candida prosthetic valve endocarditis: prospective study of six cases and review of the literature. *Clin Infect Dis* **1996**, *22* (2), 262-7.
87. Cabell, C. H.; Jollis, J. G.; Peterson, G. E.; Corey, G. R.; Anderson, D. J.; Sexton, D. J.; Woods, C. W.; Reller, L. B.; Ryan, T.; Fowler, V. G., Jr., Changing patient characteristics and the effect on mortality in endocarditis. *Arch Intern Med* **2002**, *162* (1), 90-4.
88. Ivert, T. S.; Dismukes, W. E.; Cobbs, C. G.; Blackstone, E. H.; Kirklin, J. W.; Bergdahl, L. A., Prosthetic valve endocarditis. *Circulation* **1984**, *69* (2), 223-232.

89. Habib, G.; Badano, L.; Tribouilloy, C.; Vilacosta, I.; Zamorano, J. L.; Galderisi, M.; Voigt, J. U.; Sicari, R.; Cosyns, B.; Fox, K.; Aakhus, S.; European Association of, E., Recommendations for the practice of echocardiography in infective endocarditis. *Eur J Echocardiogr* **2010**, *11* (2), 202-19.
90. Hasse, B.; Husmann, L.; Zinkernagel, A.; Weber, R.; Lachat, M.; Mayer, D., Vascular graft infections. *Swiss Med Wkly* **2013**, *143*, w13754.
91. Valentine, R. J.; Timaran Ch Fau - Modrall, G. J.; Modrall GJ Fau - Smith, S. T.; Smith St Fau - Arko, F. R.; Arko Fr Fau - Clagett, G. P.; Clagett, G. P., Secondary aortoenteric fistulas versus paraprosthetic erosions: is bleeding associated with a worse outcome? *J Am Coll Surg* **2008**, *207*(6) (1879-1190 (Electronic)), 922-7.
92. Antonios, V. S.; Baddour, L. M., Intra-arterial device infections. *Current Infectious Disease Reports* **2004**, *6* (4), 263–269.
93. Legout, L.; D'Elia, P. V.; Sarraz-Bournet, B.; Haulon, S.; Meybeck, A.; Senneville, E.; Leroy, O., Diagnosis and management of prosthetic vascular graft infections. *Med Mal Infect* **2012**, *42* (3), 102-9.
94. Conen, A.; Fux, C. A.; Vajkoczy, P.; Trampuz, A., Management of infections associated with neurosurgical implanted devices. *Expert Review of Anti-infective Therapy* **2016**, *15* (3), 241-255.
95. Robert A. McGovern; Kathleen M. Kelly, B. A.; Andrew K. Chan, B. S.; Morrissey, N. J.; II, G. M. M., Should ventriculoatrial shunting be the procedure of choice for normal-pressure hydrocephalus? *J Neurosurg* **2014**, *120*, 1458–1464.
96. Darouiche, R. O., Treatment of infections associated with surgical implants. *The New England journal of medicine* **2004**, *350* (14), 1422-9.
97. Kumar, K.; Wilson, J. R.; Taylor, R. S.; Gupta, S., Complications of spinal cord stimulation, suggestions to improve outcome, and financial impact. *Journal of neurosurgery. Spine* **2006**, *5* (3), 191-203.
98. Kurtz, S. M.; Lau, E.; Watson, H.; Schmier, J. K.; Parvizi, J., Economic burden of periprosthetic joint infection in the United States. *J Arthroplasty* **2012**, *27* (8 Suppl), 61-5.e1.
99. James, R. C.; Macleod, C. J., Induction of staphylococcal infections in mice with small inocula introduced on sutures. *Br J Exp Pathol* **1961**, *42* (3), 266-277.
100. Zimmerli, W.; Waldvogel, F. A.; Vaudaux, P.; Nydegger, U. E., Pathogenesis of foreign body infection: description and characteristics of an animal model. *J Infect Dis* **1982**, *146* (4), 487-97.
101. Conen, A.; Walti, L. N.; Merlo, A.; Fluckiger, U.; Battegay, M.; Trampuz, A., Characteristics and treatment outcome of cerebrospinal fluid shunt-associated infections in adults: a retrospective analysis over an 11-year period. *Clin Infect Dis* **2008**, *47* (1), 73-82.
102. Chiang, H. Y.; Kamath, A. S.; Pottinger, J. M.; Greenlee, J. D.; Howard, M. A., 3rd; Cavanaugh, J. E.; Herwaldt, L. A., Risk factors and outcomes associated with surgical site infections after craniotomy or craniectomy. *J Neurosurg* **2014**, *120* (2), 509-21.
103. Sneh-Arbib, O.; Shiferstein, A.; Dagan, N.; Fein, S.; Telem, L.; Muchtar, E.; Eliakim-Raz, N.; Rubinovitch, B.; Rubin, G.; Rappaport, Z. H.; Paul, M., Surgical site infections following craniotomy focusing on possible post-operative acquisition of infection: prospective cohort study. *European journal of clinical microbiology & infectious diseases : official publication of the European Society of Clinical Microbiology* **2013**, *32* (12), 1511-6.
104. Borgbjerg, B. M.; Gjerris, F.; Albeck, M. J.; Borgesen, S. E., Risk of infection after cerebrospinal fluid shunt: an analysis of 884 first-time shunts. *Acta neurochirurgica* **1995**, *136* (1-2), 1-7.
105. Kulkarni, A. V.; Drake, J. M.; Lamberti-Pasculli, M., Cerebrospinal fluid shunt infection: a prospective study of risk factors. *J Neurosurg* **2001**, *94* (2), 195-201.

106. McGirt, M. J.; Zaas, A.; Fuchs, H. E.; George, T. M.; Kaye, K.; Sexton, D. J., Risk factors for pediatric ventriculoperitoneal shunt infection and predictors of infectious pathogens. *Clin Infect Dis* **2003**, *36* (7), 858-62.
107. Arabi, Y.; Memish, Z. A.; Balkhy, H. H.; Francis, C.; Ferayan, A.; Al Shimemeri, A.; Almuneef, M. A., Ventriculostomy-associated infections: incidence and risk factors. *American journal of infection control* **2005**, *33* (3), 137-43.
108. Lozier, A. P.; Sciacca, R. R.; Romagnoli, M. F.; Connolly, E. S., Jr., Ventriculostomy-related infections: a critical review of the literature. *Neurosurgery* **2002**, *51* (1), 170-81; discussion 181-2.
109. Lyke, K. E.; Obasanjo, O. O.; Williams, M. A.; O'Brien, M.; Chotani, R.; Perl, T. M., Ventriculitis complicating use of intraventricular catheters in adult neurosurgical patients. *Clin Infect Dis* **2001**, *33* (12), 2028-33.
110. Kleber, C.; Schaser, K. D.; Trampuz, A., [Complication management of infected osteosynthesis: Therapy algorithm for peri-implant infections]. *Der Chirurg; Zeitschrift für alle Gebiete der operativen Medizin* **2015**, *86* (10), 925-34.
111. Dashti, S. R.; Baharvahdat, H.; Spetzler, R. F.; Sauvageau, E.; Chang, S. W.; Stiefel, M. F.; Park, M. S.; Bambakidis, N. C., Operative intracranial infection following craniotomy. *Neurosurgical focus* **2008**, *24* (6), E10.
112. Morton, R. P.; Abecassis, I. J.; Hanson, J. F.; Barber, J.; Nerva, J. D.; Emerson, S. N.; Ene, C. I.; Chowdhary, M. M.; Levitt, M. R.; Ko, A. L.; Dellit, T. H.; Chesnut, R. M., Predictors of infection after 754 cranioplasty operations and the value of intraoperative cultures for cryopreserved bone flaps. *J Neurosurg* **2016**, *125* (3), 766-70.
113. Riordan, M. A.; Simpson, V. M.; Hall, W. A., Analysis of Factors Contributing to Infections After Cranioplasty: A Single-Institution Retrospective Chart Review. *World neurosurgery* **2016**, *87*, 207-13.
114. Sundseth, J.; Sundseth, A.; Berg-Johnsen, J.; Sorteberg, W.; Lindegaard, K. F., Cranioplasty with autologous cryopreserved bone after decompressive craniectomy: complications and risk factors for developing surgical site infection. *Acta neurochirurgica* **2014**, *156* (4), 805-811.
115. Borgbjerg, B. M.; Gjerris, F.; Albeck, M. J.; Hauerberg, J.; Borgesen, S. V., A comparison between ventriculo-peritoneal and ventriculo-atrial cerebrospinal fluid shunts in relation to rate of revision and durability. *Acta neurochirurgica* **1998**, *140* (5), 459-64; discussion 465.
116. Olsen, L.; Frykberg, T., Complications in the treatment of hydrocephalus in children. A comparison of ventriculoatrial and ventriculoperitoneal shunts in a 20-year material. *Acta paediatrica Scandinavica* **1983**, *72* (3), 385-90.
117. Burstrom, G.; Andresen, M.; Bartek, J., Jr.; Fyttagoridis, A., Subacute bacterial endocarditis and subsequent shunt nephritis from ventriculoatrial shunting 14 years after shunt implantation. *BMJ case reports* **2014**, *2014*.
118. Sacar, S.; Turgut, H.; Toprak, S.; Cirak, B.; Coskun, E.; Yilmaz, O.; Tekin, K., A retrospective study of central nervous system shunt infections diagnosed in a university hospital during a 4-year period. *BMC infectious diseases* **2006**, *6* (1), 43.
119. Olsen, M. A.; Chu-Ongsakul, S.; Brandt, K. E.; Dietz, J. R.; Mayfield, J.; Fraser, V. J., Hospital-associated costs due to surgical site infection after breast surgery. *Archives of surgery (Chicago, Ill. : 1960)* **2008**, *143* (1), 53-60; discussion 61.
120. Spear, S. L.; Howard, M. A.; Boehmler, J. H.; Ducic, I.; Low, M.; Abbruzzese, M. R., The infected or exposed breast implant: management and treatment strategies. *Plast Reconstr Surg* **2004**, *113* (6), 1634-44.
121. Chun, J. K.; Schulman, M. R., The infected breast prosthesis after mastectomy reconstruction: successful salvage of nine implants in eight consecutive patients. *Plast Reconstr Surg* **2007**, *120* (3), 581-9.

122. Bode, L. G.; Kluytmans, J. A.; Wertheim, H. F.; Bogaers, D.; Vandenbroucke-Grauls, C. M.; Roosendaal, R.; Troelstra, A.; Box, A. T.; Voss, A.; van der Tweel, I.; van Belkum, A.; Verbrugh, H. A.; Vos, M. C., Preventing surgical-site infections in nasal carriers of *Staphylococcus aureus*. *The New England journal of medicine* **2010**, *362* (1), 9-17.
123. Greenky, M.; Gandhi K Fau - Pulido, L.; Pulido L Fau - Restrepo, C.; Restrepo C Fau - Parvizi, J.; Parvizi, J., Preoperative anemia in total joint arthroplasty: is it associated with periprosthetic joint infection? *Clin Orthop Relat Res.* **2012**, (1528-1132 (Electronic)).
124. Gurusamy, K. S.; Koti, R.; Wilson, P.; Davidson, B. R., Antibiotic prophylaxis for the prevention of methicillin-resistant *Staphylococcus aureus* (MRSA) related complications in surgical patients. *Cochrane Database Syst Rev* **2013**, (8), CD010268.
125. Jaggessar, A.; Shahali, H.; Mathew, A.; Yarlagaadda, P., Bio-mimicking nano and micro-structured surface fabrication for antibacterial properties in medical implants. *J Nanobiotechnology* **2017**, *15* (1), 64.
126. Tande, A. J.; Patel, R., Prosthetic joint infection. *Clin. Microbiol. Rev.* **2014**, *27* (1098-6618 (Electronic)).
127. Monds, R. D.; O'Toole, G. A., The developmental model of microbial biofilms: ten years of a paradigm up for review. *Trends Microbiol* **2009**, *17* (2), 73-87.
128. Chung, K. K.; Schumacher, J. F.; Sampson, E. M.; Burne, R. A.; Antonelli, P. J.; Brennan, A. B., Impact of engineered surface microtopography on biofilm formation of *Staphylococcus aureus*. *Biointerphases* **2007**, *2* (2), 89-94.
129. Maddikeri, R. R.; Tosatti, S.; Schuler, M.; Chessari, S.; Textor, M.; Richards, R. G.; Harris, L. G., Reduced medical infection related bacterial strains adhesion on bioactive RGD modified titanium surfaces: a first step toward cell selective surfaces. *J Biomed Mater Res A* **2008**, *84* (2), 425-35.
130. Raphael, J.; Holodniy, M.; Goodman, S. B.; Heilshorn, S. C., Multifunctional coatings to simultaneously promote osseointegration and prevent infection of orthopaedic implants. *Biomaterials* **2016**, *84*, 301-314.
131. Chouirfa, H.; Bouloussa, H.; Migonney, V.; Falentin-Daudre, C., Review of titanium surface modification techniques and coatings for antibacterial applications. *Acta Biomater* **2019**, *83*, 37-54.
132. Sargeant, T. D.; Rao, M. S.; Koh, C.-Y.; Stupp, S. I., Covalent functionalization of NiTi surfaces with bioactive peptide amphiphile nanofibers. *Biomaterials* **2008**, *29* (8), 1085-1098.
133. Alcheikh, A.; Pavon-Djavid, G.; Helary, G.; Petite, H.; Migonney, V.; Anagnostou, F., PolyNaSS grafting on titanium surfaces enhances osteoblast differentiation and inhibits *Staphylococcus aureus* adhesion. *Journal of Materials Science: Materials in Medicine* **2013**, *24* (7), 1745-1754.
134. Michiardi, A.; Hélarý, G.; Nguyen, P. C. T.; Gamble, L. J.; Anagnostou, F.; Castner, D. G.; Migonney, V., Bioactive polymer grafting onto titanium alloy surfaces. *Acta Biomaterialia* **2010**, *6* (2), 667-675.
135. Hélarý, G.; Noirclère, F.; Mayingi, J.; Migonney, V., A new approach to graft bioactive polymer on titanium implants: Improvement of MG 63 cell differentiation onto this coating. *Acta Biomaterialia* **2009**, *5* (1), 124-133.
136. Vasconcelos, D. M.; Falentin-Daudré, C.; Blanquaert, D.; Thomas, D.; Granja, P. L.; Migonney, V., Role of protein environment and bioactive polymer grafting in the S. epidermidis response to titanium alloy for biomedical applications. *Materials Science and Engineering: C* **2014**, *45*, 176-183.
137. Asha, A. B.; Chen, Y.; Zhang, H.; Ghaemi, S.; Ishihara, K.; Liu, Y.; Narain, R., Rapid Mussel-Inspired Surface Zwitteration for Enhanced Antifouling and Antibacterial Properties. *Langmuir* **2019**, *35* (5), 1621-1630.

138. Chen, R.; Willcox, M. D. P.; Ho, K. K. K.; Smyth, D.; Kumar, N., Antimicrobial peptide melimine coating for titanium and its in vivo antibacterial activity in rodent subcutaneous infection models. *Biomaterials* **2016**, *85*, 142-151.
139. Gerits, E.; Kucharíková, S.; Van Dijck, P.; Erdtmann, M.; Krona, A.; Lövenklev, M.; Fröhlich, M.; Dovgan, B.; Impellizzeri, F.; Braem, A.; Vleugels, J.; Robijns, S. C. A.; Steenackers, H. P.; Vanderleyden, J.; De Brucker, K.; Thevissen, K.; Cammue, B. P. A.; Fauvart, M.; Verstraeten, N.; Michiels, J., Antibacterial activity of a new broad-spectrum antibiotic covalently bound to titanium surfaces. *Journal of Orthopaedic Research* **2016**, *34* (12), 2191-2198.
140. Wei, Q.; Achazi, K.; Liebe, H.; Schulz, A.; Noeske, P. L.; Grunwald, I.; Haag, R., Mussel-inspired dendritic polymers as universal multifunctional coatings. *Angew Chem Int Ed Engl* **2014**, *53* (43), 11650-5.
141. Terranova, U.; Bowler, D. R., Adsorption of Catechol on TiO₂ Rutile (100): A Density Functional Theory Investigation. *The Journal of Physical Chemistry C* **2010**, *114* (14), 6491-6495.
142. Maier, G. P.; Butler, A., Siderophores and mussel foot proteins: the role of catechol, cations, and metal coordination in surface adhesion. *J Biol Inorg Chem* **2017**, *22* (5), 739-749.
143. Chouirfa, H.; Evans, M. D. M.; Castner, D. G.; Bean, P.; Mercier, D.; Galtayries, A.; Falentin-Daudré, C.; Migonney, V., Grafting of architecture controlled poly(styrene sodium sulfonate) onto titanium surfaces using bio-adhesive molecules: Surface characterization and biological properties. *Biointerphases* **2017**, *12* (2), 02C418.
144. Hu, X.; Neoh, K.-G.; Shi, Z.; Kang, E.-T.; Poh, C.; Wang, W., An in vitro assessment of titanium functionalized with polysaccharides conjugated with vascular endothelial growth factor for enhanced osseointegration and inhibition of bacterial adhesion. *Biomaterials* **2010**, *31* (34), 8854-8863.
145. Córdoba, A.; Hierro-Oliva, M.; Pacha-Olivenza, M. Á.; Fernández-Calderón, M. C.; Perelló, J.; Isern, B.; González-Martín, M. L.; Monjo, M.; Ramis, J. M., Direct Covalent Grafting of Phytate to Titanium Surfaces through Ti–O–P Bonding Shows Bone Stimulating Surface Properties and Decreased Bacterial Adhesion. *ACS Applied Materials & Interfaces* **2016**, *8* (18), 11326-11335.
146. Pfaffenroth, C.; Winkel, A.; Dempwolf, W.; Gamble, L. J.; Castner, D. G.; Stiesch, M.; Menzel, H., Self-Assembled Antimicrobial and Biocompatible Copolymer Films on Titanium. *Macromolecular Bioscience* **2011**, *11* (11), 1515-1525.
147. Maddikeri, R. R.; Tosatti, S.; Schuler, M.; Chessari, S.; Textor, M.; Richards, R. G.; Harris, L. G., Reduced medical infection related bacterial strains adhesion on bioactive RGD modified titanium surfaces: A first step toward cell selective surfaces. *Journal of Biomedical Materials Research Part A* **2008**, *84A* (2), 425-435.
148. Chua, P.-H.; Neoh, K.-G.; Kang, E.-T.; Wang, W., Surface functionalization of titanium with hyaluronic acid/chitosan polyelectrolyte multilayers and RGD for promoting osteoblast functions and inhibiting bacterial adhesion. *Biomaterials* **2008**, *29* (10), 1412-1421.
149. Lv, H.; Chen, Z.; Yang, X.; Cen, L.; Zhang, X.; Gao, P., Layer-by-layer self-assembly of minocycline-loaded chitosan/alginate multilayer on titanium substrates to inhibit biofilm formation. *Journal of Dentistry* **2014**, *42* (11), 1464-1472.
150. Román, M. R. A. a. J. S., *Smart Polymers and their Applications*. Woodhead Publishing: 2014.
151. Lee, S. J.; Heo, D. N.; Lee, H. R.; Lee, D.; Yu, S. J.; Park, S. A.; Ko, W.-K.; Park, S. W.; Im, S. G.; Moon, J.-H.; Kwon, I. K., Biofunctionalized titanium with anti-fouling resistance by grafting thermo-responsive polymer brushes for the prevention of peri-implantitis. *Journal of Materials Chemistry B* **2015**, *3* (26), 5161-5165.

152. Schaer, T. P.; Stewart, S.; Hsu, B. B.; Klibanov, A. M., Hydrophobic polycationic coatings that inhibit biofilms and support bone healing during infection. *Biomaterials* **2012**, *33* (5), 1245-1254.
153. Rodriguez Lopez, A. L.; Lee, M. R.; Ortiz, B. J.; Gastfriend, B. D.; Whitehead, R.; Lynn, D. M.; Palecek, S. P., Preventing *S. aureus* biofilm formation on titanium surfaces by the release of antimicrobial beta-peptides from polyelectrolyte multilayers. LID - S1742-7061(19)30160-6 [pii] LID - 10.1016/j.actbio.2019.02.047 [doi]. *Acta Biomater.* **2019**, *19* (1878-7568 (Electronic)).
154. Kazemzadeh-Narbat, M.; Kindrachuk, J.; Duan, K.; Jenssen, H.; Hancock, R. E. W.; Wang, R., Antimicrobial peptides on calcium phosphate-coated titanium for the prevention of implant-associated infections. *Biomaterials* **2010**, *31* (36), 9519-9526.
155. Malizos, K.; Blauth, M.; Danita, A.; Capuano, N.; Mezzoprete, R.; Logoluso, N.; Drago, L.; Romanò, C. L., Fast-resorbable antibiotic-loaded hydrogel coating to reduce post-surgical infection after internal osteosynthesis: a multicenter randomized controlled trial. *Journal of Orthopaedics and Traumatology* **2017**, *18* (2), 159-169.
156. Shirai, T.; Tsuchiya, H.; Nishida, H.; Yamamoto, N.; Watanabe, K.; Nakase, J.; Terauchi, R.; Arai, Y.; Fujiwara, H.; Kubo, T., Antimicrobial megaprotheses supported with iodine. *Journal of Biomaterials Applications* **2014**, *29* (4), 617-623.
157. Shibata, Y.; Suzuki, D.; Omori, S.; Tanaka, R.; Murakami, A.; Kataoka, Y.; Baba, K.; Kamijo, R.; Miyazaki, T., The characteristics of in vitro biological activity of titanium surfaces anodically oxidized in chloride solutions. *Biomaterials* **2010**, *31* (33), 8546-8555.
158. Arciola, C. R.; Campoccia, D.; Speziale, P.; Montanaro, L.; Costerton, J. W., Biofilm formation in Staphylococcus implant infections. A review of molecular mechanisms and implications for biofilm-resistant materials. *Biomaterials* **2012**, *33* (26), 5967-5982.
159. Das, K.; Bose, S.; Bandyopadhyay, A.; Karandikar, B.; Gibbins, B. L., Surface coatings for improvement of bone cell materials and antimicrobial activities of Ti implants. *Journal of Biomedical Materials Research Part B: Applied Biomaterials* **2008**, *87B* (2), 455-460.
160. Almaguer-Flores, A.; Sánchez-Cruz, Y. R.; Park, J. H.; Olivares-Navarrete, R.; Dard, M.; Tannenbaum, R.; Schwartz, Z.; Boyan, B. D., Bacterial Adhesion on Polyelectrolyte Modified Microstructured Titanium Surfaces. *MRS Proceedings* **2011**, *1277*, s6-1.
161. Song, D.-H.; Uhm, S.-H.; Kim, S.-E.; Kwon, J.-S.; Han, J.-G.; Kim, K.-N., Synthesis of titanium oxide thin films containing antibacterial silver nanoparticles by a reactive magnetron co-sputtering system for application in biomedical implants. *Materials Research Bulletin* **2012**, *47* (10), 2994-2998.
162. Cabal, B.; Cafini, F.; Esteban-Tejeda, L.; Alou, L.; Bartolomé, J. F.; Sevillano, D.; López-Piriz, R.; Torrecillas, R.; Moya, J. S., Inhibitory Effect on In Vitro Streptococcus oralis Biofilm of a Soda-Lime Glass Containing Silver Nanoparticles Coating on Titanium Alloy. *PLOS ONE* **2012**, *7* (8), e42393.
163. Westas, E.; Gillstedt, M.; Lönn-Stensrud, J.; Bruzell, E.; Andersson, M., Biofilm formation on nanostructured hydroxyapatite-coated titanium. *Journal of Biomedical Materials Research Part A* **2014**, *102* (4 %@ 1549-3296), 1063-1070.
164. Y. Shibata, T. M., *Handbook of Oral Biomaterials*, n.d. <http://www.panstanford.com/books/9789814463126.html>. 2014.
165. Yao, X.; Zhang, X.; Wu, H.; Tian, L.; Ma, Y.; Tang, B., Microstructure and antibacterial properties of Cu-doped TiO₂ coating on titanium by micro-arc oxidation. *Applied Surface Science* **2014**, *292*, 944-947.
166. Kang, M.-K.; Lee, S.-B.; Moon, S.-K.; Kim, K.-M.; Kim, K.-N., The biomimetic apatite-cefalotin coatings on modified titanium. *Dental Materials Journal* **2012**, *31* (1), 98-105.

167. Metsemakers, W. J.; Reul, M.; Nijs, S., The use of gentamicin-coated nails in complex open tibia fracture and revision cases: A retrospective analysis of a single centre case series and review of the literature. *Injury* **2015**, *46* (12), 2433-7.
168. Fuchs, T.; Stange, R.; Schmidmaier, G.; Raschke, M. J., The use of gentamicin-coated nails in the tibia: preliminary results of a prospective study. *Arch Orthop Trauma Surg* **2011**, *131* (10), 1419-25.
169. Lee, J.-H.; Moon, S.-K.; Kim, K.-M.; Kim, K.-N., Modification of TiO₂ nanotube surfaces by electro-spray deposition of amoxicillin combined with PLGA for bactericidal effects at surgical implantation sites. *Acta Odontologica Scandinavica* **2013**, *71* (1), 168-174.
170. Park, S. W.; Lee, D.; Choi, Y. S.; Jeon, H. B.; Lee, C.-H.; Moon, J.-H.; Kwon, I. K., Mesoporous TiO₂ implants for loading high dosage of antibacterial agent. *Applied Surface Science* **2014**, *303*, 140-146.
171. Chen, W.; Liu, Y.; Courtney, H. S.; Bettenga, M.; Agrawal, C. M.; Bumgardner, J. D.; Ong, J. L., In vitro anti-bacterial and biological properties of magnetron co-sputtered silver-containing hydroxyapatite coating. *Biomaterials* **2006**, *27* (32), 5512-5517.
172. Feng, Q. L.; Wu, J.; Chen, G. Q.; Cui, F. Z.; Kim, T. N.; Kim, J. O., A mechanistic study of the antibacterial effect of silver ions on Escherichia coli and Staphylococcus aureus. *Journal of biomedical materials research* **2000**, *52* (4), 662-8.
173. Zhu, Z. Y.; Zhang, F. Q.; Xie, Y. T.; Chen, Y. K.; Zheng, X. B., In Vitro Assessment of Antibacterial Activity and Cytotoxicity of Silver Contained Antibacterial HA Coating Material. *Materials Science Forum* **2009**, *620-622*, 307-310.
174. Xu, J.; Li, Y.; Zhou, X.; Li, Y.; Gao, Z.-D.; Song, Y.-Y.; Schmuki, P., Graphitic C₃N₄-Sensitized TiO₂ Nanotube Layers: A Visible-Light Activated Efficient Metal-Free Antimicrobial Platform. *Chemistry – A European Journal* **2016**, *22* (12), 3947-3951.
175. Thibaud, C.; Michel, B.; Jacques, L., Sol-gel Chemistry in Medicinal Science. *Current Medicinal Chemistry* **2006**, *13* (1), 99-108.
176. Radin, S.; Ducheyne, P., Controlled release of vancomycin from thin sol-gel films on titanium alloy fracture plate material. *Biomaterials* **2007**, *28* (9), 1721-1729.
177. Gollwitzer, H.; Haenle, M.; Mittelmeier, W.; Heidenau, F.; Harrasser, N., A biocompatible sol-gel derived titania coating for medical implants with antibacterial modification by copper integration. *AMB Express* **2018**, *8* (1), 24.
178. Lin, N.; Huang, X.; Zou, J.; Zhang, X.; Qin, L.; Fan, A.; Tang, B., Effects of plasma nitriding and multiple arc ion plating TiN coating on bacterial adhesion of commercial pure titanium via in vitro investigations. *Surface and Coatings Technology* **2012**, *209*, 212-215.
179. Lin, N.; Huang, X.; Zhang, X.; Fan, A.; Qin, L.; Tang, B., In vitro assessments on bacterial adhesion and corrosion performance of TiN coating on Ti6Al4V titanium alloy synthesized by multi-arc ion plating. *Applied Surface Science* **2012**, *258* (18), 7047-7051.
180. Ji, M.-K.; Park, S.-W.; Lee, K.; Kang, I.-C.; Yun, K.-D.; Kim, H.-S.; Lim, H.-P., Evaluation of antibacterial activity and osteoblast-like cell viability of TiN, ZrN and (Ti_{1-x}Zr_x)N coating on titanium. *J Adv Prosthodont* **2015**, *7* (2), 166-171.
181. Patterson, D. M.; Nazarova, L. A.; Prescher, J. A., Finding the right (bioorthogonal) chemistry. *ACS Chem Biol* **2014**, *9* (3), 592-605.
182. Ji, X.; Pan, Z.; Yu, B.; De La Cruz, L. K.; Zheng, Y.; Ke, B.; Wang, B., Click and release: bioorthogonal approaches to "on-demand" activation of prodrugs. *Chem Soc Rev* **2019**, *48* (4), 1077-1094.
183. Lee, M. H.; Sessler, J. L.; Kim, J. S., Disulfide-based multifunctional conjugates for targeted theranostic drug delivery. *Acc Chem Res* **2015**, *48* (11), 2935-46.
184. Yeh, J. J.; Kim, W. Y., Targeting tumor hypoxia with hypoxia-activated prodrugs. *Journal of clinical oncology : official journal of the American Society of Clinical Oncology* **2015**, *33* (13), 1505-8.

185. Rooseboom, M.; Commandeur, J. N.; Vermeulen, N. P., Enzyme-catalyzed activation of anticancer prodrugs. *Pharmacological reviews* **2004**, *56* (1), 53-102.
186. Azoulay, M.; Tuffin, G.; Sallem, W.; Florent, J. C., A new drug-release method using the Staudinger ligation. *Bioorg Med Chem Lett* **2006**, *16* (12), 3147-9.
187. van Brakel, R.; Vulders, R. C.; Bokdam, R. J.; Grull, H.; Robillard, M. S., A doxorubicin prodrug activated by the staudinger reaction. *Bioconjugate chemistry* **2008**, *19* (3), 714-8.
188. Mondal, M.; Liao, R.; Xiao, L.; Eno, T.; Guo, J., Highly Multiplexed Single-Cell In Situ Protein Analysis with Cleavable Fluorescent Antibodies. *Angew Chem Int Ed Engl* **2017**, *56* (10), 2636-2639.
189. Nilsson, B. L.; Hondal, R. J.; Soellner, M. B.; Raines, R. T., Protein Assembly by Orthogonal Chemical Ligation Methods. *Journal of the American Chemical Society* **2003**, *125* (18), 5268-5269.
190. Cohen, A. S.; Dubikovskaya, E. A.; Rush, J. S.; Bertozzi, C. R., Real-time bioluminescence imaging of glycans on live cells. *J Am Chem Soc* **2010**, *132* (25), 8563-5.
191. Matikonda, S. S.; Orsi, D. L.; Staudacher, V.; Jenkins, I. A.; Fiedler, F.; Chen, J.; Gamble, A. B., Bioorthogonal prodrug activation driven by a strain-promoted 1,3-dipolar cycloaddition. *Chemical Science* **2015**, *6* (2), 1212-1218.
192. Sustmann, R.; Trill, H., Substituent Effects in 1,3-Dipolar Cycloadditions of Phenyl Azide. *Angewandte Chemie International Edition in English* **1972**, *11* (9), 838-840.
193. Matikonda, S. S.; Fairhall, J. M.; Fiedler, F.; Sanhajariya, S.; Tucker, R. A. J.; Hook, S.; Garden, A. L.; Gamble, A. B., Mechanistic Evaluation of Bioorthogonal Decaging with trans-Cyclooctene: The Effect of Fluorine Substituents on Aryl Azide Reactivity and Decaging from the 1,2,3-Triazoline. *Bioconjugate chemistry* **2018**, *29* (2), 324-334.
194. Xu, M.; Tu, J.; Franzini, R. M., Rapid and efficient tetrazine-induced drug release from highly stable benzonorbornadiene derivatives. *Chemical Communications* **2017**, *53* (46), 6271-6274.
195. Darko, A.; Wallace, S.; Dmitrenko, O.; Machovina, M. M.; Mehl, R. A.; Chin, J. W.; Fox, J. M., Conformationally Strained trans-Cyclooctene with Improved Stability and Excellent Reactivity in Tetrazine Ligation. *Chem Sci* **2014**, *5* (10), 3770-3776.
196. Selvaraj, R.; Liu, S.; Hassink, M.; Huang, C. W.; Yap, L. P.; Park, R.; Fox, J. M.; Li, Z.; Conti, P. S., Tetrazine-trans-cyclooctene ligation for the rapid construction of integrin $\alpha v \beta 3$ targeted PET tracer based on a cyclic RGD peptide. *Bioorg Med Chem Lett* **2011**, *21* (17), 5011-4.
197. Rossin, R.; Verkerk, P. R.; van den Bosch, S. M.; Vulders, R. C.; Verel, I.; Lub, J.; Robillard, M. S., In vivo chemistry for pretargeted tumor imaging in live mice. *Angew Chem Int Ed Engl* **2010**, *49* (19), 3375-8.
198. Devaraj, N. K.; Thurber, G. M.; Keliher, E. J.; Marinelli, B.; Weissleder, R., Reactive polymer enables efficient in vivo bioorthogonal chemistry. *Proceedings of the National Academy of Sciences of the United States of America* **2012**, *109* (13), 4762-7.
199. Blackman, M. L.; Royzen, M.; Fox, J. M., Tetrazine ligation: fast bioconjugation based on inverse-electron-demand Diels-Alder reactivity. *J Am Chem Soc* **2008**, *130* (41), 13518-9.
200. Taylor, M. T.; Blackman, M. L.; Dmitrenko, O.; Fox, J. M., Design and synthesis of highly reactive dienophiles for the tetrazine-trans-cyclooctene ligation. *J Am Chem Soc* **2011**, *133* (25), 9646-9.
201. Chen, W.; Wang, D.; Dai, C.; Hamelberg, D.; Wang, B., Clicking 1,2,4,5-tetrazine and cyclooctynes with tunable reaction rates. *Chemical Communications* **2012**, *48* (12), 1736-1738.
202. Czuban, M.; Srinivasan, S.; Yee, N. A.; Agustin, E.; Koliszak, A.; Miller, E.; Khan, I.; Quinones, I.; Noory, H.; Motola, C.; Volkmer, R.; Di Luca, M.; Trampuz, A.; Royzen, M.;

- Mejia Oneto, J. M., Bio-Orthogonal Chemistry and Reloadable Biomaterial Enable Local Activation of Antibiotic Prodrugs and Enhance Treatments against Staphylococcus aureus Infections. *ACS Cent Sci* **2018**, *4* (12), 1624-1632.
203. Versteegen, R. M.; Rossin, R.; ten Hoeve, W.; Janssen, H. M.; Robillard, M. S., Click to release: instantaneous doxorubicin elimination upon tetrazine ligation. *Angew Chem Int Ed Engl* **2013**, *52* (52), 14112-6.
204. Fan, X.; Ge, Y.; Lin, F.; Yang, Y.; Zhang, G.; Ngai, W. S.; Lin, Z.; Zheng, S.; Wang, J.; Zhao, J.; Li, J.; Chen, P. R., Optimized Tetrazine Derivatives for Rapid Bioorthogonal Decaging in Living Cells. *Angew Chem Int Ed Engl* **2016**, *55* (45), 14046-14050.
205. Khan, I.; Agris, P. F.; Yigit, M. V.; Royzen, M., In situ activation of a doxorubicin prodrug using imaging-capable nanoparticles. *Chemical communications (Cambridge, England)* **2016**, *52* (36), 6174-7.
206. Cieplik, F.; Deng, D.; Crielaard, W.; Buchalla, W.; Hellwig, E.; Al-Ahmad, A.; Maisch, T., Antimicrobial photodynamic therapy - what we know and what we don't. *Crit Rev Microbiol* **2018**, *44* (5), 571-589.
207. Wilson, B. C.; Patterson, M. S., The physics, biophysics and technology of photodynamic therapy. *Physics in medicine and biology* **2008**, *53* (9), R61-109.
208. Nagata, J. Y.; Hioka, N.; Kimura, E.; Batistela, V. R.; Terada, R. S.; Graciano, A. X.; Baesso, M. L.; Hayacibara, M. F., Antibacterial photodynamic therapy for dental caries: evaluation of the photosensitizers used and light source properties. *Photodiagnosis and photodynamic therapy* **2012**, *9* (2), 122-31.
209. Fekrazad, R.; Zare, H.; Vand, S. M., Photodynamic therapy effect on cell growth inhibition induced by Radachlorin and toluidine blue O on Staphylococcus aureus and Escherichia coli: An in vitro study. *Photodiagnosis and photodynamic therapy* **2016**, *15*, 213-7.
210. Wang, C.; Chen, P.; Qiao, Y.; Kang, Y.; Guo, S.; Wu, D.; Wang, J.; Wu, H., Bacteria-activated chlorin e6 ionic liquid based on cation and anion dual-mode antibacterial action for enhanced photodynamic efficacy. *Biomaterials science* **2019**, *7* (4), 1399-1410.
211. Tyagi, P.; Singh, M.; Kumari, H.; Kumari, A.; Mukhopadhyay, K., Bactericidal activity of curcumin I is associated with damaging of bacterial membrane. *PloS one* **2015**, *10* (3), e0121313.
212. Mun, S. H.; Joung, D. K.; Kim, Y. S.; Kang, O. H.; Kim, S. B.; Seo, Y. S.; Kim, Y. C.; Lee, D. S.; Shin, D. W.; Kweon, K. T.; Kwon, D. Y., Synergistic antibacterial effect of curcumin against methicillin-resistant Staphylococcus aureus. *Phytomedicine : international journal of phytotherapy and phytopharmacology* **2013**, *20* (8-9), 714-8.
213. Kiesslich, T.; Gollmer, A.; Maisch, T.; Berneburg, M.; Plaetzer, K., A comprehensive tutorial on in vitro characterization of new photosensitizers for photodynamic antitumor therapy and photodynamic inactivation of microorganisms. *BioMed research international* **2013**, *2013*, 840417.
214. Anagnostakos, K., Therapeutic Use of Antibiotic-loaded Bone Cement in the Treatment of Hip and Knee Joint Infections. *J Bone Jt Infect* **2017**, *2* (1), 29-37.
215. Anagnostakos, K.; Kelm, J., Enhancement of antibiotic elution from acrylic bone cement. *Journal of biomedical materials research. Part B, Applied biomaterials* **2009**, *90* (1), 467-75.
216. Anagnostakos, K.; Furst, O.; Kelm, J., Antibiotic-impregnated PMMA hip spacers: Current status. *Acta orthopaedica* **2006**, *77* (4), 628-37.
217. Cui, Q.; Mihalko, W. M.; Shields, J. S.; Ries, M.; Saleh, K. J., Antibiotic-impregnated cement spacers for the treatment of infection associated with total hip or knee arthroplasty. *The Journal of bone and joint surgery. American volume* **2007**, *89* (4), 871-82.

218. Kühn, K.-D., *Management of Periprosthetic Joint Infection. A global perspective on diagnosis, treatment options, prevention strategies and their economic impact*. Springer: 2018.
219. Brown, T. S.; Petis, S. M.; Osmon, D. R.; Mabry, T. M.; Berry, D. J.; Hanssen, A. D.; Abdel, M. P., Periprosthetic Joint Infection With Fungal Pathogens. *The Journal of Arthroplasty* **2018**, *33* (8), 2605-2612.
220. Cobo, F.; Rodriguez-Granger, J.; Sampedro, A.; Aliaga-Martinez, L.; Navarro-Mari, J. M., Candida Prosthetic Joint Infection. A Review of Treatment Methods. *J Bone Jt Infect* **2017**, *2* (2), 114-121.
221. Okano, A.; Isley, N. A.; Boger, D. L., Total Syntheses of Vancomycin-Related Glycopeptide Antibiotics and Key Analogues. *Chemical reviews* **2017**, *117* (18), 11952-11993.
222. Smith, K.; Perez, A.; Ramage, G.; Gemmell, C. G.; Lang, S., Comparison of biofilm-associated cell survival following in vitro exposure of meticillin-resistant *Staphylococcus aureus* biofilms to the antibiotics clindamycin, daptomycin, linezolid, tigecycline and vancomycin. *Int J Antimicrob Agents* **2009**, *33* (4), 374-8.
223. Bruniera, F. R.; Ferreira, F. M.; Saviolli, L. R.; Bacci, M. R.; Feder, D.; da Luz Goncalves Pedreira, M.; Sorgini Peterlini, M. A.; Azzalis, L. A.; Campos Junqueira, V. B.; Fonseca, F. L., The use of vancomycin with its therapeutic and adverse effects: a review. *European review for medical and pharmacological sciences* **2015**, *19* (4), 694-700.
224. Bassetti, M.; Nicco, E.; Ginocchio, F.; Ansaldi, F.; de Florentiis, D.; Viscoli, C., High-dose daptomycin in documented *Staphylococcus aureus* infections. *Int J Antimicrob Agents* **2010**, *36* (5), 459-61.
225. Taylor, S. D.; Palmer, M., The action mechanism of daptomycin. *Bioorganic & medicinal chemistry* **2016**, *24* (24), 6253-6268.
226. Corona Perez-Cardona, P. S.; Barro Ojeda, V.; Rodriguez Pardo, D.; Pigrau Serrallach, C.; Guerra Farfan, E.; Amat Mateu, C.; Flores Sanchez, X., Clinical experience with daptomycin for the treatment of patients with knee and hip periprosthetic joint infections. *The Journal of antimicrobial chemotherapy* **2012**, *67* (7), 1749-54.
227. Eisenstein, B. I.; Oleson, F. B., Jr.; Baltz, R. H., Daptomycin: from the mountain to the clinic, with essential help from Francis Tally, MD. *Clin Infect Dis* **2010**, *50* Suppl 1, S10-5.
228. Byren, I.; Rege, S.; Campanaro, E.; Yankelev, S.; Anastasiou, D.; Kuropatkin, G.; Evans, R., Randomized controlled trial of the safety and efficacy of Daptomycin versus standard-of-care therapy for management of patients with osteomyelitis associated with prosthetic devices undergoing two-stage revision arthroplasty. *Antimicrobial agents and chemotherapy* **2012**, *56* (11), 5626-32.
229. J.H., W., The Formation of Mussel Byssus: Anatomy of a Natural Manufacturing Process. . In *Case S.T. (eds) Structure, Cellular Synthesis and Assembly of Biopolymers. Results and Problems in Cell Differentiation (A Series of Topical Volumes in Developmental Biology)*, Springer, Berlin, Heidelberg ed.; 1992; Vol. 19.
230. Lee, B. P.; Messersmith, P. B.; Israelachvili, J. N.; Waite, J. H., Mussel-Inspired Adhesives and Coatings. *Annu Rev Mater Res* **2011**, *41*, 99-132.
231. Lee, H.; Scherer, N. F.; Messersmith, P. B., Single-molecule mechanics of mussel adhesion. *Proc Natl Acad Sci U S A* **2006**, *103* (35), 12999-3003.
232. Burzio, L. A.; Waite, J. H., Cross-Linking in Adhesive Quinoproteins: Studies with Model Decapeptides†. *Biochemistry* **2000**, *39* (36), 11147-11153.
233. LaVoie, M. J.; Ostaszewski, B. L.; Weihofen, A.; Schlossmacher, M. G.; Selkoe, D. J., Dopamine covalently modifies and functionally inactivates parkin. *Nat Med* **2005**, *11* (11), 1214-21.

234. Kang, S. M.; Rho, J.; Choi, I. S.; Messersmith, P. B.; Lee, H., Norepinephrine: material-independent, multifunctional surface modification reagent. *J Am Chem Soc* **2009**, *131* (37), 13224-5.
235. Lee, H.; Dellatore, S. M.; Miller, W. M.; Messersmith, P. B., Mussel-inspired surface chemistry for multifunctional coatings. *Science* **2007**, *318* (5849), 426-30.
236. Faure, E.; Falentin-Daudré, C.; Jérôme, C.; Lyskawa, J.; Fournier, D.; Woisel, P.; Detrembleur, C., Catechols as versatile platforms in polymer chemistry. *Progress in polymer science* **2013**, *38* (1), 236-270.
237. Kucukdurmaz, F.; Parvizi, J., The Prevention of Periprosthetic Joint Infections. *Open Orthop J* **2016**, *10*, 589-599.
238. Brauner, A.; Fridman, O.; Gefen, O.; Balaban, N. Q., Distinguishing between resistance, tolerance and persistence to antibiotic treatment. *Nature Reviews Microbiology* **2016**, *14* (5), 320-330.